DEMOCRATIC AND POPULAR REPUBLIC OF ALGERIA

Ministry of Higher Education and Scientific Research

University of Tlemcen

جامعة أبو بكر بلقايد

UNIVERSITÉ DE TLEMCEN

Pan African University

Institute of Water and Energy Sciences

PAN AFRICAN UNIVERSITY

Institute of Water and Energy Sciences (Incl. Climate Change)

DESIGN AND PERFORMANCE ANALYSIS OF A PARABOLIC TROUGH POWER PLANT UNDER TAMANRASSET CLIMATOLOGICAL CONDITIONS

Benhadji Serradj Djamal Eddine

Date: 28/08/2016

Master in Energy Engineering track

Members of Jury:

Abdellah Khellaf	President	Professor	CDER-Algiers
Ben Sebitosi	Supervisor	Professor	Stellenbosch S.A
Abdelatif Zerga	External examiner 1	Professor	U.A.B-Tlemcen
Sofiane Amara	Internal examiner 2	Doctor	U.A.B-Tlemcen

Academic Year: 2015-2016

This research thesis is submitted in partial fulfillment of the requirements of Master Science in Energy Engineering at Pan African University Institute of Water and Energy Sciences (including Climate Change)-(PAUWES) at the University of Tlemcen in Algeria.

August 2016.

DECLARATION

I, **Djamal Eddine Benhadji Serradj** do hereby declare that this thesis is my original work and to the best of my knowledge, it has not been submitted for any award in any University or Institution.

Signed_____ Date _____

Djamal Eddine Benhadji Serradj

CERTIFICATION

This thesis has been submitted with my approval as the supervisor

Signed_____Date_____

Prof. A. Ben Sebitosi

ABSTRACT

In this study the current status of the energy resources, supply and demand in Algeria is reviewed. The different sources of renewable energy and their contribution to the present and future electricity supply of the country are also analyzed. Low electricity price in Algeria is one of the major challenges facing the development of renewable energies in the country. Since the energy prices are low, country's energy consumption is one of the highest in Africa at 1277 kWh per capita per annum where the average per capita energy consumption for Africa is 543 kWh [1]. Conventional resources, especially natural gas are the primary sources exploited for electricity production. However, the latter resources emit a great amount of greenhouse gases. The huge solar energy potential in Algeria and its different applications can be utilized to meet the escalating energy demand with minimal greenhouse gases.

In this study, the site of Tamanrasset was taken as the case study because of the high direct normal irradiation (DNI) received in the city. Tamanrasset is an oasis city and capital of Tamanrasset province in southern Algeria, in the Ahaggar Mountains. In summer there is an escalation of power demand due to the cooling load. The capacity of the existing transmission infrastructure cannot meet this additional load and hence there is periodic shortage of electricity. The most suitable technology for harvesting (DNI) is concentrating solar power (CSP) and has been chosen for this project.

To support the existing installed power capacity connected to Tamanrasset, the electricity demand of the city was initially determined for two critical periods in the year (winter and summer), where the winter peak load was found during the night at a value of 73 MW and in summer peak load was in the afternoon and late in the evening at 87 MW. A parabolic trough power plant of 100 MWp with 6 hours of storage was designed and simulated to assess the city's load demand portion that power produced from the designed power plant could meet. Different parameters were taken into account during the design to minimize the impact of the environmental conditions on the performances of the plant.

Initially Meteonorm weather resource assessment software was used to generate the annual weather data file at a suitable site in Tamanrasset (Latitude: 22.79, longitude: 5.526). Using this file System Advisor Model software was then used to simulate the designed parabolic trough

power plant considering two different condensers types; evaporative and air-cooled in consideration of water constraint in the selected location.

The two different cooling technologies were compared based on the power plant electricity production and water consumption. The results have shown that for the whole year, energy produced from the one using water for cooling was higher than the one using air cooling system. Therefore, the capacity factor of the evaporative cooling power plant was higher by 4% more than the opponent technology. However, water consumption was very high for water cooling power plant reaching almost 14 times more than the air cooled technology. Since the water consumed in evaporative cooled power plant was enormous comparing to its availability in Tamanrasset the load, economic and greenhouse analysis was done only for dry cooled power plant.

The electricity production was compared after to the real load of the city during the month of January and August. It was found that during the month of January (winter) the power plant was able to cover 78% from the needs of the city. On the other hand, during the month of August (summer) even with the high electricity production the power plant provided the city with only 60% of the needs and that was due to the high demand of the city. On the other hand, the energy losses of the power plant were analyzed and it was found that the biggest share of energy losses was in form of parasitic losses in the power plant heat transfer pumps and also in the receiver in form of thermal losses.

Economic analysis of the power plant was undertaken and the levelized cost of electricity was found as 8.19 DA/kWh with a payback period of 8.78 years and benefit-cost ratio of 1.73. Sensitivity analysis when varying the solar multiple of the power plant and also the size of the thermal energy storage was done and shown for each solar multiple process an optimum number of hours of storage that gives the optimum LCOE. Moreover, it was found also that whenever the storage hours increase the Levelized cost of electricity increases too. A cash flow analysis was performed also to analyze the assets of project.

Environment impact analysis of the power plant was done and established, the designed power plant avoided greenhouse gas emissions were estimated using the emissions that could be released if the power plant was using natural gas in a combined cycle plant.

Key words: Renewable energy, Direct Normal Irradiation, Concentrating Solar Power, Meteonorm, System Advisor Model.

PREFACE

Dans cette étude, l'état actuel des ressources énergétiques, l'offre et la demande en Algérie ont été passée en revue. La contribution des énergies renouvelables à l'alimentation d'électricité au présent et au future sont également analysées. Le prix bas de l'électricité en Algérie est l'un des défis majeurs du développement des énergies renouvelables dans le pays. Puisque le prix de l'énergie est très bas, la consommation annuelle est l'une des plus élevées de l'Afrique avec 1277 kWh par habitant où la consommation moyenne par habitant en Afrique est de 543 KWh [1]. Les ressources conventionnelles, dont le gaz naturel en particulier sont les principales sources d'énergie exploitées pour la production d'électricité. Cependant, les ressources précitées émettent une grande quantité de gaz à effet de serre. L'immense potentiel d'énergie solaire en Algérie et ses différentes applications peuvent être utiliser pour faire face à l'escalade de la demande d'énergie avec un minimum d'émissions de gaz à effet de serre.

Dans cette étude, le site de Tamanrasset a été pris comme cas d'étude en raison de la forte irradiation directe à incidence normale reçue dans la ville. La ville de Tamanrasset est une oasis et elle est la capitale de la province de Tamanrasset dans le sud de l'Algérie, dans les montagnes du Hoggar. En été, il y a une augmentation de la demande d'électricité en raison de la charge causée par l'utilisation des climatiseurs. La capacité de l'infrastructure existante ne peut pas répondre à cette charge supplémentaire et par conséquent il y a des pénuries périodiques d'électricité. La technologie la plus appropriée pour l'utilisation d'irradiation direct à incidence normale est l'Energie Solaire a Concentration (ESP), thème qui a été choisi pour l'étude de ce projet.

Afin de soutenir la capacité installée existante reliée à Tamanrasset, la demande d'électricité de la ville était initialement déterminée pour deux périodes critiques au cours de l'année (hiver et été), où la charge de pointe hivernale est pendant la nuit à une valeur de 73 MW et en été dans l'après-midi et tard dans la nuit à 87 MW. Une centrale électrique utilisant des miroirs parabolique d'une puissance de 100 MW et 6 heures de stockage a été conçu et simulée pour évaluer la part de la demande que la centrale va couvrir. Différents paramètres ont été pris en compte lors de la conception afin de minimiser l'impact des conditions environnementales sur les représentations de la centrale.

Au départ, le logiciel d'évaluation des ressources météorologiques Meteonorm a été utilisé pour générer les données météorologiques annuelles à un site approprié à Tamanrasset (Latitude : 22.79, longitude : 5.526). Le logiciel System Advisor Model a ensuite été utilisé pour simuler une centrale électrique fonctionnant avec des miroirs paraboliques conçues en considérant deux types de condenseurs différents ; refroidissement a air et le deuxième utilisant l'eau en tenant compte de la contrainte des ressources en eau dans l'endroit choisi.

Les deux différentes technologies de refroidissement ont été comparées à la base de la production d'électricité de la centrale et de la consommation d'eau. Les résultats ont montré que pour l'ensemble de l'année, l'énergie produite par celle utilisant de l'eau comme un refroidisseur était plus élevé que celle utilisait le refroidissement à air. Par conséquent, le facteur de capacité de la centrale à refroidissement par l'eau a été plus élevé de 4 % que l'autre technologie. Toutefois, la consommation d'eau a été très élevée pour le refroidissement hydraulique atteignant presque 14 fois plus que la technologie refroidie par air. Puisque l'eau consommée dans la centrale a refroidissement par évaporateur était énorme comparée à sa disponibilité à Tamanrasset, l'analyse de la charge économique et de l'impact environnementale n'a été faite que pour la centrale électrique utilisant l'air pour le refroidissement.

La production d'électricité a été comparée après à la charge réelle de la ville durant le mois de Janvier et Août. Il a été constaté que, pendant le mois de janvier (hiver) La centrale électrique a été en mesure de couvrir 78 % des besoins de la ville. D'autre part, à cause de la forte demande durant le mois d'août (été) même avec une production élevée d'électricité, la centrale fournit seulement 60% de la demande

L'analyse économique de la centrale a été effectuée et le coût moyen actualisé de l'électricité est de 8,19 DA / kWh avec un délai de récupération de 8,78 ans et un rendement bénéfices/coûts de 1,73. L'analyse de sensibilité en variant le multiple solaire la centrale et également la taille de stockage d'énergie thermique a été réalisé et illustré pour chaque processus le multiple solaire traité, un nombre optimal des heures de stockage qui donne le LCOE optimale. En outre, il a été constaté aussi que, lorsque les heures de stockage augmentent le coût de l'électricité augmente aussi, ainsi une analyse des flux de trésorerie a été effectuée aussi pour analyser les actifs du projet.

L’analyse de l'impact sur l'environnement de la centrale électrique a été fait et établi, la centrale conçue évite les émissions de gaz à effet de serre, à noter que ces derniers ont été estimées en utilisant les émissions qui pourraient être libérées si la centrale utilisait du gaz naturel dans un cycle combiné.

Mots clé : Energie renouvelable, irradiation directe à incidence normale, énergie solaire a concentration, Meteonorm, System Advisor Model.

ACKNOWLEDGEMENTS

I am thankful to Allah for the gift of life and strength to press on to this far. Without Him I wouldn't have made it to this point in life.

With all due respect, I am thankful to the African Union Commission for awarding me a Master's scholarship that has seen me through PAUWES. I am grateful to the respective sponsors, partners and administration of the institute and the Algerian government at large.

I am deeply grateful to my supervisor, Professor A. Ben Sebitosi, for having accepted to supervise me. His tireless support and encouragement are remarkable. I am also thankful to Professor Dinter from Solar Thermal Energy Research Group (STERG) of Stellenbosch university for his support and guidance.

I would like to express my deepest gratitude to my parents and family members for their continuous encouragement, understanding and support. Their trust in my potential and push has kept me going and overcoming obstacles in life.

Thank you to all friends and fellow students at PAUWES, especially Nicholas Mukisa with whom I traveled with everywhere I went in the previous two years and for being supportive throughout.

LIST OF CONTENT

LIST OF FIGURES

.

LIST OF TABLES

NOMENCLATURE

ACC:	Air Cooled Condenser
BC:	Before Christ
CDER:	Center of Development of Renewable Energies
CF:	Capacity Factor
$CO_{2:}$	Carbon Dioxide
CSP:	Concentrating Solar Power
DLR:	National Center for Aerospace
DNI:	Direct Normal Irradiance
EPW:	Energy Plus Weather
HCE:	Heat Collecting Element
HTF:	Heat Transfer Fluid
IAM:	Incident Angle Modifier
IEA:	International Energy Agency
LCOE:	Levelized Cost of Electricity
MENA:	Middle East and North Africa region
PCM:	Phase Change Material
pH:	potential of Hydrogen
PTC:	Parabolic Trough Collector
PTT:	Parabolic Trough Technology
PV:	Photovoltaic
RTR:	Reversible Thermochemical Reaction
SAM:	System Advisor Model
SM:	Solar Multiple
SONELGAZ :	Société National de l'Electricité et du Gaz
STC:	Solar Thermal Conversion
STEC:	Solar Thermal Electric Components
TES:	Thermal Energy Storage
TMY:	Typical Meteorological Years
TRNSYS:	Transient Simulation Software

Chapter 1. INTRODUCTION

Outline:

1.0 Introduction

This section presents the current status of the energy sector in Algeria, with the impact of the reliance on the conventional resources on the economy of the country and also the development of the conventional resources. The key parameters such as energy consumption, energy resources with their respective share in electricity production and the renewable energy program are highlighted.

1.1 Background Information

The economy of Algeria has negatively been affected by changes in oil prices on the world market. Over the last years the price of a barrel dropped drastically from around 10,847.5 DA to 3515.4 DA which has pushed Algerian government to take austerity measures to mitigate the deficit in the budget [2]. The price of electricity in Algeria is one of the lowest in the world at 3 DA/kWh which is due to the major share of the cost being covered by subsidies [3].

However, from the beginning of 2016 the government started implementing measures to raise prices of fossil fuels and electricity in order to ensure smooth running of the country and avoid depletion of the government coffers.

Algeria being one of the biggest producers of gas and oil in the world, it emits a big amount of greenhouse gas emissions. The country plays an important role in hydrocarbons sector with a production exceeding 1.4 million barrels per day of crude oil, of which 85% is exported, and 86.5 billion cubic meters of natural gas, of which 70% is exported specifically to Europe. In addition to that, due to the fast demographic growth of population, rural exodus and also the constant growth of the economy, energy demand has been estimated to double by the year 2020 [4].

According to the report released in 2015 by the ministry of energy, the installed capacity increased in the last 10 years by 230% rising from 7,492 MW in 2005 to 17,238 MW in 2015. Table 1.1 below shows the share of the different sources of energy in the installed capacity of the country. The share of conventional resources in electricity production exceeds 97% of the total generation. However, installed capacity from renewable energies and hybrid systems presents almost a neglected share of 3% [5]. Such factors escalade the generation of greenhouse gases,

while the international trends advocate for the opposite; less emission, more sustainable and environmental solutions.

Table 1.1: Installed capacity by source

	Gas	Diesel	Hydro	Hybrid	Renewables
Installed capacity (MW)	16514	345	172	173	34

Source: (Boudghene S. et al., 2012)

As the conventional energy resources cannot be renewed, relying on them is likely to lead to energy insecurity in the long run. Algerian reserves of fossil fuels and natural gas can only sustain electricity generation for the next 50 years and according to the International Energy Agency, the energy consumption forecast is at an increase of about 53% [4]. In addition to that, the current high energy consumption and low efficiency of the systems affect the sustainable development of the different energy sectors in the country.

Algeria like any other country has drawn a roadmap for the use and promotion of renewable energy. Encouraged by its commitment to the international community in the fight against global warming backed by the abundance and one of the greatest solar potential fields in the world. The Algerian government launched a program dedicated to solar thermal and photovoltaic. Project tests and pilots were implemented in the first phase of the program in order to identify the different technologies and their response under the climate conditions of the selected sites. Figure 1.1 below shows the share of each renewable energy resource and its planned power capacity installation to which solar thermal energy using concentrating solar power constitutes 10% of the total installed capacity [6].

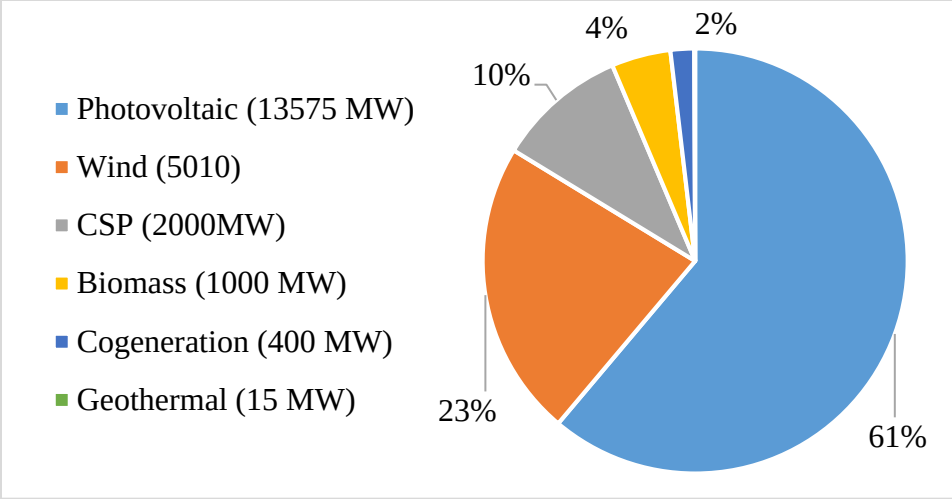

Source: (CDER, 2013)

Figure 1.1: Installed power capacity in 2030

To meet the targeted installed power capacity, Algeria inaugurated in 2011 its first hybrid (solar/natural gas) project in Hassi R'mel situated in the southern east of the country. The power plant capacity is 150 MW and the share coming from solar energy is 30 MW [7]. The environmental impact of the project is reducing CO_2 gas emissions by an amount of 33,000 tons and also a decrease in gas consumption, thus savings because of using the solar field rather than burning gas for electricity production which can reach 7 million cubic meters [8].

According to A. Boudghene Stambouli (2012), the government is venturing into the exploitation of the huge solar potential with the installation of two concentrating solar power plants with thermal storage of 150 MW each in addition to the hybrid station in Hassi R'mel. On the other hand, the decision makers aim also to create the industry for the local manufacturing of solar mirrors, heat transfer fluids, thermal storage equipment and power block components. Based on the government's plan to invest in concentrating solar plants this study assesses the possibility and potential of Tamanrasset as one of the location to be considered for these power plants [4]. The aim of this study is to carry out a performance analysis of concentrating solar power plant under the climate conditions of Tamanrasset.

1.2 Problem Statement

The utilization of only direct normal irradiation by concentrating solar power leads to disparity between the performance of a system depending on the geographical locations. Algeria

has a huge solar potential due to its geographical position in the sun belt, endowed with its Sahara, concentrating solar power technology merges as a suitable solution to mitigate the increase in energy demand and dependency on hydrocarbons in the country. SONELGAZ, the only distribution utility in the country has done enormous efforts to cover almost 99% of the population, where more than 80% is in the north [9]. However, during the past summers many provinces across the country experienced power shortages due to the high demand of electricity, especially the southern part where the population experience hot day reaching 45°C. The desert which is the potential hub for solar energy has hindering factors, such as dust waves and water unavailability that could compromise the potential of these sites. In this study, emphasis was put on the design of a concentrating solar power, evaluating the performances of such project in the selected province situated in the south of Algeria.

1.3 Objectives

General objective

i. To design a CSP power plant and simulate the system under climatological conditions of the selected location in order to select the best option for the implementation of such projects.

Specific objectives:

The specific objectives of this study are to:

i. Review and comparison of concentrating solar power technologies.
ii. Design and simulate solar thermal power plant in Tamanrasset using System Advisor Model software.
iii. Analyze the costs of the designed solar thermal power plant in order to determine the levelized costs of electricity.

1.4 Study Justification

Due to the effect of global warming which leads to temperature increase on earth, the well-being of human race in the future cannot be clearly anticipated. In order to mitigate climate change, policies toward the pillars constituting sustainable development; energy security economic growth, environment protection and social responsibilities are compulsory to be concretized [10].

In the recent decades, energy with its important role (in energy security, reducing CO_2 emissions, enforcing employment etc.) is becoming the center of international debates. Renewable energies offer the most acceptable solution in hindering the over exploitation of fossil fuels. Algeria with its enormous potential of solar and its international commitment started reform process and regulatory incentives have been introduced to face effectively environments concerns.

According to Sonia (2012), population protested in Tamanrasset against repetitive power cuts which lasted for longer periods in summer when actually electricity was most needed for cooling systems [11]. Furthermore, many traders confirmed the loss of more than 50$ of goods after each power cuts which persist for more than 6 hours. In the other hand, the Electricity and Gas utility justified the power cuts due to the high demand of electricity and undersized high voltage transmission lines. However, the cost of upgrading transmission lines that connect existing power plant to cities situated deep in the desert is very high because of the long distances and climate constraints of Sahara. Consequently, implementation of decentralized CSP plant project in the affected location would render the best option to combat these challenges.

Finally, Predicting the performances of CSP power plants under the Sahara climate plays a key role in choosing the location for installation and also the technology for future investment in order to satisfy the needs of the population.

1.5 Scope of the study

The area under research in this study is Tamanrasset province situated in the Algerian Sahara. System advisor model will be used to simulate the selected configuration of parabolic trough power plant using the available weather data from Meteonorm. The performances of the selected technology under the specific climatological conditions thereafter be evaluated. The

assessment of dust effect on the mirrors can only be done with experiment on the ground. Therefore, apart from dust, the climate conditions of the selected region (wind, humidity, ambient temperature, solar irradiation, water availability) are taken into account. The study focused mainly on the performance of the solar field and the selected thermal energy storage technology. After the electricity generated from the power plant was evaluated, Costs of the power plant were approximated in order to determine the levelized cost of electricity generated from the selected configuration. Finally, the environmental impact of the power plant was assessed without taking into account the effect the power plant on the population of the province.

Chapter 2. LITERATURE REVIEW

Outline:

2.0 Introduction

In the following section, the potential of different renewable energies in Algeria especially solar energy is shown in detail. The location of the case study site with its geographical, social and infrastructures characteristics were highlighted. A brief history of concentrating solar energy, their types and their current status with a comparison in order to choose the best option was performed. Storage systems and heat transfer mediums were reviewed with a detailed information about concentrating solar power plant systems.

2.1 Renewable Energy Potential in Algeria

Algeria is endowed not only with hydrocarbons, but also with a huge potential diversity of renewable energy resources. Solar energy represents the most important source of renewable energies in the world, in addition to that, as shown in Figure 2.1 below, MENA (the region indicated by an arrow in solar potential) is where solar energy is mostly concentrated with a typical yield of 250 GWh/Km²/year and with the highest energy density of all renewable energy sources in Algeria. Wind, hydro, geothermal and biomass energy potential also exist but only with lower importance [12].

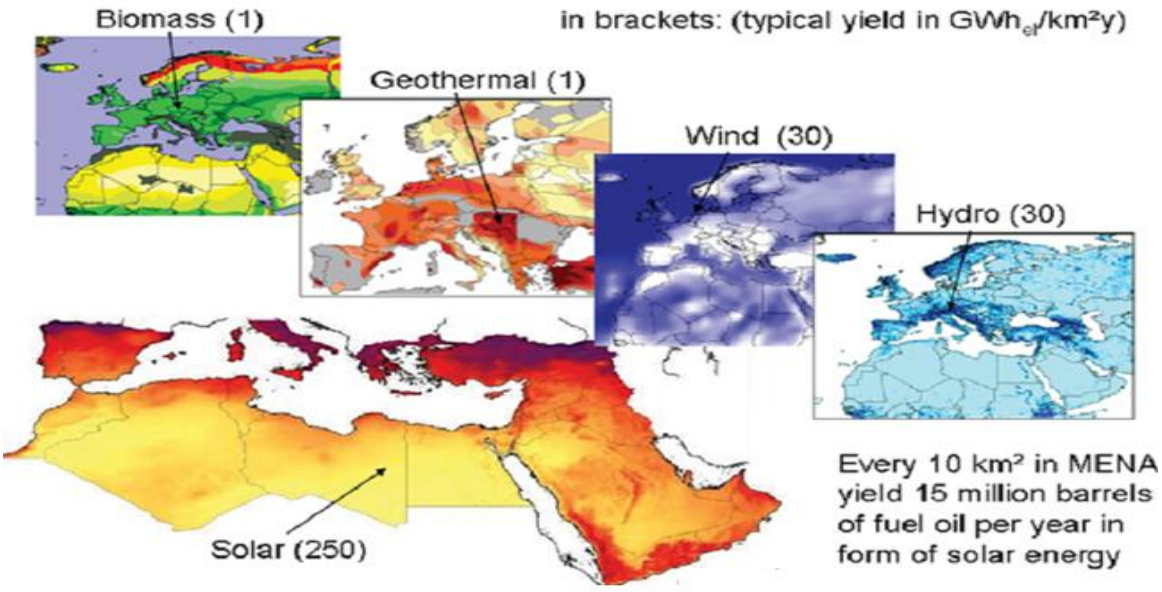

Source: (Schnatbaum L., 2009)

Figure 2.1: Typical electrical yield of renewable energies in MENA and western Europe

2.2 Solar Energy Potential in Algeria

Of the countries in the Northern African region, Algeria lies in a strategic position in the sun belt between the 38-35° of latitude north and 8-128° longitude east, with 2, 381,741 km² as the biggest country in Africa of which the Sahara takes 86% of the area of the country. The climate is transitional between maritime (north) and semi-arid to arid (middle and south) [13] .

According to satellite imaging done by the German aerospace agency (DLR) in an effort to measure the solar energy potential of Algeria, the country showed the biggest tract for concentrating solar thermal power in the Mediterranean basin with 1,787,000 km² [13].

Due to the different climate conditions in Algeria, the solar potential varies from one location to another. Table 2.1 below shows the different important parameters related to solar energy of different regions constituting the country. The mean yearly sunshine duration is 2,650 hours in the coastal areas and 3,500 hours in the southern part. The Sahara region has daily sunshine duration of 8 hours and can exceed 11 hours during summer, solar resource in the area is available throughout the year [14].

The solar irradiation received over the Algerian territory exceeds an average of 4.5 kWh/m² per day in the north, whereas in the south it reaches 7.26 kWh/m² on average. Calculations on yearly basis deduce that the potential in the Sahara (more than 80% of the area) is around 2,650 kWh/m² [14].

Table 2.1: Regional daily solar energy and sunshine duration in Algeria

Region	Coastal line	Highland	Sahara
Area (Km²)	95,271	238,174	2,048,296
Mean daily sunshine duration (h)	7.26	8.22	9.59
Solar daily energy density (kWh/m²)	4.66	5.21	7.26
Potential daily energy (10^{12} Wh)	443.96	1240.89	14,870.63

Source: (Boudries R. et al., 2012)

Figure 2.2 below shows the potential of solar energy in Algeria mapped by Center of Development of Renewable Energies (CDER) which demonstrates Algeria as one of the countries

with the highest solar potential in the world. The solar energy potential for power generation is enormous compared to regional and global energy demands—roughly 10% of the Algerian Sahara Desert could meet the European demand [4].

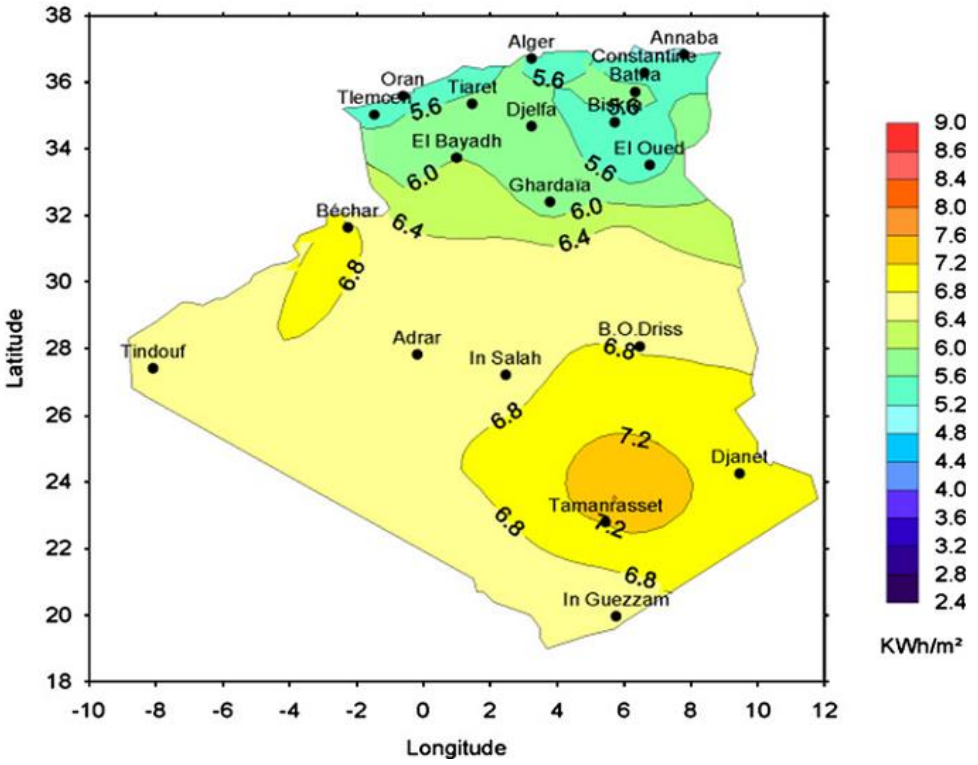

Source: (Boudghene S. et al., 2012)

Figure 2.2: Overall daily exposure received in (kWh/m^2)

2.3 Case study

The selected province for the implementation of the power plant is Tamanrasset. It is situated deep in south at a latitude of 22°.47, longitude 5°31 E and an altitude of 1,377 m above the sea level. With a surface area of 619,360 km² Tamanrasset is the biggest province in Algeria with a population of 205,220 inhabitants. The location experiences hot and long summer seasons, where the average temperature during the day is 30°C exceeding 38°C in some days between the period of June to September, the average annual rainfall is 43 mm, thus, the weather is extremely dry during the whole year. The topography of the site is flat surrounded by some massif desert mountains. The city is endowed with the biggest solar potential in the country with a direct normal irradiation exceeding 2,800 kWh/m^2/year and an average of daily irradiation of 7.7 kWh/m^2, it is important to note that most of the concentrating solar power plants in the world are installed in areas where the yearly average DNI does not reach 5.9 kWh/m^2 [15] [16] .

Source: (Algerie-monde, 2010)

Figure 2.3: Wilaya of Tamanrasset

The city is connected to the main grid with 1,584 km of transmission lines. The main grid is covering almost 90% of the population, communities in remote area far from the city use stand-alone photovoltaic installations. The connection to natural gas line is at 11%, restricted only to Ain Salah, a town in the north of the province situated at about 665 km from Tamanrasset Wilaya [15].

2.4 Climate Condition

2.4.1 Water availability

Algeria's Saharan regions are characterized by mostly flat, unproductive desert land and insufficient underground water resources which is mainly saline water. Mamdouh Shahin (2009) noted that three basins exist under the Algerian desert as shown in Figure 2.4 below.

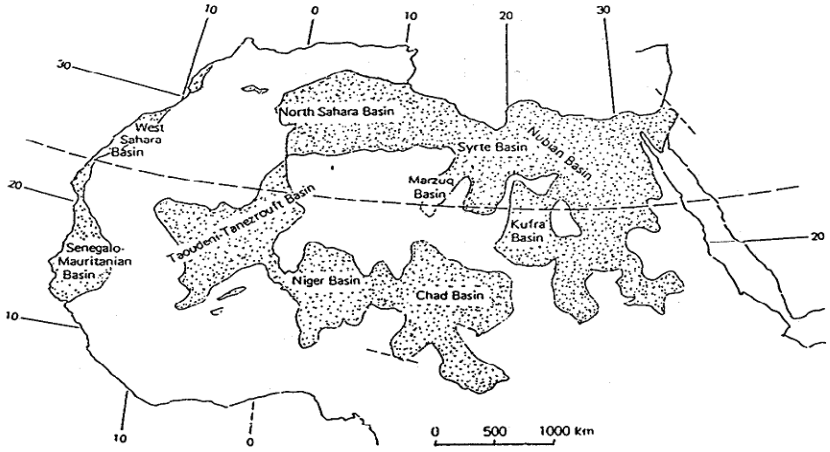

Source: (Shahin M., 2009)

Figure 2.4: Map showing groundwater basins in North Africa

Under the same perspective of assessing the water resources in Algeria Taqiy eddine Boukelia, (2012) noted that the current concentrating solar thermal systems need water, first and called it a primary need is for cooling the power cycle and renewing the heat transfer fluid when the system uses steam for electricity generation. The remaining needs are for maintaining the solar field, where water is used for cleaning mirrors from aerosol deposit and other impurities.

The use of water in CSP plants range between 3 to 3.5 m^3/kWh. For the most recent used technologies, 95% of water is used in the cooling system while the remaining 5% is for washing the mirrors and regeneration of the heat transfer fluid used [9].

2.4.2 Wind resource

According to Honghang Sun (2014), wind with its major concern in affecting the mirrors in solar thermal power plants need to be determined. For instance, the cost of the mirrors

constitutes a big share from the total investment costs that can even exceed sometimes 30%. On the other hand, wind loads can seriously distort the mirrors shape and cause losses of efficiency. Moreover, when the wind speed is too high, the mirrors are turned into stow position to avoid any damage that could affect the strength of the structures. All those effect show that wind should be taken into consideration during any feasibility study concerning concentration solar power plant [17].

Farouk Chellali (2010), found out that Algeria has a moderate wind speed especially in the northern part, however, the southwestern part (Sahara) is perceived to have an important wind load reaching 6 m/s. The two reasons why the southwestern region own that significant wind load is because of:

- Location of the region in an area of pressure difference.
- The near distance between the region and the Atlantic Ocean which causes high weather disturbances intensity.

The following map in Figure 2.5 shows the wind distribution throughout the country.

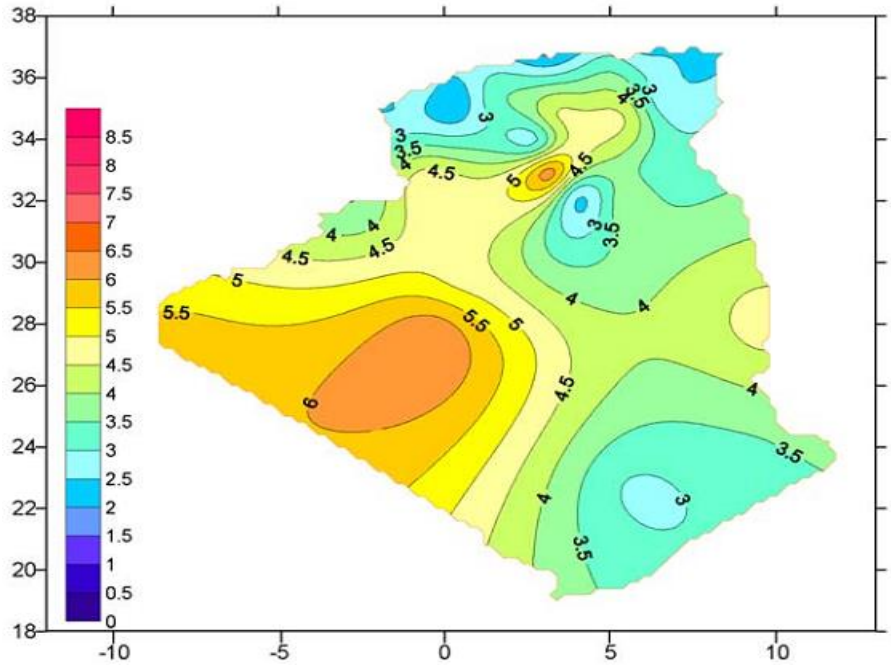

Source : (Chellali F. et al., 2010)

Figure 2.5 Annual maps of wind speed in Algeria at 10 m high

The output of any concentrating solar power system is highly related to the availability of solar irradiance and spectral content. However, another environmental factor apart from wind speed and water availability mentioned previously can affect the performance of the systems in such desert climate like dust [18].

2.4.3 Dust

North Africa is widely recognized as the biggest source of dust in the world [19]. According to Travis Sarver (2013), over the last 70 years of solar research, many studies have shown the negative effect of dust on the performance of the reflecting and absorbing devices of solar systems. In addition to that, the effect of dust on mirrors is more important than in photovoltaic panels because scattered irradiation can still be absorbed by light trapping devices to produce energy in PV technology. However, the formation of a dust layer on parabolic mirrors, Fresnel lenses or heliostats hinders the direct normal irradiation to reach reflective surfaces. Unfortunately, the locations that have the highest direct beam solar irradiation are in the desert, where the dust concentration is as well high [18].

Previous studies on the effect of dust on the performance of solar system devices have shown different results depending on the locations around the world. In the beginning, studies were conducted in USA specifically in Boston, Massachusetts, over three months of experiment on a glass plate with a tilt angle of 30°, Hottel and Woertz evaluated the losses of incident irradiation and found them to be around 1%, and 4.7% of degradation as a maximum during that period. After the solar technologies spread out in other parts of the world, other studies came up. Comparing the performances of a selected technology of PV modules in different regions, Kazmerski et al. (2010), found out that the dust effect is more important in other regions (North Africa, Middle East and Asia) than the one founded in USA. For example, the effect caused in few hours by dust in some places was the same for many months in other places [18]. Therefore, mitigating dust deposit on the CSP mirrors and assessing its effect according to time are of a great importance to finally find out the way of maximizing the efficiency of solar systems [20].

2.5 Concentrating Solar Thermal

2.5.1 Brief History

The discovery of the concentrating solar irradiation concept was introduced by Archimedes in 212 BC in order to push the fleet of Romans from the coast of Syracuse [21]. Early in the second century BC, Diocles the Greek mathematician described the optical characteristics of parabolic trough mirrors. In 1746 the French naturalist Comte de Buffon described the improvement in the design of heliostats after which Augustin Mouchot presented a dish driven steam engine at the universal exhibition in Paris in 1878 [22].

Source: (Cosman T., 2010)

Figure 2.6: Parabolic trough driven pumping system

Figure 2.6 above presents the first parabolic trough field used for pumping water for irrigation, the system was concretized by Frank Schuman in 1913. Furthermore, within the twentieth century many other prototypes and experiments were done with the aim of developing the concentrating solar technologies. However, due to the eminent development of internal combustion engines and low prices of fossil fuels, the interest in concentrating solar energy technologies development and renewables in general was lost [23].

In the 1980s, the revolution in concentrating solar power began in USA specifically in California with the shifting from prototypes and experiments to industrial level. With governmental incentives regarding taxes and mandatory long-term power purchase contract, nine power plant based electricity generation were constructed in USA with an installed capacity of 354

MW. The technology that was used is concentrating parabolic trough using oil as heat transfer fluid and steam turbine in the power block for electricity generation. Running over 20 years, the nine implemented power plants have shown success and their maturity as renewable energy technology. In addition to that, having the climate change and its harmful impact on the environment in the center of international debates led to having parabolic trough technology (PTT) with its asset of being able to reduce the greenhouse emissions spreading out through many other countries situated in the sunbelt for example Spain, Morocco, Algeria and etc. [22].

2.5.2 Concentrating solar technologies

In order to use sunlight to reach high temperatures, concentrating solar power technologies are deployed to operate on only the direct normal irradiation [24]. CSP power plants with their several types are constituted of three main parts as shown in the Figure 2.7 below. First, the sun irradiation is concentrated on the solar receivers using means of collector systems, after which the radiation energy is converted into thermal energy in the receiver using heat transfer fluids (HTF). Carrying high temperature HTF, solar receivers drive the fluid to the power block where the thermal energy is converted to mechanical energy as a first step, the last step being transforming the later into electrical energy and fed to the grid [25].

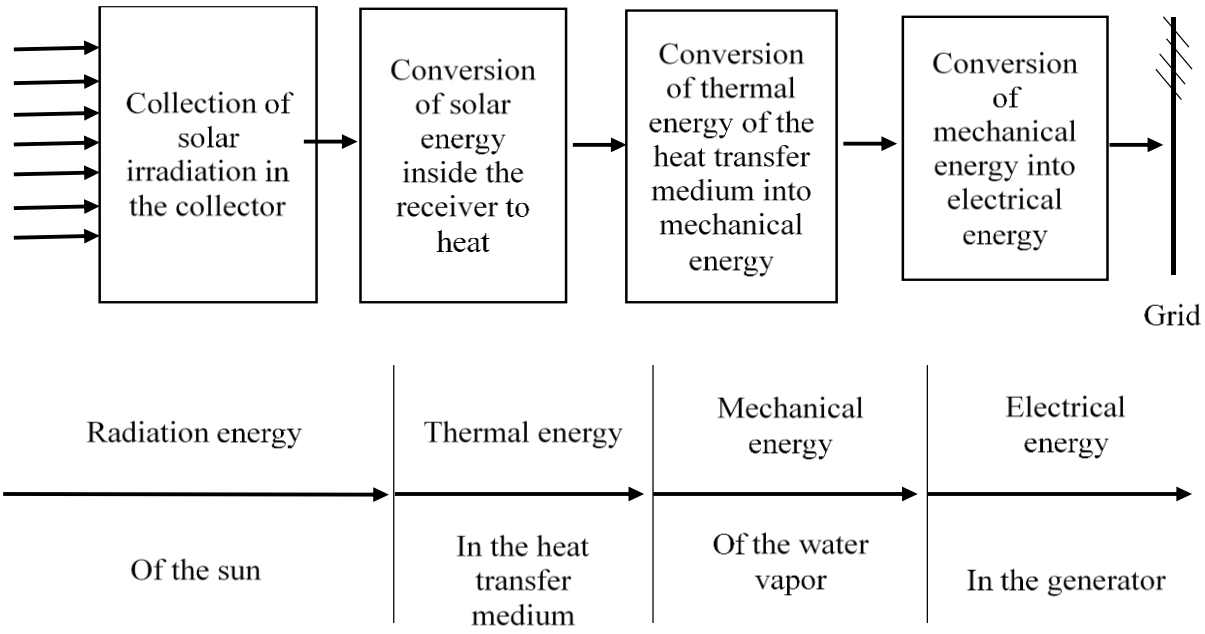

Source: (Kaltschmitt M. et al., 2007)

Figure 2.7: Energy conversion chain of STC generation

This section gives a brief description of the different concentrating solar power technologies. Four main CSP technologies exist under two subsystems; line focus and point focus. According to Lovegrove K. (2012), the current possible systems that can be designed and implemented are:

- Parabolic trough.
- Linear Fresnel.

} Line focus

- Central receiver tower.
- Parabolic dishes.

} Point focus

2.5.3 Central receiver tower

Tower solar power plant is composed of several heliostats called also mirrors that reflect the direct irradiation onto a central receivers situated at the top of the tower. Energy in form of concentrated photons is converted in the receiver to heat through a selected medium which can be water, molten salt, liquid sodium or air. Generated steam from the thermal bloc run through the turbine that converts the thermal energy to mechanical energy, whereas the generator covert the latter to electricity [26].

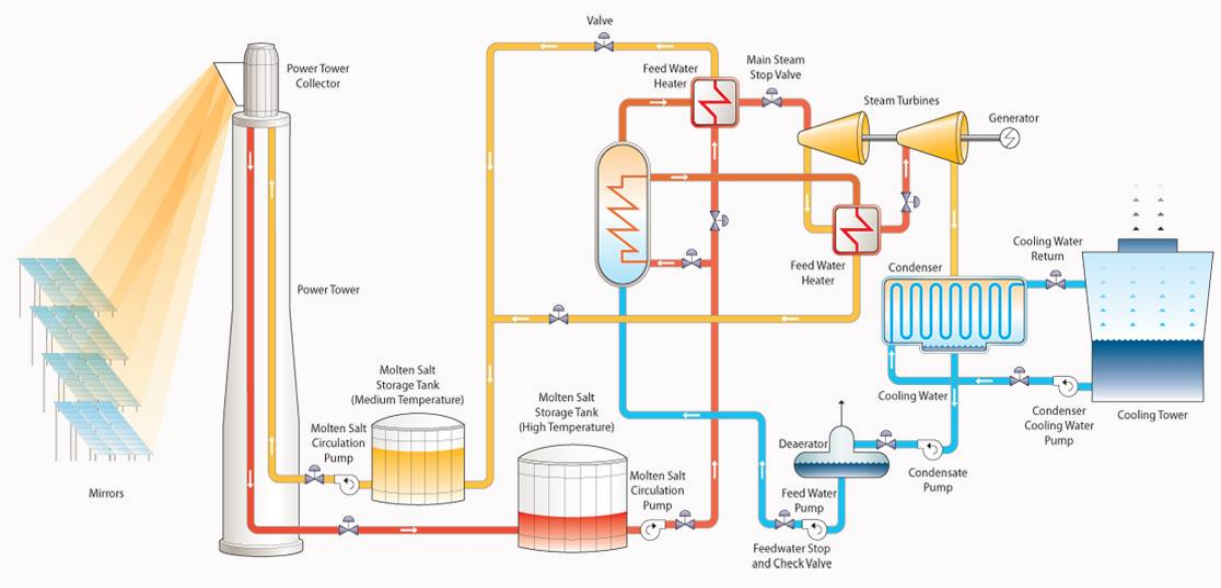

Source: (Pavlovich T. et al., 2012)

Figure 2.8: Power tower process diagram

Exhausted steam from the turbine is collected by the condenser, the condensate thereafter is pumped into the receiver where it is again heated by the solar received, and the cycle is repeated as shown in figure 2.8 above [26].

The technology has been proven in USA under a successful project Solar One whose operation lasted for 6 years from 1982 to 1988, in that time the plant was the biggest in the world and its installed capacity was 10 MW in high irradiation days in summer. The performance of the tower plants depends highly on the medium used, in the beginning water was the main HTF. However, most of the recent power plants use molten nitrate salt that is not flammable, non-toxic, and is better as a storage of heat than water. Solar power towers can operate when combined with conventional fossil-fired plants such as the natural gas combined-cycle and coal-fired or oil-fired Rankine plants. In hybrid plants solar energy can be used to reduce the use of fossil fuel or to increase the power input to the steam turbine [26].

2.5.3.1 Heliostats

One of the key components in solar tower power plants is the mirrors, since they account for more than 50% of the total cost of investment. Basically one heliostat is composed of several mirrors, frame, support pedestal, tracking system, foundations and power box Figure 2.9. Generally, many configurations may be applied in the selection of the materials. However, in the front polymer type, the surface is laminated with a silvered polymer reflector, separated from the rear membrane with a vacuum pressure that help in adjusting the length of the focal point [27].

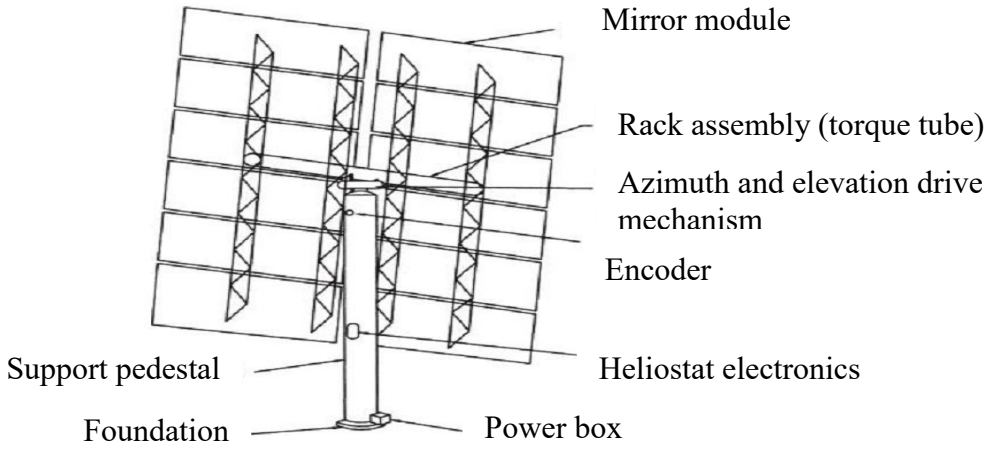

Source: (Goswami D., 2012)

Figure 2.9: Heliostat structure

2.5.3.2 Receiver

Also called power tower collector, the receiver role is to absorb the maximum solar irradiation in order to deliver it to the heat transfer fluid at high temperature. Receivers are classified into two types; direct and indirect receivers, it is called indirect when the heat transfer fluid is passing through set of tubes that are absorbing sun irradiation. However, the direct configuration allows the fluid to receive irradiation directly from the heliostats [27].

Figure 2.10 below shows the different types of tower receivers depending on how the heat transfer fluid absorbs energy coming from the sun.

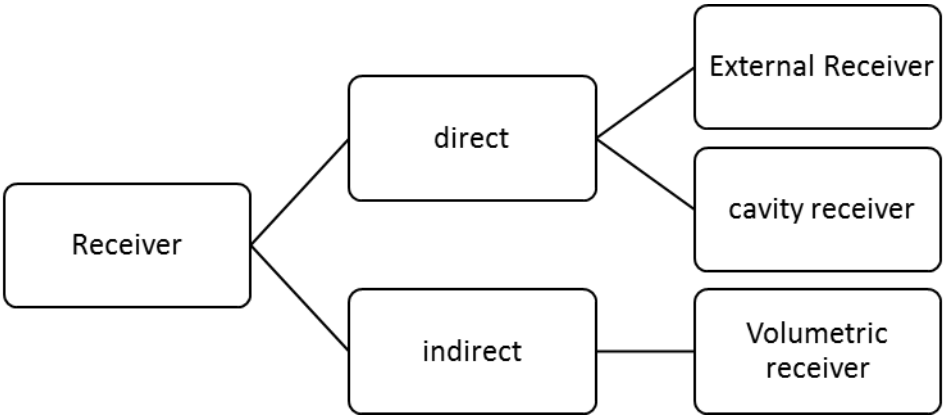

Figure 2.10: Type of receivers

Remark: Apart from parabolic dish system, parabolic trough, lineair fresnel and central tower have the same configuration for the thermal power cycle.Therfore, the power cycle is discussed separately in section (2.5.15)

2.5.4 Parabolic dish system

Dish concentrating solar power systems belong to point focus technologies, the systems are composed of parabolic mirrors in form of dishes, tracking systems and most of the time Stirling engine are coupled with a generator for electricity production as shown in Figure 2.11 below. Because of the two axes tracking system which makes the installation all the time directed towards the sun, the cosine losses that exist in all other configuration systems are avoided. The technology offers the highest efficiency (in CSP technologies) reaching 30% in converting solar irradiation into electricity [24].

Once the solar irradiation is reflected onto the receiver, the phase change working fluid (e.g. sodium) flowing in the receiving pipes is heated. The latent evaporation heat is transferred from the radiated absorber surface to the engine heater tubes and from there to the heat transfert fluid of the Stirling motor. The performance of the stirling engine depends highly on the type of the gas used, most of stirling systems use hydrogene or hylium between 600 and 800°C as working gas temperatures [25].

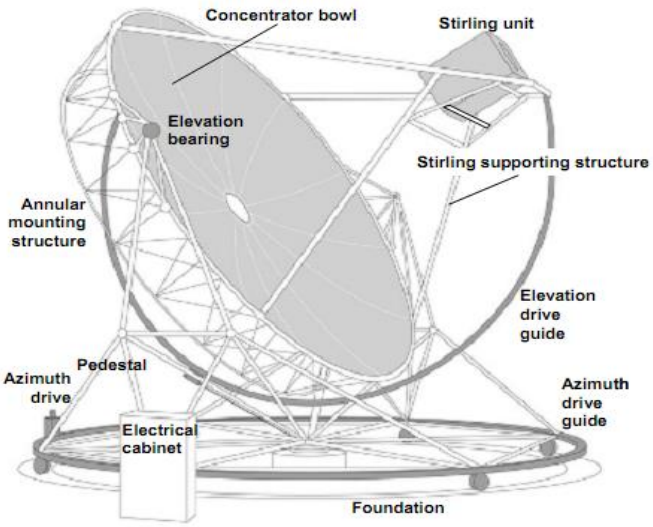

Source: (Kaltschmitt M et al., 20007)

Figure 2.11: Dish/Stirling systems

Figure 2.12 present the thermodynamic cycle of stirling engine, it is composed from two isothermal and isochoric processes. the selected gas is compressed at constant temperature from point 1 to 2, the process is achieved by a heat rejection. The fluid is then heated at constant volume from state 2 to 3 by suplyin heat to the process, after that the gas expands at constant temperature by heat addition at the highes temperature. Finally, the gas is cooled accompanied by heat rejection from state 4 to 1 [27].

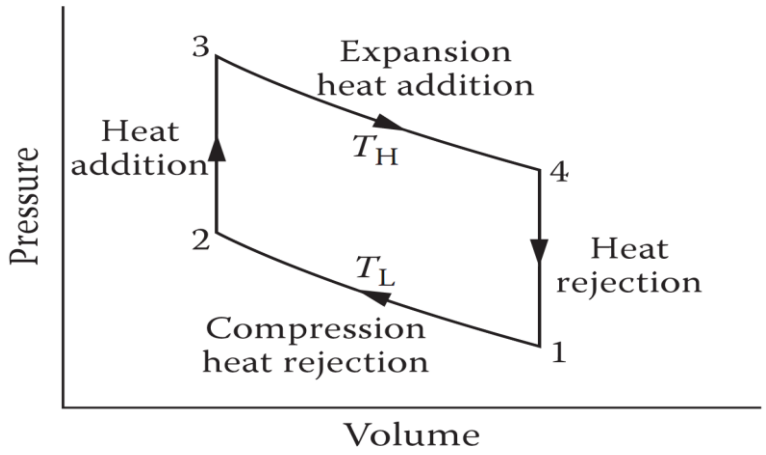

Source: (Goswami D., 2012)

Figure 2.12: P-V diagram of Stirling engine

2.5.5 Linear Fresnel systems

Concentrating solar thermal power plants using Fresnel reflectors belong to line focus technologies. They are composed of flat mirrors that reflect sun irradiation towards a fixed cylindrical collector that contains the HTF fluid. Using only one axis tracking system, Fresnel mirrors follow the trajectory of the sun during the day time. After absorbing sun irradiation, the HTF with its high temperature run through the power bloc in order to generate electricity [26].

Firstly, when the Fresnel thermal plants were designed, the purpose targeted was low to medium temperatures applications for example, heat generation for commercial or residential demand, and water treatment. the current status of the technology surpassed the first level, and now are more often designed for high temperature application large scale heat generation electricity supply [28].

Figure 2.13 shows the design of linear Fresnel arrangement including one array of flat mirrors concentrating solar irradiation onto a fixed receiver. Comparing to parabolic trough technology linear Fresnel technology has lower thermal and optical efficiency due to the nature of the configuration where the reflector body is moving and the receiver is fixed. In addition to that, with one axis tracking system Fresnel technology has the highest cosine losses among all concentrating solar technologies [28].

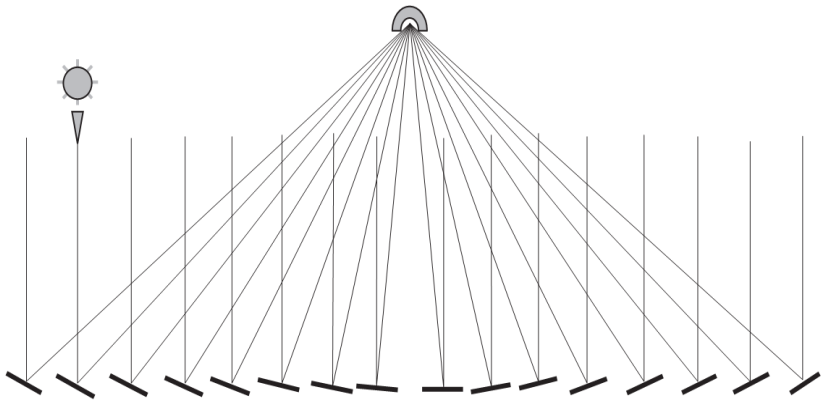

Source: (Guangdong Z. et al., 2013)

Figure 2.13: Basic linear Fresnel reflector configuration

According to Guangdong Z. et al. (2013), lots of efforts were done concerning the design of the receiver to increase the thermal and optical performances of the collector. Many configurations are possible when designing receivers, Figure 2.14 shows trapezoidal cavity receivers arrangement developed by Areva Solar where instead of only one absorber pipe the receiver has a multitude of absorber tubes allowing the increase of absorbing surface and also the collector intercept factor. The sidewalls are insulated to avoid thermal losses. However, in Fresnel technology most of the time the receivers are not evacuated because of the low working temperatures, thermal losses coefficient is considered to be highly significant when temperatures go beyond 400°C [28].

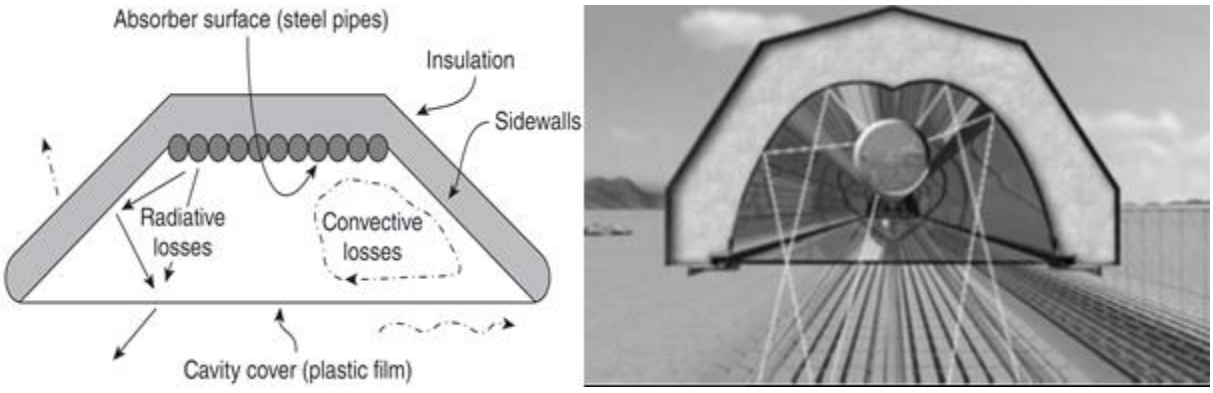

Source: (Guangdong Z. et al., 2013)

Figure 2.14: Linear Fresnel receiver

2.5.6 Parabolic trough power plant

Apart from the sun irradiation collector system, parabolic trough power plant does not differ from central receiver tower or linear Fresnel plants. Parabolic trough collectors are linear focus technology that operate in the temperature range of 150-400°C. In order to develop the technology present research aims to reach 500°C by increasing the collector, receiver and working fluid performances. Commonly, parabolic trough collectors use only one axis tracking system to maximize the received irradiation. Once the sun irradiation hits the parabolic mirrors, the concentrated irradiation is absorbed in form of heat by the selected medium in the receiver pipe. The main working fluid in parabolic trough technology is thermal oil. However, the use of water directly in the system is under investigation because of the high pressure that water can generate inside the pipes [29].

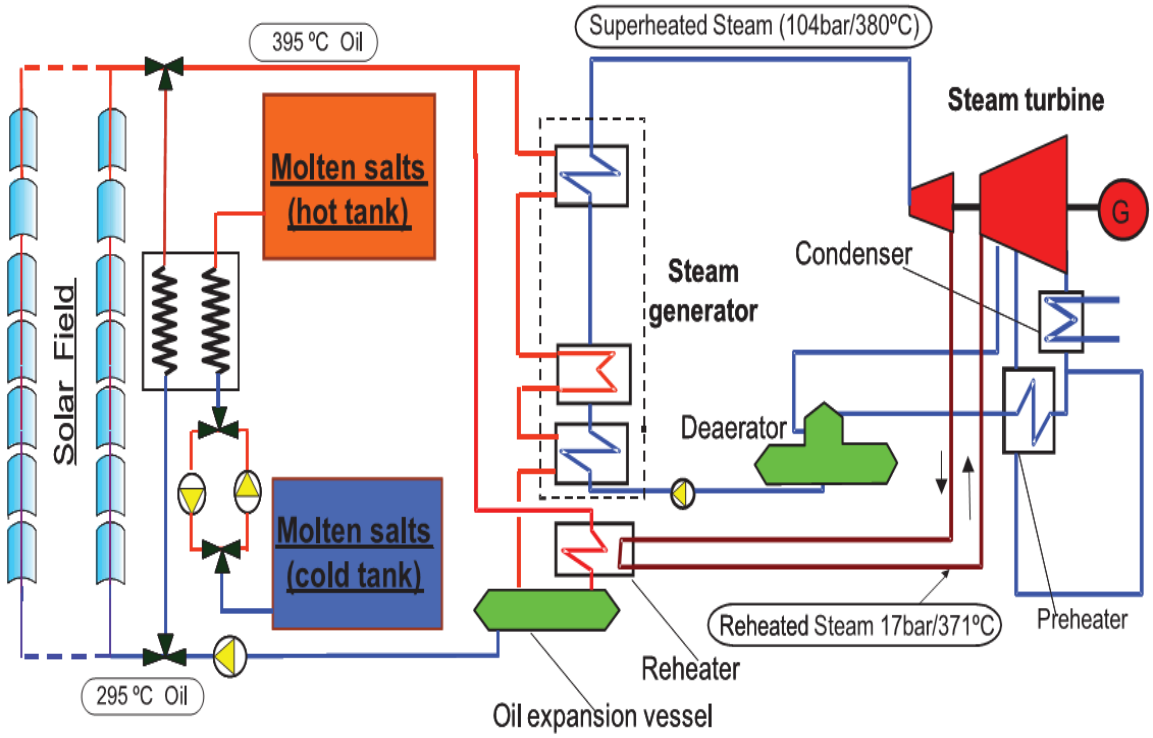

Source: (Manuel R., 2014)

Figure 2.15: Parabolic-trough plant introducing a molten-salt circuit with two storage tanks to increment capacity factor

Under parabolic trough technology two main configurations are possible; direct steam generation (use of water directly in the receivers) and indirect steam generation shown in Figure 2.15 above (use of oil in the receiver and a heat exchanger to heat the water in the power block).

However, other designs also exist for example, hybrid configurations where there is a combination of the two previous systems, also integrated solar combined cycle in which a gas turbine is added to the system instead of using backup [30] [29].

2.5.6.1 Parabolic trough collectors (PTC)

PTC are parabolic devices that concentrate solar irradiation onto an absorber pipe located in the focal line. The choice of manufacturing materials depends mainly on the manufacturer, for example there are mirrors that contain a thin layer of silver layer and low-iron float glass, other designs also exist under specific manufacturer characteristics. By increasing the quality of the mirrors where the reflectivity can reach 98%, the amount of concentrated irradiation hitting the absorber is high, therefore the overall performance of the system is high [31]. The concentration ratio is an important parameter that determine the concentration of solar irradiation, two ways are possible to define the concentration ratio.

- The first definition of concentration ratio C is the ratio of the aperture surface A_{ap} to the absorber surface A_{abs}.

$$C = \frac{A_{ap}}{A_{abs}} = \frac{W * l}{\pi * d_0 * l} = \frac{W}{\pi * d_0} \quad (1)$$

- The second definition of concentration ratio is the ratio of the radiation flux density G_{ap} at the aperture level and the corresponding value G_{abs} of the absorber.

$$C = C_{flux} = \frac{G_{ap}}{G_{abs}} \quad (2)$$

Where: d_0 is the outer diameter of the receiver steel pipe, l is collector length and W is the parabola width.

Acceptance angle, β is the second important parameter for parabolic trough systems. It is the maximum angle that can be formed between two rays on a plane transversal to the collector aperture in such a way that, when they are reflected by the parabolic mirrors, they intercept at the absorber pipe. The wider the collector acceptance angle β is, the less the sun tracking system accuracy necessity becomes, since the collector will not need to update its position as frequently.

Small acceptance angles are associated with high concentration ratios, which require the installation of very accurate solar tracking systems and consequently, higher costs [22]. The two previous parameters are presented in the Figure 2.16 below.

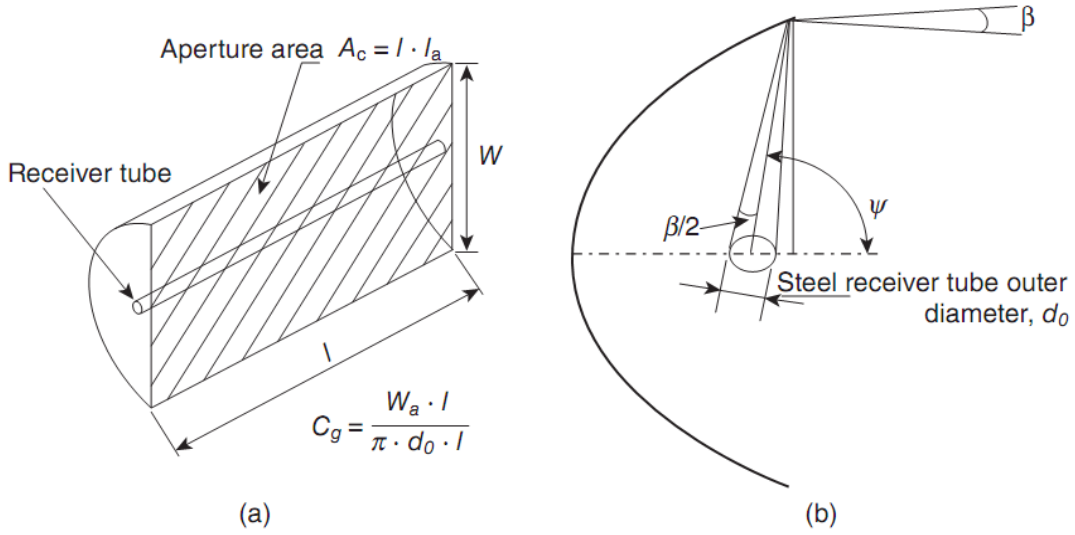

Source: (Lovegrov K. et al., 2012)

Figure 2.16: (a) Geometric concentration ratio, Cg and (b) acceptance angle, β and aperture

Parabolic trough receivers can be classified under two categories; evacuated and non-evacuated receivers. Figure 2.17 shows a typical evacuated parabolic trough receiver composed from two concentric tubes, this configuration of receivers is commonly used for electricity generation applications where the temperatures of the heat transfer fluid are above 300°C, the vacuum existing between the concentric pipes plays an important role in avoiding thermal losses with the surrounding [32].

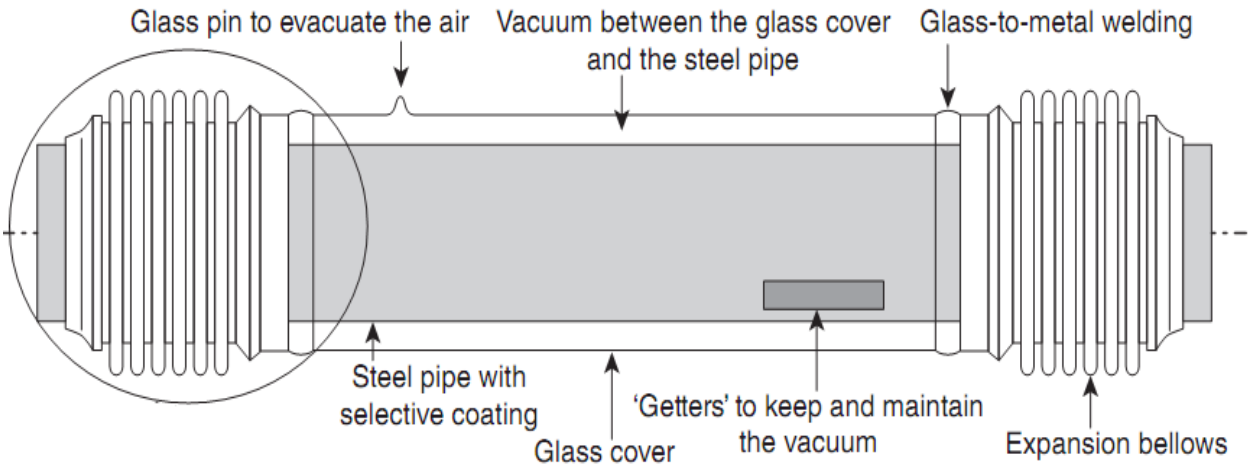

Source: (Zarza E. et al., 2012)

Figure 2.17: Typical parabolic trough receiver

2.5.7 Technology Comparison

Table 2.2 below presents a brief summary of technical and economical performances of the previous presented concentrating solar technologies [33] [34].

Table 2.2: Summary of the solar thermal technologies

	Parabolic troughs		***Central receiver***		***Dish/engine***		***Fresnel***	
Technique	line focus		Point focus		Point focus		line focus	
Power unit	30–140 MW		10–100 MW		5–25 kW			
Temperature operation	390°C		565°C		750°C		300°C	
Annual capacity factor	23%–50%		20%–77%		25%		22%-24%	
Peak efficiency	23–27%		20–27%		29.4–31.25%		18–22%	
Net annual efficiency	15–16%		15–17%		26%		8–10%	
Commercial status	Mature		Early projects		Prototypes		Prototypes	
Technology risk	Low		Medium		High		medium	
Thermal storage	Yes		Yes		Batteries		yes	
Hybrid schemes	Yes		Yes		Yes		Not proven	
Tracking system	1-Axis		2-Axis		2-Axis		1-Axis	
Application	grid-connected plants, industrial heat process		grid-connected large scale plants		Limited to small load applications		grid-connected plants, industrial heat process	
First commercial plant	SEGS I has generated 14 MWe since 1984		PS10 has generated 10 MWe since 2007		Tooele Army Depot plant (under construction)		Stanwell generated 14 MWe since 2000	
Cost/kWh with storage	19 DA/kWh		24 DA/kWh		-		24 DA/kWh	
	Num	MW	Num	MW	Num	MW	Num	MW
Current projects and total capacity	62	2751.41	8	64.42	0	0	6	59.65
Under construction plants	20	2122	4	602	0	0	0	0
Under development plants	4	400	5	1000	0	0	0	0

According to Dhyia (2015), parabolic trough technology is a full mature technology in both aspects: technical and commercial. Furthermore, the technology is also able to incorporate other sources of energy whether it is conventional resource or thermal storage. Currently among the four concentrating solar energy technologies, the lowest cost of energy is generated from parabolic trough technology using thermal energy storage with 19 DA/kWh. Nowadays, the most utilized technology with more than 95% commercial implemented project is parabolic trough technology, it accounts for 62 operational plants with a total installed capacity of 2,751.41 MWe. Other projects are also under the construction phase with almost the same installed capacity of current operating plants. However, the capacity is generated from 20 projects only, which shows clearly that all projects are directed to commercial purposes with the aim of reducing the levelized cost of electricity to make it more competitive with conventional projects [34].

Having a peak efficiency of about 20%, Linear Fresnel technology has the lowest efficiency in all concentrating solar energy technologies, thus it is considered as a technology under experimental phase. In the other hand, Linear Fresnel use less land that all remaining CSP technologies which allows its implementation in urban areas. The technology can also be integrated with conventional energy resources specially when the area is limited Fresnel technology constitutes the best option. With 6 operational projects having an installed capacity of 59.65 MWe Linear Fresnel technology own less than 2.1% of the total CSP installed capacity share. Currently only 5 projects are under construction with an installed capacity of 166 MWe. Hence, the projects are in form of experimental prototypes aiming to investigate more in the technology [34].

Power tower is a recent technology comparing to parabolic trough. However, since the successful project PS10 implemented in 2007 the technology was introduced in the commercial market as a proven technology. The cost of electricity generated from such technology is highly related to the installed capacity, large scale power plants with thermal energy storage offer the lowest LEC of 24 DA/kWh. However, due to the layout of heliostats, the technology has the highest land use requirement, thus preferable in places with abundant land space. Hybrid configurations are also possible with conventional energy resources or thermal storage, and offer the lowest LEC of the technology. At the moment, 8 operational projects with generating capacity 64.42 MWe which represents 2.24% of the total installed capacity from CSP technologies. On the

other hand, concerning projects under construction the technology has a share of 20% aiming to make it more competitive with parabolic trough technology which is leading in the economical perspective as shown in the Table 2.2 above [34].

Endowed with a high efficiency, solar dish technology constitutes the best choice for individual use or when grouped for small scale projects. The technology has no water consumption which is ideal for location where the water is only directed for population and agricultural use. However, because of the high cost of the electricity coming from the technology, its introduction to the market is difficult, thus only one plant is under construction in USA with and installed capacity of 1.5 MWe which represents 0.052% of the total generating capacity of under-construction CSP projects [34].

Finally, parabolic trough technology has shown its dominance over 28 years of commercial operation with the ability of generating electricity whether as a stand-alone or in hybrid systems at the lowest levelized cost of electricity and lower technical and economic risks for the investors. However, with more than 60% of projects under development phase, solar tower technology is also merging up as a future competitor in the field of solar concentrating power generation [34].

2.5.8 Solar energy notions

This section presents some solar energy details that define the portion of solar irradiation reaching surfaces.

Solar irradiation is the summation of the diffuse irradiation and beam irradiation, however, in concentrating solar receivers, only the beam irradiation is useful, also called direct solar irradiation. Beam irradiation is the energy received from the sun without having been scattered in the atmosphere [35].

In order to determine the direct solar irradiation absorbed by the receiver tubes, the position of the sun relative to the receiver should be determined [36].

$$Q_{abs} = DNI * \cos\theta * IAM * R_s * End\ losses * \eta_{field} * \eta_{HCE} * A_{ref} \qquad (3)$$

Q_{abs} = solar radiation absorbed by the receiver tubes

θ = angle of incidence

IAM = incidence angle modifier

R_s = Row Shadow

End Loss = performance factor that accounts for losses from ends of HCEs

η_{fiels} = field efficiency that accounts for losses due to mirror optics and imperfections

η_{HCE} = HCE efficiency that accounts for losses due to HCE optics and imperfections

A_{ref} = reflective area

Different angles are used to describe the position of the sun according the selected location and time. The following part defines the most important parameters used to the calculation of the sun position [35].

The incidence angle (θ): is the angle between the beam radiation on the collector and the normal to the collector.

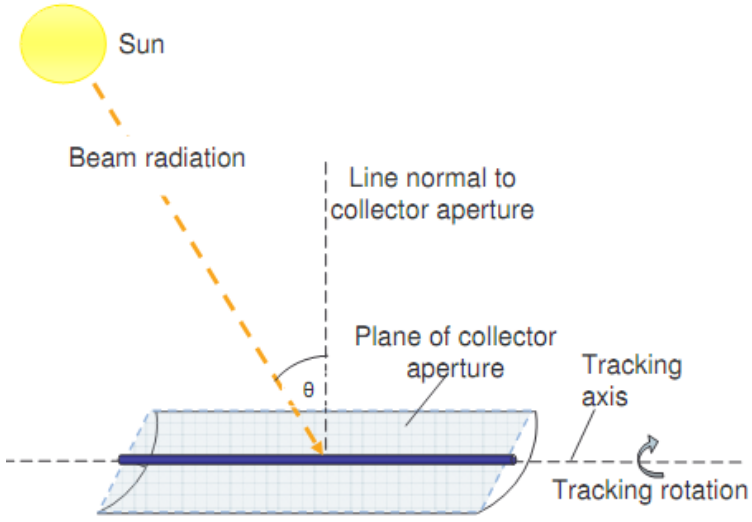

Source: (Patnode A., 2013)

Figure 2.18: Angle of incidence on a parabolic trough collector

Figure 2.18 above shows that the incidence angle varies during the day depending on the sun position and the collector orientation

In order to determine the position of the sun during the year, other angles such as the declination angle δ, this angle represents the angular location of the sun at solar noon, with respect to the plane of the equator should be determined.

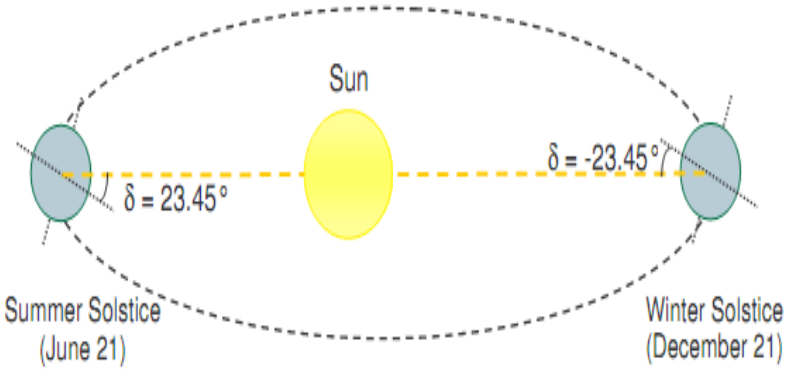

Source: (Patnode A., 2013)

Figure 2.19: Declination angle variation

Figure 2.19 above shows the rotation of the earth around the sun throughout the year, which makes the declination angle varying within a range of $-23.45° \leq \delta \leq 23.45°$ [35].

The declination angle is given by:

$$\delta = 23.45 \sin\left(360 * \frac{284 + n}{365}\right) \quad (4)$$

Where: n is the day number of the year.

The position of the Sun is also dependent on the hour angle, that represents the angle between the local meridian and the plane containing the center of the Sun. The hour angle is zero when the Sun is in the line with the local meridian. This angle comes as a result of the rotation of the Earth, which spins on its axis at a rate of 15º per hour, and is given by [35]:

$$\omega(degree) = 15 * (t_s - 12) \quad (5)$$

t_s: solar time in hours.

To determine the solar time, it is necessary to adjust the local time (LCT) with the following relation:

$$t_s = LCT - DST + \frac{L_{st} - L_{loc}}{15} + E(\frac{1h}{60min}) \quad (6)$$

DST: Daylight savings time adjustment

L_{st}: standard meridian for the local time zone

L_{loc}: the local meridian of the collector site

E: equation of time

The equation of time defines the perturbations that occur during the earth rotation which affect the time the sun crosses the observer's meridian:

$$E = 229.18(0.000075 + 0.001868\cos(B) - 0.032077\sin B - 0.014615\cos(2B) - 0.04089\sin(2B)) \quad (7)$$

With, $B = \frac{360}{365}(n-1)$

For the calculation of the incidence angle θ, the only remaining angle is the azimuth angle θ_z. given by:

$$\cos\theta_z = \cos\delta * \cos\varphi * \cos\omega + \sin\varphi * \sin\delta \quad (8)$$

φ: Latitude of the location

Therfore, the incidence angle for a plane rotated about a horizontal north-south axis with continuous east-west tracking to minimize the angle of incidence is given by [35]:

$$\cos\theta = \sqrt{\cos^2\theta_z + \cos^2\delta\sin^2\omega} \quad (9)$$

2.5.9 Solar field size and layout

A typical Parabolic trough plant is composed of several parallel rows of multiple parabolic trough collectors connected in series. The temperature of the medium increases while passing through the inlet to the outlet of each row as shown in Figure 2.20 below [37].

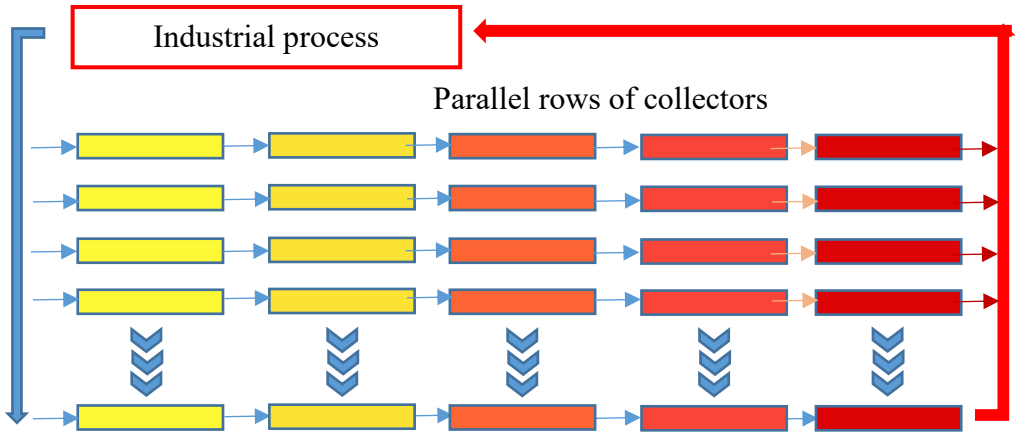

Source: (Goswami D. et al., 2016)

Figure 2.20: Typical solar field with parabolic trough collectors

Several parameters are used in order to design the solar field for a given power plant. The first step from the design is to define the "design point" that determine the performance of the solar field. Below are the parameters taken into account while defining the design point [37]:

- Collector orientation
- Date and time of design point
- DNI and surrounding temperature for the selected location and time
- Geographical location
- Thermal needed from the solar field
- Solar collector soiling factor
- Selected medium
- Fluid inlet and outlet temperature
- Nominal fluid flow rate

The step that follows the definition of the designed point is the determination of the number of rows and collectors that should be connected in series. In order to calculate the two previous

parameters, characteristics of the selected PTC (peak optical efficiency, incidence angle modifier, heat loss coefficient, and aperture area) and working fluid (density, heat capacity, and dynamic viscosity) should be known. If the heat transfer fluid that passes through the steam generator is the same used in solar field, the field outlet temperature approximation should exceed the required temperature in the generator by 15°. This difference is used to compensate the thermal losses between the outlet of the solar field and the boiler, and also the boiler pinch point which is on the order of 5 to 7°C [37].

The number of collectors contained in one single row depends mainly on the nominal temperature difference between solar field inlet and outlet ΔT, and single collector temperature variation ΔT_c.

The number of collector N is given by:

$$N = \frac{\Delta T}{\Delta T_c} \tag{10}$$

After the calculation of the number of collectors connected in series in one single row, the required number of strings is then determined. The number of rows depends mainly on the thermal power needed by the industrial process and the existence of the thermal energy storage. The absence of the storage makes the calculation simple because the number of rows is found when calculating the ratio between the power demanded by the generation block and the energy output of one single string at designed point. However, when the thermal energy storage is needed, the number of rows is given by the ratio of the next two parameters that should be calculated; the useful energy delivered by one row from sunrise to sunset for the design day and thermal energy demanded during the complete day (24 hours) by the electricity generation block [37].

After the sizing of the solar field, connection of pipes in the field should be lied out according to the three basic designs shown Figure 2.21 below which also presents their respective advantages and disadvantages.

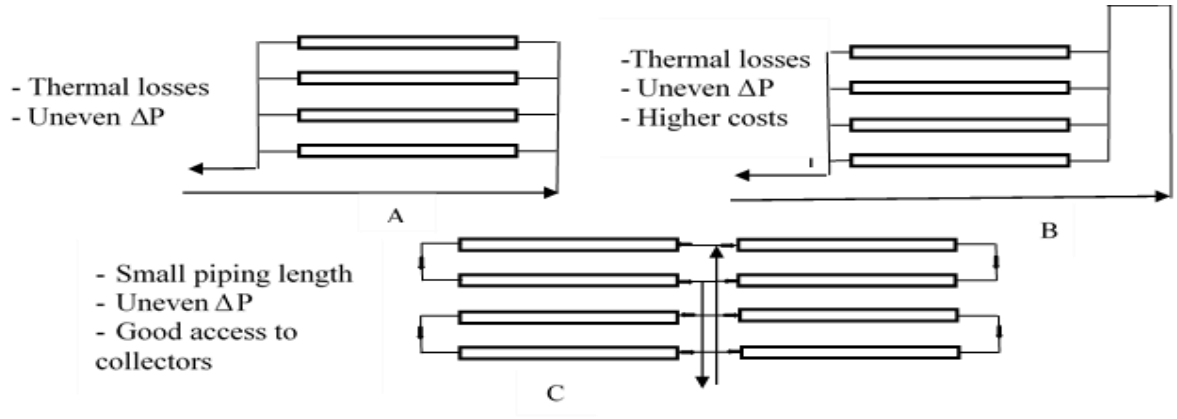

Source: (Goswami D. et al., 2016)

Figure 2.21: Solar field layouts for parabolic-trough collectors: (A) direct return, (B) inverse return, and (C) central feed

2.5.10 Oil expansion vessel

An expansion vessel or tank is used in the solar plant to absorb the differences in volume of the heat transfer fluid when its temperature increases. It is generally placed at the highest location in the power plant next to the solar field. The tank is approximately designed to handle phases of the fluid; first, when the fluid is cold the tank is full at 25%, and when the system is in normal operation 75%. The free space in the tank is therefore filled with nitrogen at high pressure to avoid chemical reaction in the tank and also to hinder the entrance of air and moisture from the surrounding to the system [27].

2.5.11 Parabolic trough collector losses

Before the heat reaches the heat transfert fluid, significant losses occur because of different factors. The losses are devided into three types, which in the descending order of importance are [37]:

1. Optical losses.
2. Thermal losses from the absorber pipe to the ambient.
3. Geometrical losses.

The optical losses are depending four parameters Figure 2.22 below, which are as follow:

Reflectivity (ρ): the typical reflectivity of parabolic trough mirrors is around 0.93. However, the deposit of dust specially in desert regions decreases gradually this parameter. In the commercial level, troughs are washed once the reflectivity reach 0.90 to 0.88 [37].

Intercept factor (ϒ): a part from the irradiation that is reflected by the mirror does not reach the receiver due to some microscopic or macroscopic imperfection of its shape. These imperfections occur during manufacturing process or in the field for example, during assembly or high load of wind. The share of losses caused by the interception factor is approximately 93% [37].

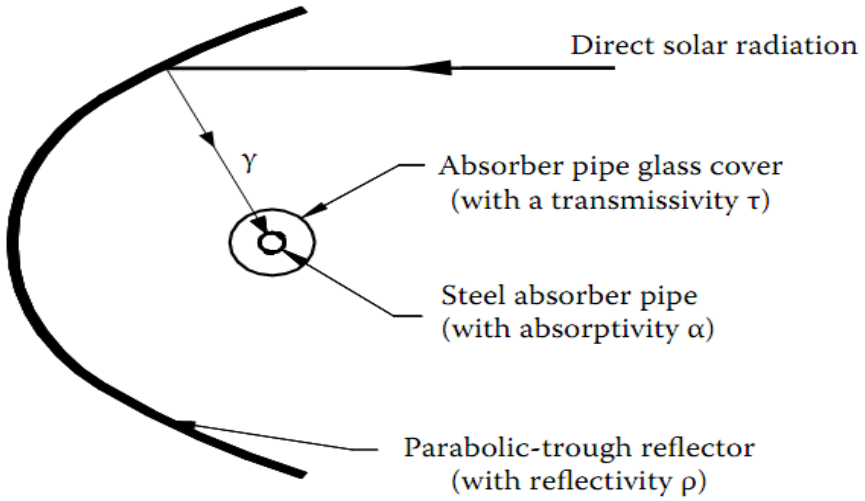

Source: (Goswami D. et al., 2016)

Figure 2.22: Optical parameters of a parabolic-trough collector

Transmissivity of the glass tube (τ): as it was mentioned before, the absorber situated inside the receiver is covered by a glass tube in order to decrease thermal losses, thus increasing its efficiency. However, it is well known that perfect transmitters do not exist, therefore, a typical glass cover can only leave 93% from the reflected irradiation to reach the absorber [37].

Absorptivity of the receiver (α): once the irradiation reaches the absorber, only 95% from it can be absorbed in a typical receiver with a cermet coating while it is slightly lower for pipes coated with black nickel or chrome [37].

The following relation gives the optimum optical efficiency of the collector when the incidence angle is equal to zero:

$$\eta_{opt,0^\circ} = \rho * \tau * \gamma * \alpha|_{\varphi=0^0} \quad (11)$$

The Incidence Angle Modifier (IAM) is a factor that corrects the optical losses mentioned before, this factor is correlated to the incidence angle by an empirical equation deduced from experiments data for a given collector type. IAM values range from 1 to 0 and it is obtained using the following equation:

$$IAM = \frac{K}{\cos\theta} \quad (12)$$

With, K is:

$$K = \cos\theta - k_1\theta - k_2\theta^2 \quad (13)$$

where k_1 and k_2 are characteristic coefficients of each type of collector, obtained experimentally [36].

Thermal losses in the absorber are divided into three heat transfer modes, which constitute the total thermal losses from PTC. The equation presenting losses is as follow:

Radiative heat loss from the steel absorber pipe to ambient is:

$$Q_{collector \to ambient} = U_{l,abs} * \pi * d_0 * l * (T_{abs} - T_{amb}) \quad (14)$$

$U_{l,abs}$: thermal loss coefficient

d_0: outer diameter of the steel absorber pipe

T_{abs} : absorber temperature

l : absorber pipe length

T_{amb}: ambient temperature

It is clearly shown in the previous equation that the thermal losses are highly related to the difference in temperature between the absorber and the ambient. Therefore, the thermal losses can always be determined using a second-order polynomial equation with a, b and c coefficients experimentally deducted, thus the equation is given by:

$$U_{l,abs} = a + b * (T_{abs} - T_{amb}) + c * (T_{abs} - T_{amb})^2 (\frac{W}{m_{abs}^2 K}) \quad (15)$$

A typical value of $U_{l,abs}$ for absorber tubes with vacuum in the space between the inner steel pipe and the outer glass tube is lower than 5 $W/m_{abs}^2.K$ [37]. More details about heat Collecting Element heat transfer are presented in the next section.

In addition to thermal and optical losses, geometric factor also constitutes a source of energy loss in parabolic trough collector. The incidence angle varies according to the position of the sun in the sky and the day of the year. Furthermore, commercial parabolic trough concentrators use one axis tracking system, therefore, the incidence angle is not equal to zero. This factor causes losses of a part of direct normal irradiation at the end of the heat collectors, Figure 2.23 below shows the losses that occur at the end of the collector [36].

$$End\ losses = 1 - \frac{f * \tan(\theta)}{L_{sca}} \quad (16)$$

Where:

θ: incidence angle

f: focal length of the collectors

L_{sca}: length of a single solar collector assembly

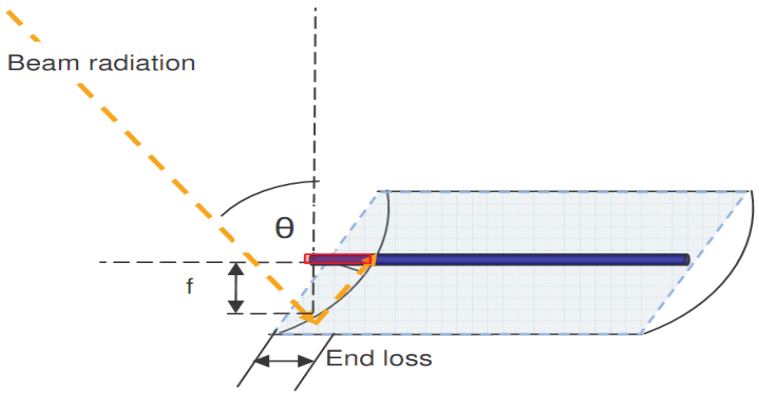

Source: (Patnode A., 2013)

Figure 2.23: End losses of PTC

2.5.12 Row Shadow (Rs)

Shading in the solar field occur when the altitude of the sun is low whether early in the morning or late in the evening. It is also considered as source of energy losses that depends on the area shaded as well as the solar insolation available during that particular time. Therefore, in order to find the actual energy losses in a collector field the proportion of shading must be defined [36].

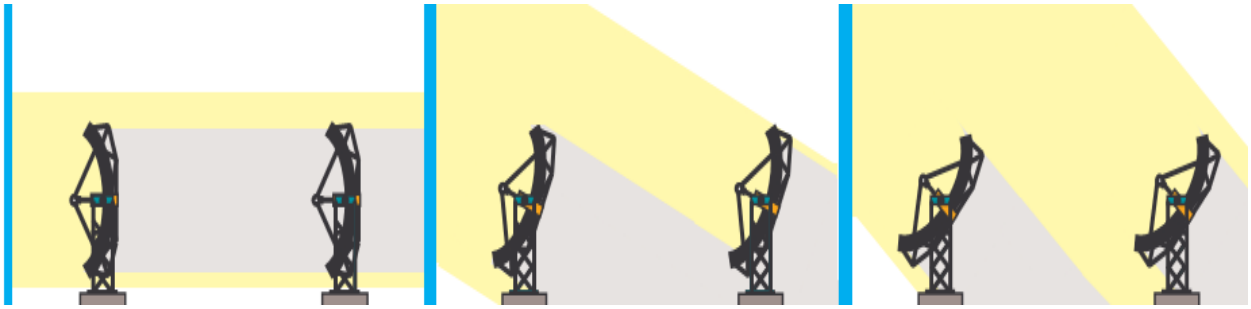

Source: (Patnode A., 2013)

Figure 2.24 Collector shading during the day

Row shading decreases the collector performance by decreasing the amount of radiation incident on the collectors Figure 2.24 above. The value of row shading is given by:

$$Row\ Shadow = \frac{W_{eff}}{W} = \frac{L_{spacing}}{W} * \frac{\cos(\theta_z)}{\cos(\theta)} \quad (17)$$

Where:

W_{eff} = effective (unshaded) width of mirror aperture (m)

$L_{spacing}$ = length of spacing between troughs (m)

W = collector aperture width (m)

θ_z = zenith angle

θ = angle of incidence

2.5.13 Absorber / Heat Collecting Element (HCE)

Also called The parabolic trough linear receiver, HCE is a device composed of two concentric tubes separated by a vacuum. The vacuum between the pipes is not necessary because most of the designed tubes currently use air-stable absorber pipes. The inner tube carries the heat transfer fluid, and the surrounding is a glass tube generally made of low-iron borosilicate in order to get a high transmittance coefficient regarding concentrated solar irradiation. On the other hand, without the cover, the convectional heat transfer coefficient between the absorber and the environment would be very high because of the buoyancy around the receiver. Therefore, covering the absorber with a glass tube minimizes significantly the thermal losses due to free convection. The absorber is made of a selective material with a high absorption coefficient and low emittance of infrared irradiation. Furthermore, the recommended absorber surface is a black material that absorb the irradiation of wavelength between 0.3µm and 2.5µm [22].

Figure 2.25 below shows the one-dimensional steady-state energy balance for a cross-section of an HCE, with and without the glass envelope intact [38].

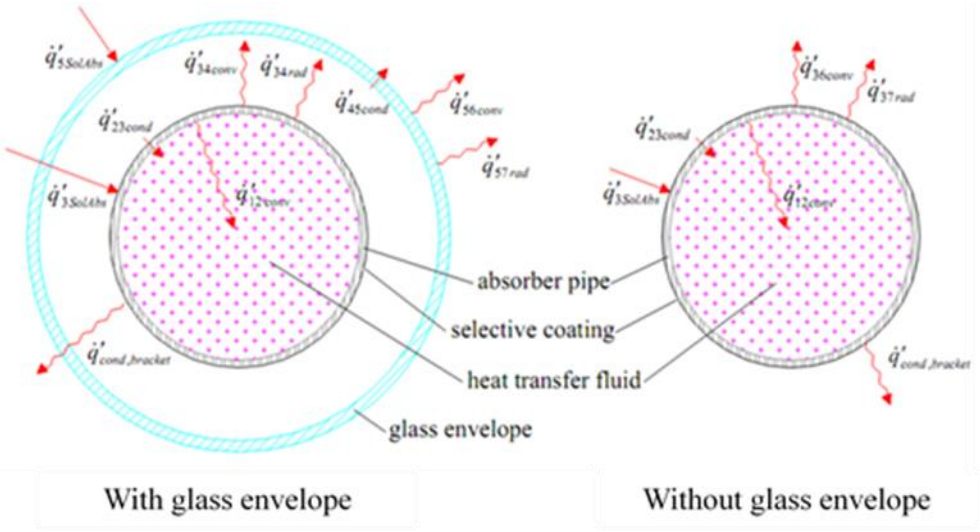

Source: (Foristall R., 2003)

Figure 2.25: One-dimensional energy balance for the receiver

The energy balance equations are determined by conserving energy at each surface of the HCE cross-section, both with and without the glass envelope intact.

With the glass envelope:

$$\dot{q}'_{12conv} = \dot{q}'_{23cond}$$

$$\dot{q}'_{3SolAbs} = \dot{q}'_{34conv} + \dot{q}'_{34rad} + \dot{q}'_{23cond} + \dot{q}'_{cond,bracket}$$

$$\dot{q}'_{34conv} + \dot{q}'_{34rad} = \dot{q}'_{45cond}$$

$$\dot{q}'_{45cond} + \dot{q}'_{5SolAbs} = \dot{q}'_{56conv} + \dot{q}'_{57rad}$$

$$\dot{q}'_{HeatLoss} = \dot{q}'_{56cinv} + \dot{q}'_{57rad} + \dot{q}'_{cond,bracket}$$

Without the glass envelope:

$$\dot{q}'_{12conv} = \dot{q}'_{23cond}$$

$$\dot{q}'_{3SolAbs} = \dot{q}'_{36conv} + \dot{q}'_{37rad} + \dot{q}'_{23cond} + \dot{q}'_{cond,bracket}$$

$$\dot{q}'_{HeatLoss} = \dot{q}'_{36cinv} + \dot{q}'_{37rad} + \dot{q}'_{cond,bracket}$$

Table 2.3: Heat Flux Definitions

Heat Flux (W/m) *	Heat Transfer mode	Heat Transfer Path	
		From	To
$\dot{q}'_{12conv}$	Convection	inner absorber pipe surface	heat transfer fluid
$\dot{q}'_{23cond}$	Conduction	outer absorber pipe surface	inner absorber pipe surface
$\dot{q}'_{3SolAbs}$	Solar irradiation absorption	incident solar irradiation	outer absorber pipe surface
$\dot{q}'_{34conv}$	Convection	outer absorber pipe surface	inner glass envelope surface
$\dot{q}'_{34rad}$	Radiation	outer absorber pipe surface	inner glass envelope surface
$\dot{q}'_{45cond}$	Conduction	inner glass envelope surface	outer glass envelope surface
$\dot{q}'_{5SolAbs}$	Solar irradiation absorption	incident solar irradiation	outer glass envelope surface
$\dot{q}'_{56conv}$	Convection	outer glass envelope surface	Ambient
$\dot{q}'_{57rad}$	Radiation	outer glass envelope surface	Sky
$\dot{q}'_{36conv}$	Convection	outer absorber pipe surface	Ambient
$\dot{q}'_{37rad}$	Radiation	outer absorber pipe surface	Sky
$\dot{q}'_{cond,bracket}$	Conduction	outer absorber pipe surface	HCE support bracket
$\dot{q}'_{HeatLoss}$	Convection and radiation	heat collecting element a	ambient and sky
***Per unit aperture length**			

Source: (Forristall, 2003)

The following different heat transfer modes that govern the system can be calculated in order to assess the performance of the receiver [38]:

- Convection Heat Transfer between the HTF and the Absorber
- Conduction Heat Transfer through the Absorber Wall
- Heat Transfer from the Absorber to the Glass Envelope
- Conduction Heat Transfer through the Glass Envelope
- Heat Transfer from the Glass Envelope to the Atmosphere

- Solar Irradiation Absorption
- Heat Loss through HCE Support Bracket
- No Glass Envelope Case

2.5.14 Tracking system

Because of the tracking system, parabolic trough collectors can also be defined as dynamic devices. It allows the PTCs to follow the position of the sun in order to capture and concentrate the maximum direct normal irradiation into the receiver. One hydraulic drive unit is sufficient to rotate a multiple modules connected in series moving as one collector. However, for small collectors (aperture area <100m²) tracking systems composed of electric motor and gear box are used [37].

Centralized control units are used in order to command the tracking system when to move and in which direction to track the sun. Currently two units which are depending on the device used to track the sun are commercially available. These two categories are classified bellow:

1. Control units based on sun sensors.
2. Control units based on astronomical algorithms.

The first category uses photo cells in order to detect the position of the sun in the sky. However, the one using astronomical algorithms are more accurate because of the very precise mathematical algorithms that find the sun elevation and azimuth every second and measure the angular position of the rotation axis by means of electronic devices [37].

Currently all commercial power plants use single axis tracking system. However, two axis tracking system were tested in the past but they showed low cost effectiveness comparing to the single axis systems. Although the two axis tracking system could not compete with the lower price of the single axis tracking, its existence allows the trough to track the sun with an incidence angle equal to zero, thus reducing optical losses while increasing the absorbed heat by the receiver. There is further need to investigate their maintenance and cost effectiveness in order to compete in the market [37].

2.5.15 Power conversion system

The power conversion system is where the heat gained by the heat transfer fluid from the solar field and the thermal energy storage is transformed to electricity by means of a steam Rankine cycle using superheating and reheating systems to increase the efficiency of the cycle.

2.5.15.1 Steam generation system

The steam generator system in parabolic trough plants is similar to conventional plants, the main parts are as follow [37]:

- Preheater: where the water is preheated to a temperature close to evaporation.
- Evaporator: where the preheated water is evaporated and converted into saturated steam.
- Super heater: the saturated steam produced in the evaporator is heated in the super-heater to the temperature.

The different components mentioned before in a power plant are all of them set of heat exchangers that transfers heat from the medium circulating in the solar field to water in order to produce a superheated steam to generate electricity. Figure 2.26 below show the common configuration of shell-and-tube heat exchanger with one shell pass and one tube pass [39].

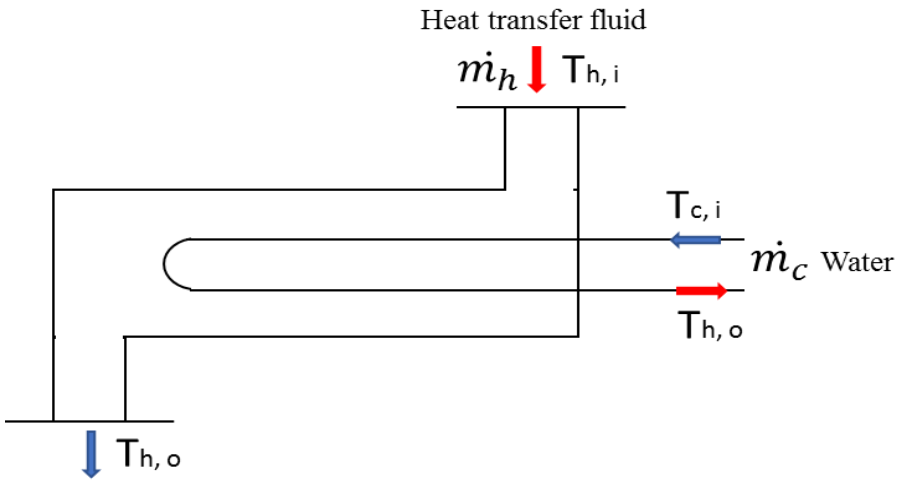

Figure 2.26: Shell-and-tube heat exchanger with one shell pass and one tube pass

The ratio of the real heat transfer rate to the maximum possible heat transfer rate is called effectiveness off heat exchangers, this parameter defines the performances of the steam generation components.

$$\varepsilon = \frac{q}{q_{max}} \tag{18}$$

Other effectiveness formulae exist for other heat exchanger configurations; they are detailed in [39].

Reheater is a set of pipes incorporated in the boiler. The use of super heater in the Rankine cycle is to avoid wet steam in the turbine. However, it causes another problem of high temperature inlet in the turbine. To fix this issue, the exhausted steam from the high pressure turbine is expanded to an intermediate pressure and directed to reheater. After that, the steam is expanded in a second stage of the steam turbine [40].

Different design of the power block gives different thermodynamic cycles, in the following part the previous schematic of parabolic trough plant with (reheater, preheater and super heater) is taken as an example. Figure 2.27 below, shows an ideal Rankine cycle temperature–entropy (T–s) diagram for steam as a working fluid.

The cycle is composed of the following process:

5 → 6: Saturated liquid from the condenser at state 1 is pumped to the boiler at state 6 passing through two bleeding from the low pressure turbine.

6 → 8: Liquid is heated in the boiler at constant pressure. The temperature of the liquid rises until it becomes a saturated liquid. Further addition of heat vaporizes the liquid at constant temperature until all of the liquid turns into saturated vapor. additional heat superheats the working fluid to state 8.

8 → 10: Steam expands isentropically through the high pressure turbine to state 9; where the steam will be reheated to reach the point 10.

10 → 13: Steam expands once again in the low pressure turbine to reach point 13 passing through two bleeding.

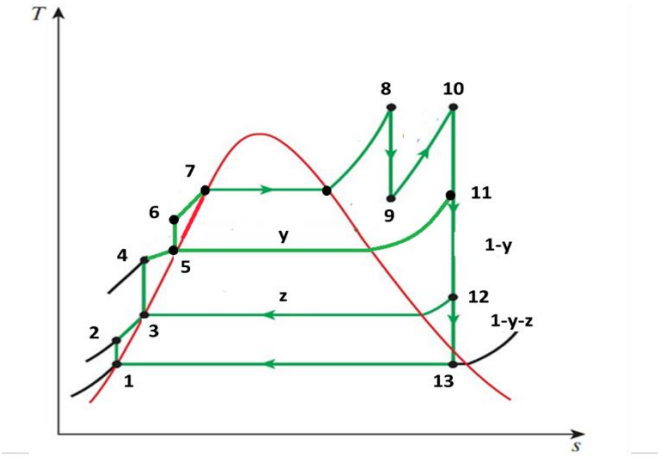

Figure 2.27 Rankine cycle with vapor reheating T(s) diagram

13 → 1: Steam exiting from low pressure turbine is condensed at constant pressure until it returns to state 1 as saturated liquid.

The performance of the cycle is given by:

Turbine work:

$$w_{tur} = (h_8 - h_9) + (h_{10} - h_{11}) + (1 - y)(h_{11} - h_{12}) + (1 - y - z)(h_{12} - h_{13})$$

Pump work:

$$w_{pump} = (h_6 - h_5)$$

Preheater work:

$$w_{pre} = (1 - y - z)(h_3 - h_1) + (1 - y)(h_5 - h_3)$$

Reheater work:

$$w_{reh} = (h_{10} - h_9)$$

Cycle efficiency:

$$\eta_{cycle} = \frac{Net\ work\ output}{heat\ input} \tag{19}$$

$$= \frac{(h_8 - h_9) + (h_{10} - h_{11}) + (1 - y)(h_{11} - h_{12}) + (1 - y - z)(h_{12} - h_{13})}{(h_6 - h_5) + (h_{10} - h_9) + (1 - y - z)(h_3 - h_1) + (1 - y)(h_5 - h_3)}$$

where h represents enthalpy.

2.5.15.2 Condenser

A condenser is a critical device in solar thermal plants that involves two phase heat exchanger to condensate the working fluid from vapor state to saturated liquid state. Generally, the most used type of condensers is shell- and tube-type heat exchanger where the cooling fluid is water which passes through the pipes and hot air from the turbine across the shell side. The efficiency of the power block depends highly on the performances of the condenser. Therefore, the latter should be designed in such a way to have the lowest pressure possible to get the lowest temperature of the condensate. Cooling towers are used generally to evaporate some of the cooling water in order to have a low wet-bulb temperature of the cooled water [27].

Table 2.4 below shows the difference between the performances of a thermal power plant using an Air Cooled Condenser (ACC) and Evaporative condenser during two different seasons where the ambient temperature of the location fluctuates. Evaporative cooling presents a clear advantage regarding the efficiency of thermal power plants especially during high temperature seasons. However, during winter season the difference is marginal to conclude that evaporative cooling performs better than the opponent system. This difference is mainly due to the ambient temperature that affect directly the amount of heat rejected therefore the performances of air cooled condensers [41].

Table 2.4: Comparison of thermal power plant performances for different cooling systems and ambient temperatures

	Winter 6 ºC		**Summer 30 ºC**	
	P (MW)	Efficiency $\boldsymbol{\eta}$ %	P (MW)	Efficiency $\boldsymbol{\eta}$ %
Wet cooling	411.7	57.6%	363.5	56%
ACC	408.1	57%	345.4	53.3%

Source: (Kehlhofer, 2009)

Using dry cooling technologies currently increases the cost of cooling by 3.3 times above the technologies using water, affecting the overall efficiency as well [9]. Dry cooling can push up the cost of electricity by 10%. As mentioned before, the nature of water in the desert is saline. In addition, the amount of fresh water is limited and committed mostly to agricultural uses

[42].Therefore, the use of dry cooling technologies which is similar to the one adopted in Hassi R'mel at present offers an accepted solution to mitigate the absence of water.

Many configuration of air cooled condensers exist; the system uses finned coils where the steam coming from the turbine flows through over which the ambient air is blown. Figure 2.28 below shows an A - frame condenser in which the steam flows through the finned coils oriented at angles of 45°to 60° to the horizontal.

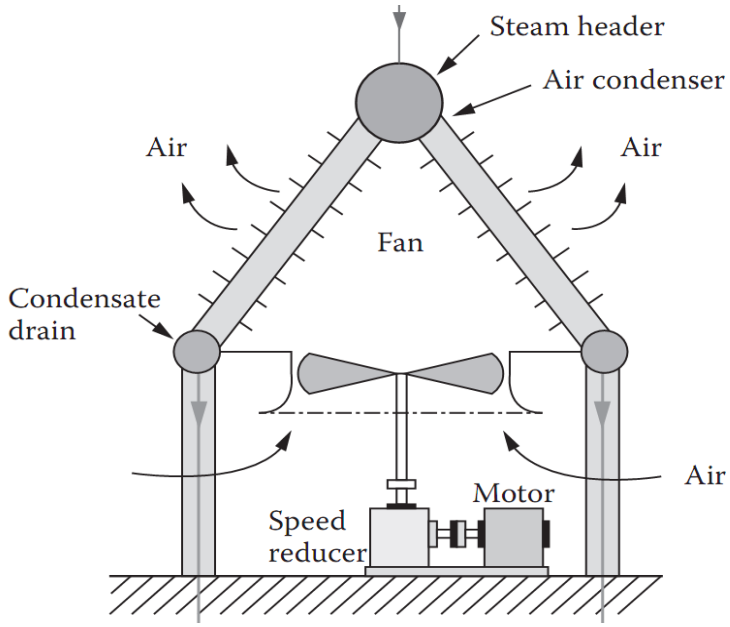

Source: (Goswami D., 2013)

Figure 2.28 Configuration of an A frame air-cooled condenser

The use of dry cooling systems has shown a number of advantages, such as:

- Low costs of maintenance (no chemical additives or periodic cleaning required).
- Absence of the cooling tower infrastructure.
- Plant siting flexibility
- Lower environmental impact because the system emits only warm and clean air.

On the other hand, the disadvantages of dry cooling are:

- Lower heat-transfer coefficients; therefore, bigger heat exchanger area.

- Additional energy consumed because of the use of the fan to reach higher heat transfer coefficient.
- Performance highly related to the temperature of the surrounding that variate according to seasons.
- Lower power plant efficiency.

2.5.15.3 Deaerator

The deaerator is an essential component in the power block due to its role of removing dissolved oxygen, carbon dioxide and other non-condensable gases, on the other hand, deaeration is a mechanical process that increases the life span of the steam generation system. The presence of oxygen and Carbon dioxide lower pH levels in the power block causing severe acid attack throughout the boiler system. In order to control gases in the power block and mitigate low pH levels, addition of chemical substances that control their existence is possible, however, removing those gases mechanically (deaeration) is more economical and thermal efficient [43].

The working principle of a deaerator is based on the two following scientific theories:

1- Henry's Law, states: "Gas solubility in a solution decreases as the gas partial pressure above the solution decreases."
2- "Gas solubility in a solution decreases as the temperature of the solution rises and approaches saturation temperature."

When a liquid attains its saturation temperature, the solubility of a gas in it is zero but it can be achieved only when the liquid is subjected to turbulence by properly stirring the fluid to ensure complete deaeration. Both of these theories are used in deaerator operation for removal of dissolved gases from boiler feed water, which at the same time gains some temperature from the heating medium [44].

2.6 Thermal energy storage

In the following section, different types of Thermal energy storage mechanisms, heat transfer fluids and their importance in the operation of solar thermal power plants will be presented.

The electricity generated by a solar thermal power plant is highly dependent on the weather conditions and the nature of the source. Due to the intermittency of sun irradiation, weather conditions and its full absence during night time the capacity factor of the power plants is low. Using parabolic trough technology with the high potential of direct normal irradiation, the capacity factor of the plant can reach 25%. However, using a thermal storage can increase the capacity factor to reach 50% or more [31]. The use of thermal energy storage is already attractive and exists in many thermal solar power plants around the world and its maturity was proven. However, if shifting of energy production is possible from low to high tariff periods, benefits can cover more storage system expenses [22] [45].

Thermal storage in concentrating solar power plants constitutes an important advantage compared to storage in photovoltaic or wind energy where storing energy in form of electricity is expensive [46]. Thermal storage in solar plants can positively affect the system in multiple manners as shown Figure 2.29 below [22]:

- Increasing the value of electricity production by making transition in electricity generation from low load to periods where the demand is high.
- Decreasing the capacity of back up based fossil fuels which has a high investment cost and low thermal efficiency.
- Increasing the system efficiency by avoiding the transients in the power cycle caused by clouds.
- Minimizing start up time by using the thermal storage to preheat the absorber.

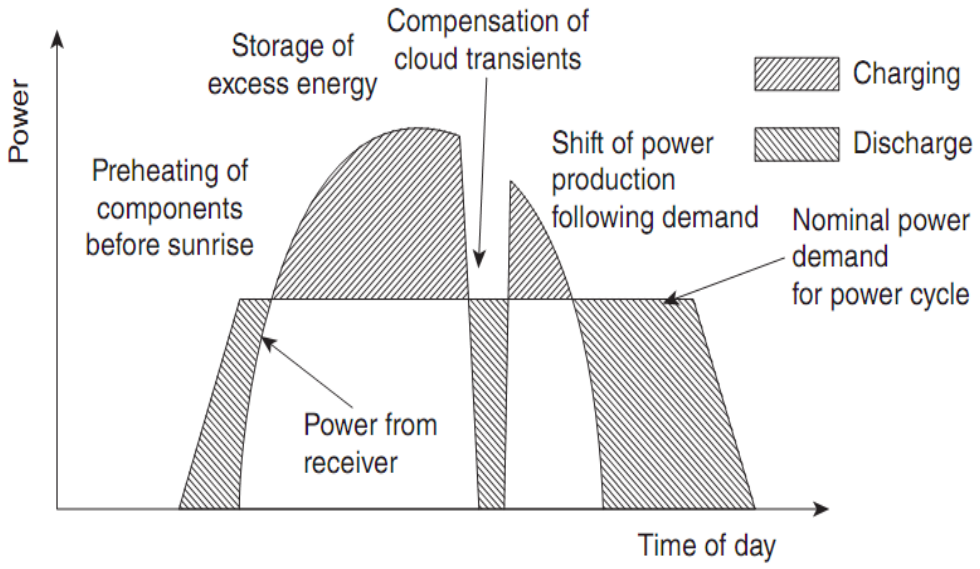

Source: (Lovegrove K. et al., 2013)

Figure 2.29 Various functions of thermal storage in a CSP plant

One hour of thermal energy storage is defined as the capacity of the system to continue running the power plant at it rated output power P_{out} for one hour. As mentioned before, the capacity factor can be improved by using a thermal storage which will increase the energy output during the year, the capacity factor is given by [45]:

$$CF = \frac{W_a}{P_{out} * 87600} \tag{20}$$

Where: W_a is annual electric energy output.

When designing a storage system, the solar multiple is the ratio that defines the capacity of the thermal power plant to deliver energy during cloudy day, it is defined by the produced power from the solar field during (P_{Re}) the designed point divided by the inlet nominal power of the cycle (P_{Cy}) [45].

$$SM = \frac{P_{Re}}{P_{Cy}} \tag{21}$$

2.6.1 Different types of thermal storage

According to Sarada Kuravi (2013), thermal storage systems are divided into two type systems; active and passive. If the medium is a fluid and it has the ability to circulate between the storage tanks it is called active storage. However, if the heat transfer fluid role is only charging

and discharging where the storage material is solid, the storage is called passive. Under active storage two subsystems exist; first is when the heat transfer fluid and the medium used in the storage are the same, the storage type is called direct active storage. When an additional heat exchanger exists in the system and its role is to transfer heat from HTF to storage medium or the opposite, the subsystem is named indirect active storage. The following diagram, Figure 2.30 shows the different type of thermal storage discussed above [47].

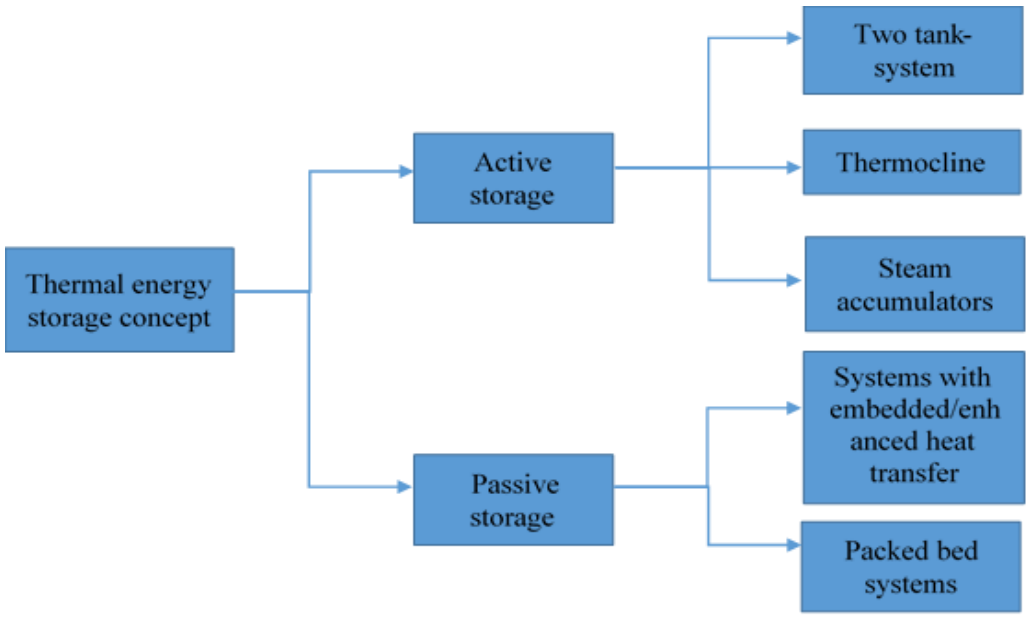

Source: (Kuravi S. et al., 2013)

Figure 2.30 Categorization of TES systems

2.6.2 High temperature thermal energy storage materials

Different materials are used in high temperature thermal energy storage depending the application and the temperature ranges of the process. Three categories of materials exist as listed below:

2.6.2.1 Sensible heat storage materials

Sensible heat materials store thermal energy from the solar field without undergoing phase change within the temperature range of the application. The quantity of thermal energy stored by the medium in a mass of material can be expressed by:

$$Q = \rho * C_p * V * \Delta T \quad (22)$$

where Q is the amount of heat stored [J], ρ is the density of the storage material [kg/L], C_p is the specific heat over the temperature range of operation [J/ (kg K)], V is the volume of storage material used (L), and ΔT is the temperature range of operation.

The materials used in this type can be whether solid media or liquid media. Currently, the main solid material utilized are concrete and castable ceramics in packed bed thermal storage, where the use of heat transfer fluid is necessary. One of the advantages of using solid materials like concrete or rocks is the low cost of purchasing the material and its abundance [48].

Liquid materials such as (molten salts, mineral oils and synthetic oils) are the main used material for thermal storage in concentrating solar energy. Due to the difference of density between cold and hot fluids, these mediums maintain naturally the thermal stratification. The only requirement when using these fluids is that in the storage tank the hot fluid is supplied from upper part during charging and cold material from down during discharging. However, in order to avoid mixing, there is other mechanisms like using stratification devices or separating tanks of hot and cold fluid [48].

2.6.2.2 Latent heat storage media

In some substances, thermal energy can be stored almost isothermally as the latent heat of phase change. Heat transition can be done by liquefaction from solid to liquid or vaporization from liquid to vapor. However, currently, the main phase change process used is from solid to liquid and the materials under this type are called phase change materials (PCM) [48].

Latent storage systems are more energy efficient than sensible thermal heat storage due to the advantage of small temperature difference operating conditions between charging and discharging. On the other hand, this category of materials has higher energy density comparing to sensible heat mediums. Therefore, lower size of heat storage system. Though the system design and selection of the material are difficult and their performance in the ground has shown degradation after a low number of freeze–melt cycles [48].

2.6.2.3 Chemical heat storage

Chemical storage requires full reversible reaction substances, the thermal energy produced from the solar field is used to arouse an endothermic chemical reaction, in order to recover the same energy, the thermal reaction should be completely reversible. This type of thermal materials offers many advantages, first the thermal densities is very comparing to the remaining materials, secondly the period of storage is unlimited as long as it is kept under ambient temperature. However, the development level of reversible thermochemical reaction (RTR) is already at a very early stage [48].

For high temperatures concentrating solar electricity generation applications, the main fluids that are used are either molten salt or synthetic oil. Currently two-tank thermal energy storage system is the most commercialized mature system in the industry, when other technologies are in their level of maturity. Two-tank technology can be direct and indirect active technology, when it is direct the synthetic oil or molten salt are used as heat transfer fluid and storage medium, while in the indirect active system the oil is used as HTF and molten salt in the tank like storage material [47] . In addition to its maturity, the technology is widely used, for example, the Solar Two power tower in California and Several parabolic trough power plants under development and in operation in Spain and the U.S [47]

2.7 Heat Transfer Fluids

According to Vignarooban K. (2015), heat transfer fluids are critical components for transferring and storing energy in concentrating solar thermal power plants. Different heat transfer fluids were subject of investigation in this paper, that is; Air and other gases, Water/steam, Thermal oils, Organics, Molten-salts and Liquid metals.

Water can be used in parabolic trough plants as HTF. Otherwise, a non-based water HTF is used to carry heat from HTC to steam generator and then transferred to water in the power block. Recent research demonstrated that the use of water in the system as HTF and working fluid increases the overall efficiency of the plant and reduces the cost of produced energy up to 11% comparing to other configurations. However, as mentioned previously the main problem with the use of water is its availability and cost in the selected location [49].

Thermal oils are currently used in some commercial solar thermal plants around the world (example: Saguaro CSP plant located at Redrock, Arizona, USA). They are produced from non-toxic petroleum based oil with optimum purity and performance, and they have almost the same thermal conductivity of 0.1W/ (m K). One of the disadvantages of thermal oils and reason why they are not used in high temperature and highly efficient solar thermal system is that they are thermally stable only up to 400°C. In addition to that, thermal oils are the most expensive HTF fluid with a cost reaching 5$ per Kg [49].

Molten salts are the most used HTF in commercial solar thermal plants. In addition to their viscosity being comparable to water at high temperature, including similar viscosity and low vapor pressure they are thermally stable at high temperatures (up to 500°C). Molten salts with their previous properties make an excellent heat transfer fluid. Furthermore, molten salts have also another important advantage that is the ability to be used in thermal energy storage systems. Currently the main issue of using molten salt fluids based on nitrates/nitrites is that the worldwide nitrate salt production is restricted and the largest mines are only in Chile and Peru. The IEA's target of the CSP in 2050 would require 30 times the current mine production of nitrate salts from Chile and Peru. Alternative HTFs made from inexpensive and earth abundant materials are being intensively investigated [49].

The use of metal liquids date back to 1940s in nuclear industries. Nowadays, this category of fluids is under investigation for use in commercial solar thermal systems as HTFs and thermal energy storage media. With an operating temperature range of 98–883°C Liquid sodium was first used as a HTF and storage medium in 1981 in a test plant (500 kWe) located in Almeria, Spain. The main disadvantages of liquid sodium are its high combustibility when in contact with water and its cost exceeding 4 times the price of molten salts [49].

2.8 Environmental impact

In this section, the analysis of different environmental facts related to the implementation of parabolic trough projects (that is, construction, normal operation and end of operation) are discussed.

2.8.1 Manufacture and construction

The effect of solar thermal plant on the environment begins with the process of plant components production and represents the largest share, same as conventional power plants and other industrial production processes. However, the period of environmental impact is restricted to a very short duration. In addition to that, in many countries they are subject to strict legislative requirements and regulations. In General, solar thermal projects are installed in remote locations where the population density is very low. Therefore, the effect of such projects on human beings and environment is so far only a very limited knowledge [22].

2.8.2 Normal operation

During operation, solar thermal power plants have also effects on environment same as the remaining thermal plants. Some aspects of these are discussed below.

2.8.2.1 Land requirements and emissions:

Due to the low energy density of solar energy technologies, implementation of such project require large solar concentrators. Therefore, large areas of land as shown in Table 2.5. Since the locations where such projects are preferably installed are deserts or steppes, the land requirements (extensive drainage systems, compacted and levelled soil, ecosystem interference) are generally fulfilled [22].

Table 2.5: Space requirements of solar thermal plants (K. Lovegrove, 2012)

Tower power plants	20 – 35 m^2/kW
Line-focusing power plants	10 – 25 m^2/kW
Parabolic trough power plant	15 – 30 m^2/kW

Source: (K. Lovegrove, 2012)

Greenhouse gas emissions in concentrating solar power plants are restricted only to hybrid systems using fossil fuels as source of electricity generation. On the other hand, sound pollution may take place in the power plant, mainly emanating from pumps and turbines. However, since

the power block in most of the power plants is located in the central position of the solar field and also is subjected to many environment regulation, noise emissions in the plant are negligible [22].

2.8.3 End of operation

Environment effects of dismantling concentrating solar power have not been reported so far. However, due to the nature of the components used in solar plants which are similar to the conventional systems, it puts them under the same legal restriction that monitors and assesses environmental impacts [22].

2.9 Previous Simulation Studies

In order to investigate more to find out the optimum design of parabolic trough technologies in Algeria, Ameur Trad (2014) used a method called "demand-supply balancing analysis" to determine the best option from 7 designs proposed. The simulation was performed in Naama (South of Algeria), and the best technologies were selected to go through an economic, financial and sensitivity analysis. The prefeasibility study has shown that the design D3 with a dry cooling system, 100 MW_{el} installed capacity and with 8 full load hours of thermal energy storage is the most suitable regarding Benefit/Cost ratio recovering more than 28% of its total investments, rendering it the most promising design to be followed [50].

Using System Advisor Model (SAM), Abdou Messai Y. B. (2013) designed a 30 MW_e parabolic trough power plant without storage system. The plant power generation was compared under the conditions of 20 locations situated in Algeria. The best site was Djanet situated in the southern east of the country, the simulation results showed that Djanet is the site where a plant should be implemented rather than what was found in the previous study. It was found that the cost of energy is highly related to the location where the project is installed [8].

Another research study also was done in order to evaluate the technical and economical performances. Using STEC (solar thermal electric components) model library under TRNSYS simulation software, Abdelkader Zaaraoui (2012) evaluated the performances of 30 MW parabolic trough power plant. Apart from natural gas-fired hybrid block. The plant was designed similarly to SEGS VI situated in the Mojave Desert in California, the system was composed of a Rankine cycle with reheat and feed water heating. For simplicity, each heat exchanger network, consisting

of preheater (economizer), steam generator (boiler) and super heater is treated as a single heat exchanger. The simulation was conducted in 4 sites having a relatively direct normal irradiance exceeding 2000 kWh/m².yr. The generation of meteorological data was performed using the software METEONORM. Followed by an economic analysis, the best location that have the lowest cost of electricity was Bechar [51].

Chapter 3. METHODOLOGY

Outline:

3.0 Introduction

The following section contains some brief description of the two used software tools for the simulation (Meteonorm and System Advisor Model) used. The different parameters of the simulated power plant; solar field, power block and storage system were exposed. The load of the city where the power plant was simulated was determined for two extreme months.

3.1 Simulation software

In this study, System Advisor Model (SAM) software was used to simulate the technical and economical performances of the thermal power plant. The software was developed in 2005 by the National Renewable Energy Laboratory in collaboration with Sandia National Laboratories. In the beginning the software was called Solar Advisory Model, but with the introduction of new technologies apart from solar technologies the name changed to Systems Advisor Model to show the existence of the remaining options. In 2007, with the release of the first public version it was possible for solar energy professionals to evaluate photovoltaic and concentrating solar power systems [52].

System advisor model is an open source simulation software which is used by different categories of professionals (project developers, academic researchers, policy makers and manufacturers). Companies use SAM in order to test and evaluate performances of their products and their impact on the efficiency or cost reduction of installed systems. Furthermore, the software can also be used to analyze different configuration of a selected technology to maximize the benefits of projects. Finally, Policy makers and designers use the model to experiment with different incentive structure [52].

System advisor model requires weather data of the selected location, financial regulation and project technical specifications as inputs. First, the software runs using weather data in form of TMY2, TMY3 or EPW files containing the different weather conditions of the site including (temperatures, wind speed, solar irradiation etc.). On the other hand, technical performances are generated using hourly weather data, therefore hourly energy output is estimated and then yearly performances of the system and its components are calculated resulting the total annual output. Finally, the software offers many financial and economical type of analysis for energy projects

using as inputs to the analysis period equivalent to the system lifetime, discount rate, inflation rate, loan amount and loan rate [52]. The following diagram Figure 3.1 shows the different steps of system advisor model working principle and how the flow of information occur in the software [53].

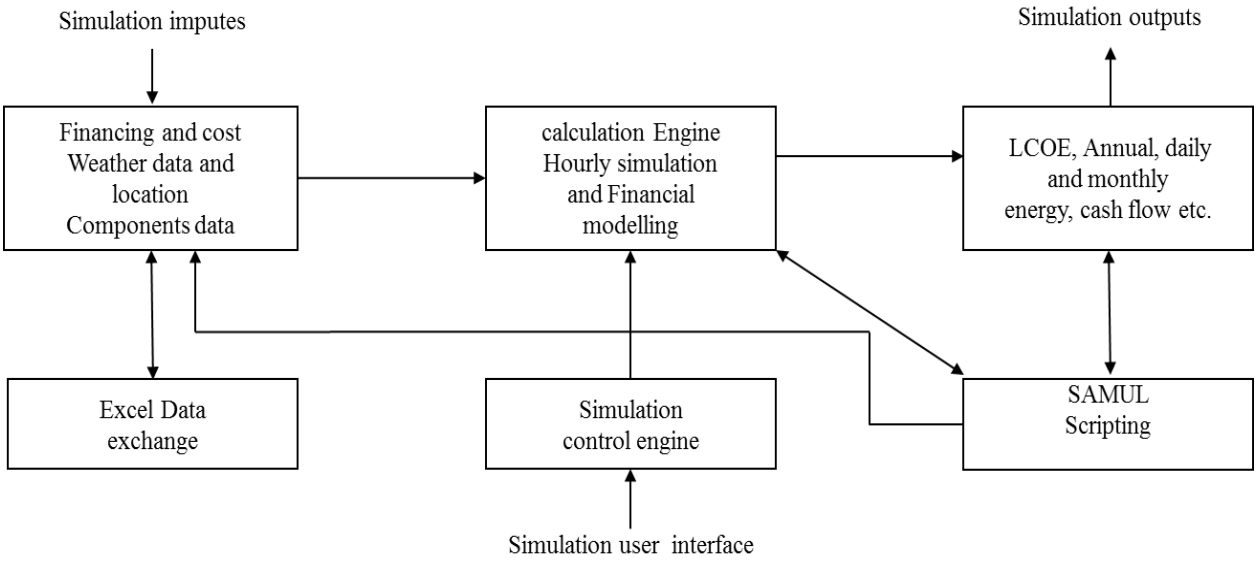

Source: (Kariuki K., 2013)

Figure 3.1: SAM model structure flow

3.2 Weather Data

In order to simulate the parabolic trough power plant, System Advisor Model requires meteorological data of the selected location. Typical Meteorological Year 3 (TMY3) weather file data format was generated using Meteonorm version. 7.1. The used software is developed by Meteotest institute; it uses ground stations and satellites images weather measurements. For the locations where there are no weather measurements stations the software uses results that are interpolated between locations where data is available. The software has some uncertainties that range between 2 to 10% according to the methods used in measurements (satellite images, ground measurements and interpolated data) [54].

The weather file incorporates different hourly measurements for different parameters (shown in the appendix Figure I.1 and I.2), it generates data of one year considered as typical year because it represents an average of all years where measurements were available [55]. Figures 3.2,

3.3 and 3.4 below present the hourly direct normal irradiation, ambient temperature and wind speed of the location:

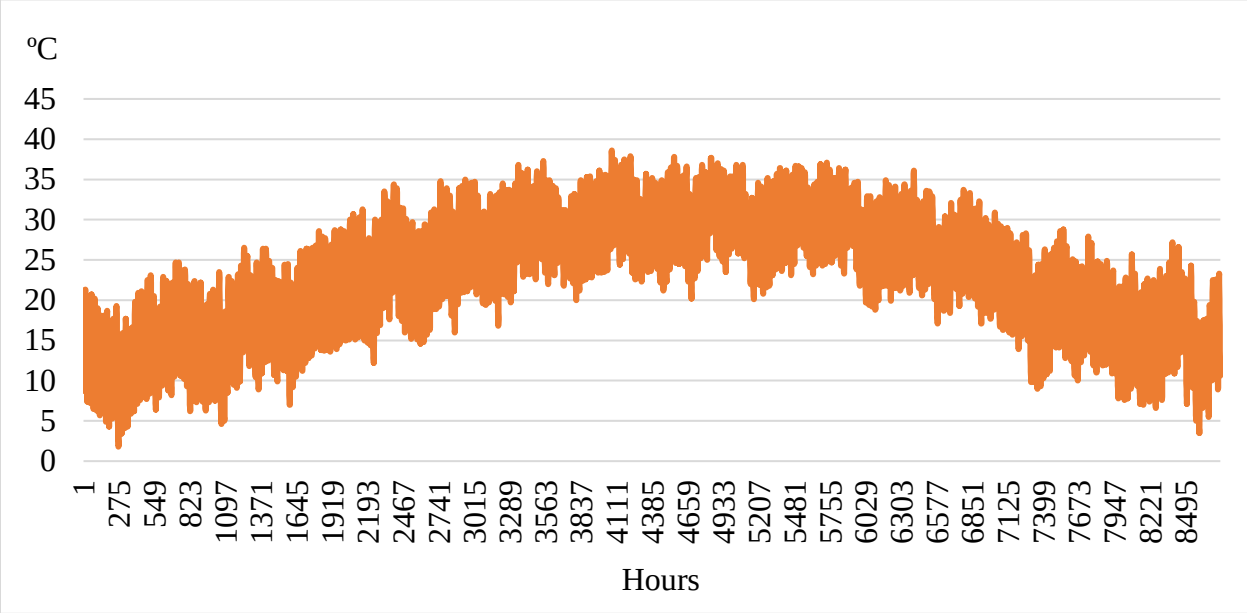

Figure 3.2: Hourly ambient temperature

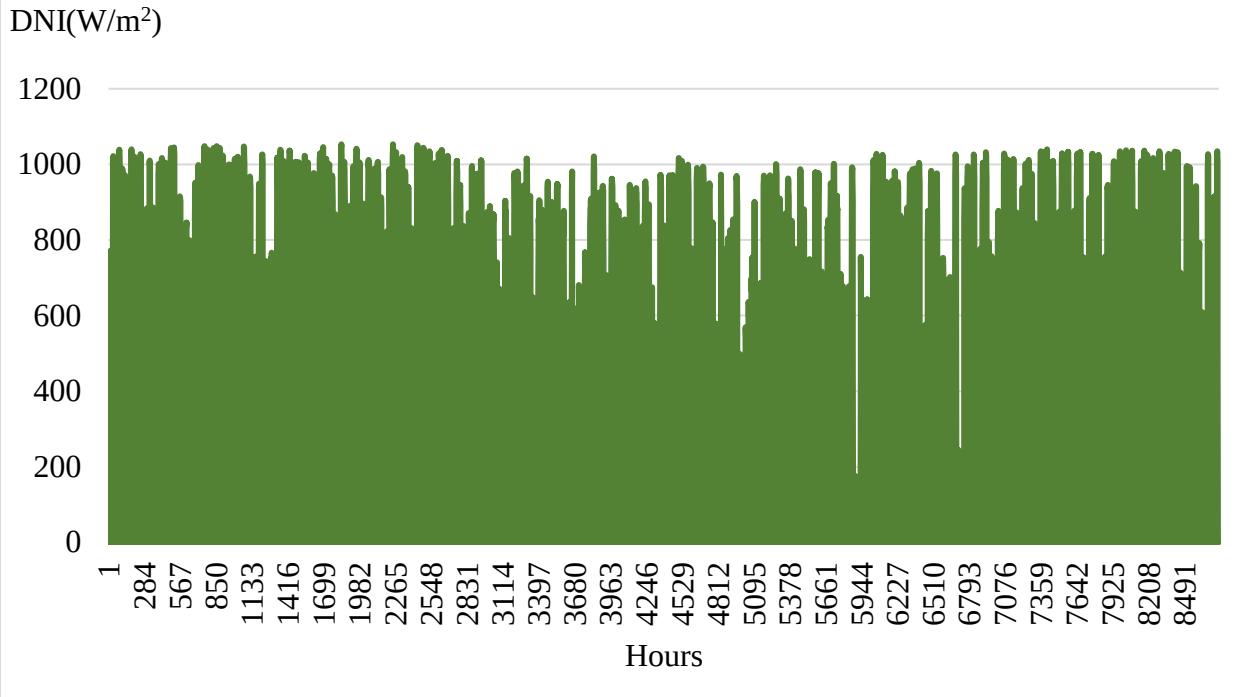

Figure 3.3: Resource Beam Normal Irradiation

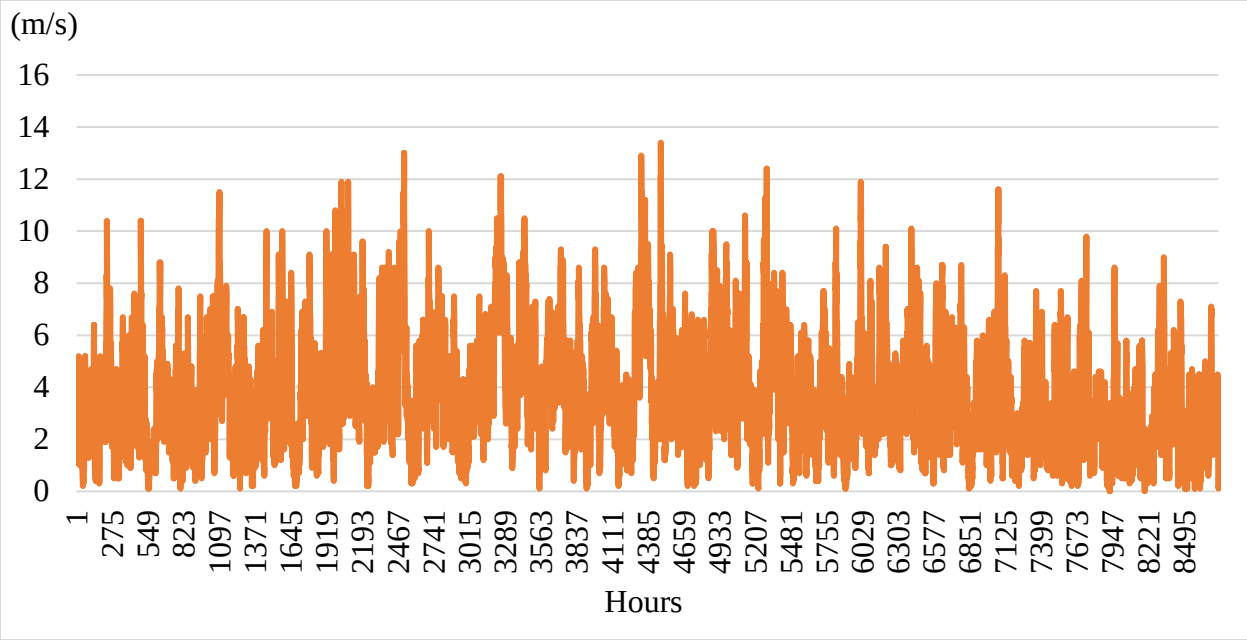

Figure 3.4: Hourly wind speed

The software gives uncertainties depending the chosen location, for Tamanrasset the software indicated the following possible range of errors of measurements:

1. Mean irradiance of global radiation horizontal: 3%
2. Irradiance of beam: 6%
3. Ambient temperature: 0.3 °C

3.3 Load profile

In order to size the parabolic trough power plant so that it meets the needs of the population living in Tamanrasset, the load profile had to be determined. Since the data of electricity demand was not available through the local utility for the selected location, another city with almost the same population number and weather condition was taken into account to estimate the location load profile.

The data collected from the utility were expressed in Mega Volts Amperes (MVA) for each 15 minutes for the whole year of 2015. For better sizing of the system, the apparent power (S) is more suitable than the active power (P) since the latter takes into account imperfections of the grid and consumer side. The following equation express the relation between the two terms of power [56]:

$$P(W) = S(VA) * PF \quad (23)$$

Where: PF is the power factor of the system.

Due to the location of the Tamanrasset in the Algerian desert, the city experience extremely hot days. Therefore, the use of air conditioning systems become necessary for the well-being of the citizens. These extreme weather conditions specially during winter and summer seasons affect the load profile, Figure 3.5 below, shows the daily electricity demand of the city for the months of January and August 2015. The selected location experiences during summer high electricity demand during afternoon hours between 1pm and 5 pm in the evening and also late in the evening between 9 and 11pm. However, during winter time the peak hours occur only late in the evening around 8pm with a demand lower than the one in summer. Therefore, in this research the sizing of the power plant was done based on the summer load.

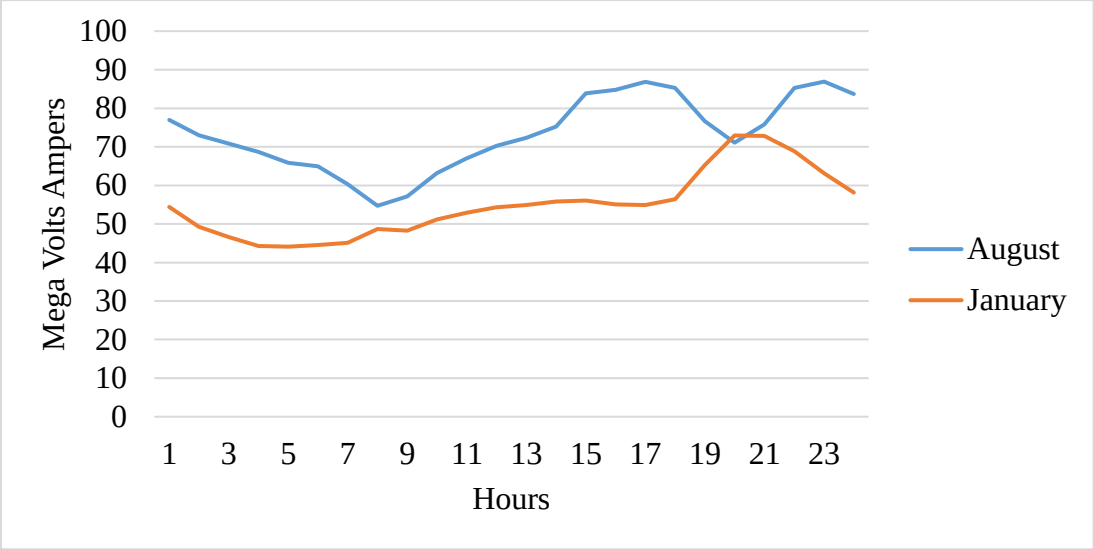

Figure 3.5: Load profile of Tamanrasset

3.4 Solar field system design and sizing

In this section, the design of the considered parabolic trough power plant and its different parameters are presented.

In order to support the current power delivered to the city, a power plant of 100 MWe (Net output at design point) using steam Rankine cycle was simulated to analyze its technical and

economical performances. Furthermore, the energy produced from the power plant was compared to the high demand loads of the city during the two selected months of the year.

The solar field dimensions can be determined in the software by two different ways. The first option gives the user the possibility to size the solar field by choosing the desired solar multiple, then the number of parabolic collectors, number of loops, area of the solar field and thermal output are automatically calculated by the software. However, the second option allows the user to determine the number of collectors then after the solar multiple and the different other parameters are determined by the system. In the present system, the number of collectors was determined using the estimated thermal output of the plant and also the load.

The heat transfer fluid plays a key role in the calculation of solar field parameters. Different commercial heat transfer fluids are available in the system. The inlet and outlet temperatures of the medium and its flow rate range in the loops is fixed by the user. Furthermore, it is also possible to define new properties of a selected fluid that are not available in the software. Due to its low freezing temperature which leads to a low electricity consumption by the power plant to keep the fluid in liquid state, Therminol VP-1 was used in the solar field to absorb the solar irradiation. Table 3.1 shows the different properties of Therminol VP-1

Table 3.1: Therminol VP-1 properties

Name	Type	Minimal operating temperature	Minimal operating temperature	Freeze point	Comment
Therminol VP-1	Mixture of Biphenyl and Diphenyl Oxide	12ºC	400ºC	12ºC (crystallization point)	Standard for current generation oil HTF systems

The solar field configuration is constituted from several loops; each loop contains a multitude of solar collectors Figure 3.6. The number of loops and collectors in each loop depends on the thermal energy needed by the power block.

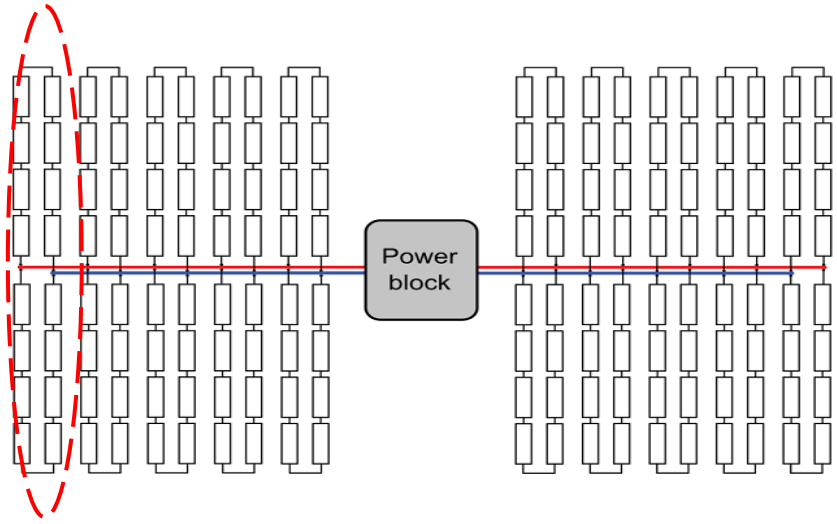

Source: (Kariuki K., 2013)

Figure 3.6: Alignment of the Solar field

The library of the software contains several types of solar collectors and receivers, but only four types are possible to be chosen for one loop. the selection of the two components was done according to their cost and technical performances comparing to the remaining available options [57].

The characteristics of the parabolic trough collector and the heat collector receiver are presented in the two tables below Table 3.2 and 3.3 [58] [59].

In other to support the demand of the power block and also a to have solar multiple of 2, it was necessary to have a solar field with 146 loops and a reflective area of 954840 m^2.

Table 3.2: Euro trough ET 150 characteristics

Euro trough ET 150	
Focal Length	1.71 m
Absorber Radius	3.5 cm
Aperture Width	5.77 m
Aperture Area	817.5 m^2
Collector Length	148.5 m
Number of Modules per Drive	12
Number of Absorber Tubes	36
Mirror reflectivity	94%
Weight of steel structure and pylons, per m^2 aperture area	18.5 kg

Table 3.3: Schott PTR 70 Receiver characteristics

SCHOTT PTR 70 Receiver	
Length	4.060 m
Outer diameter	70 mm
Solar absorptance	0.95
Glass envelope	Borosilicate glass Outer diameter 125 mm Antireflective coating Solar transmittance: $\tau \geq 97\%$
Operating pressure	$\leq$ 41 bar (Absolute)

The amount of thermal energy produced from the solar field is determined by the software and it mainly depends on the direct normal irradiance (DNI), velocity of the HTF entering the solar field, ambient temperature and the wind speed and other parameters provided by the weather file. This is shown in Figure 3.7 below [60].

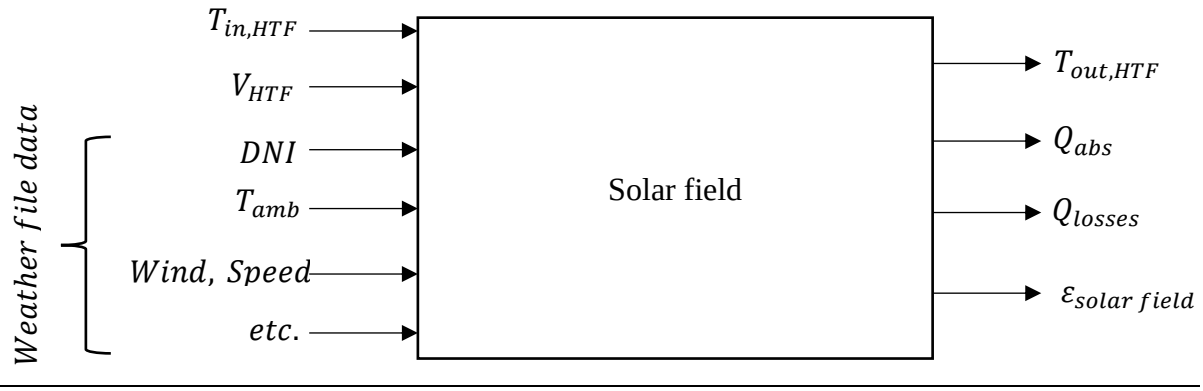

Source: (Kariuki K., 2013)

Figure 3.7: Flow of information in the solar field

N.B: The Average hourly data presented in Figure 3.4 was used to determine the design point of the solar field.

Because of the negative effect of dust deposit on the mirrors and it high abundance in the desert. The number of washes per year was increased to 96 (2 washed per week) Figure 3.8.

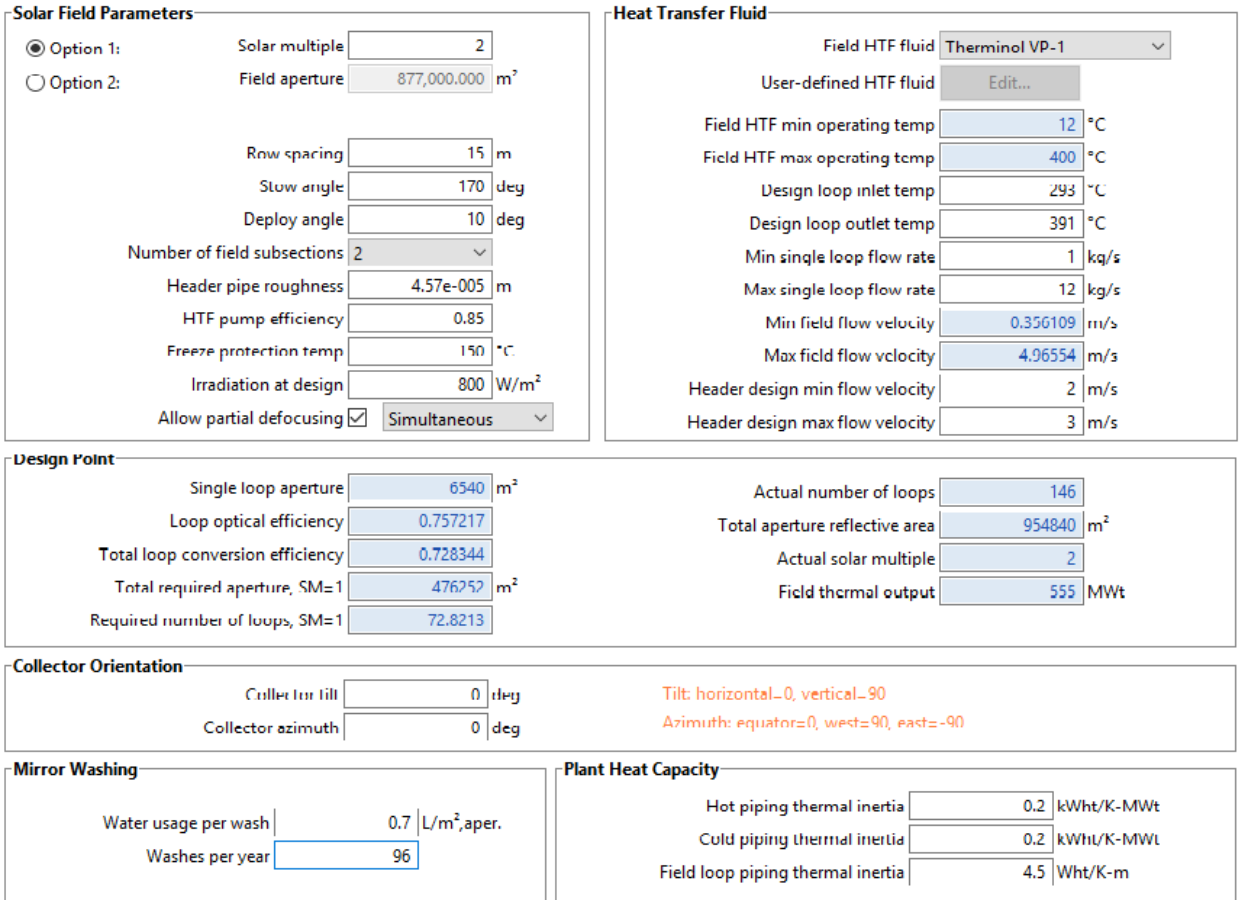

Figure 3.8: Solar field characteristics

3.5 Power cycle

The power cycle configuration selected in this research was the same explained above in the literature review. The electricity output from the power plant was then assessed. Furthermore, two different technologies of condensers were used in the simulation in order to analyze the performances of the plant using evaporative (wet) cooling and dry cooling technologies. The different characteristics of the system used are defined below in Figure 3.19.

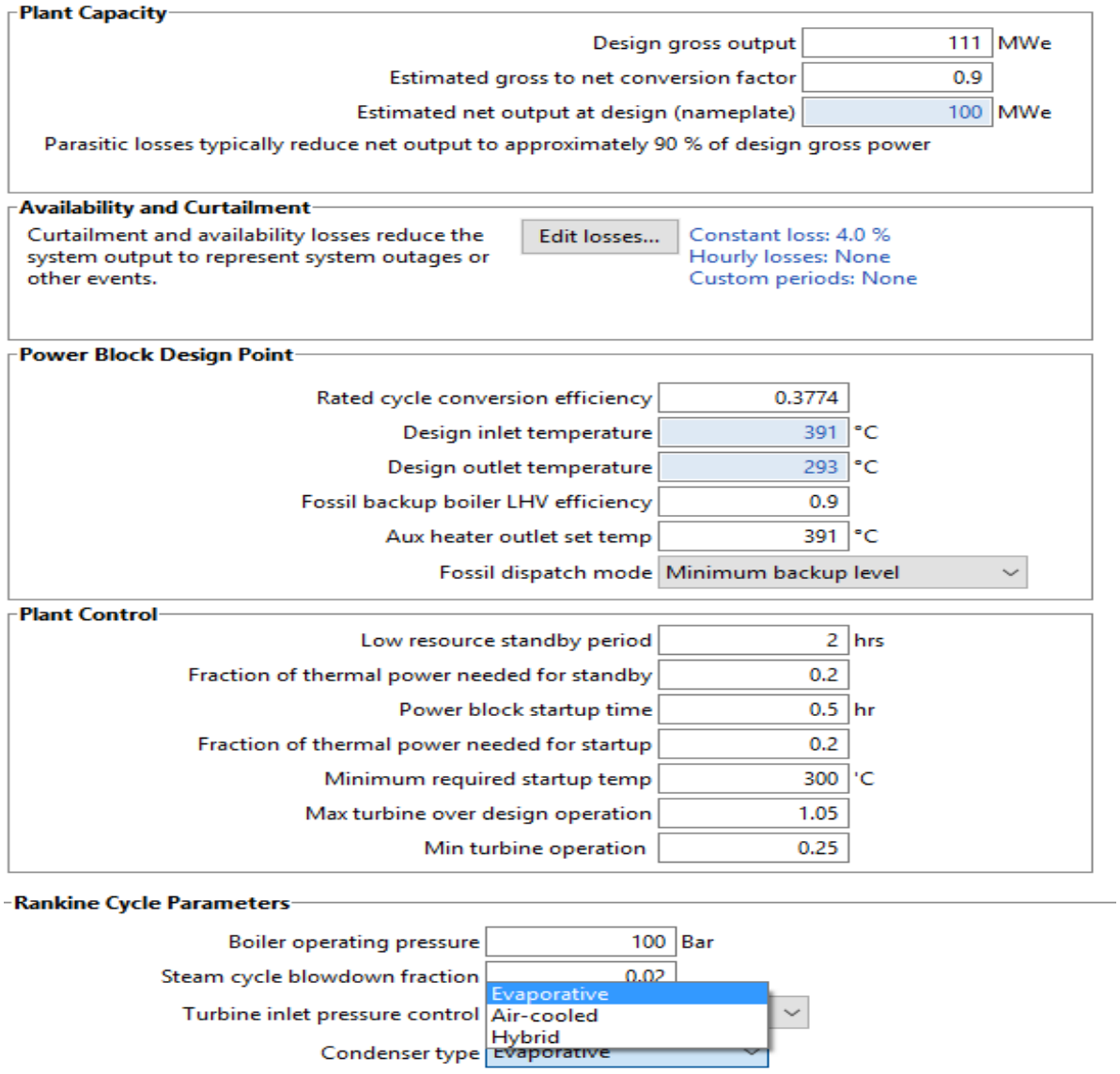

Figure 3.9: Power cycle system in SAM

3.6 Storage system

The power plant included a two tank thermal storage system with indirect active storage system using Therminol VP-1 in the solar field and in the storage tank molten salt. Table 3.4 shows the different properties of the heat transfer fluid used in the thermal energy storage.

Table 3.4: Hitec solar salt properties

Name	Type	Minimal operating temperature	Minimal operating temperature	Freeze point	Comment
Hitec solar salt	Nitrate salt	238ºC	593ºC	238ºC (crystallization point)	Standard for current to tank storage systems

The tank was sized according to the needs of electricity during night times (based peak load design). The maximum number of hours of storage were fixed at 6 hours in order to avoid the oversizing of the backup, where the latter will not be fully charged during the whole time of simulation.

The different properties of the storage system are defined below in Figure 3.10.

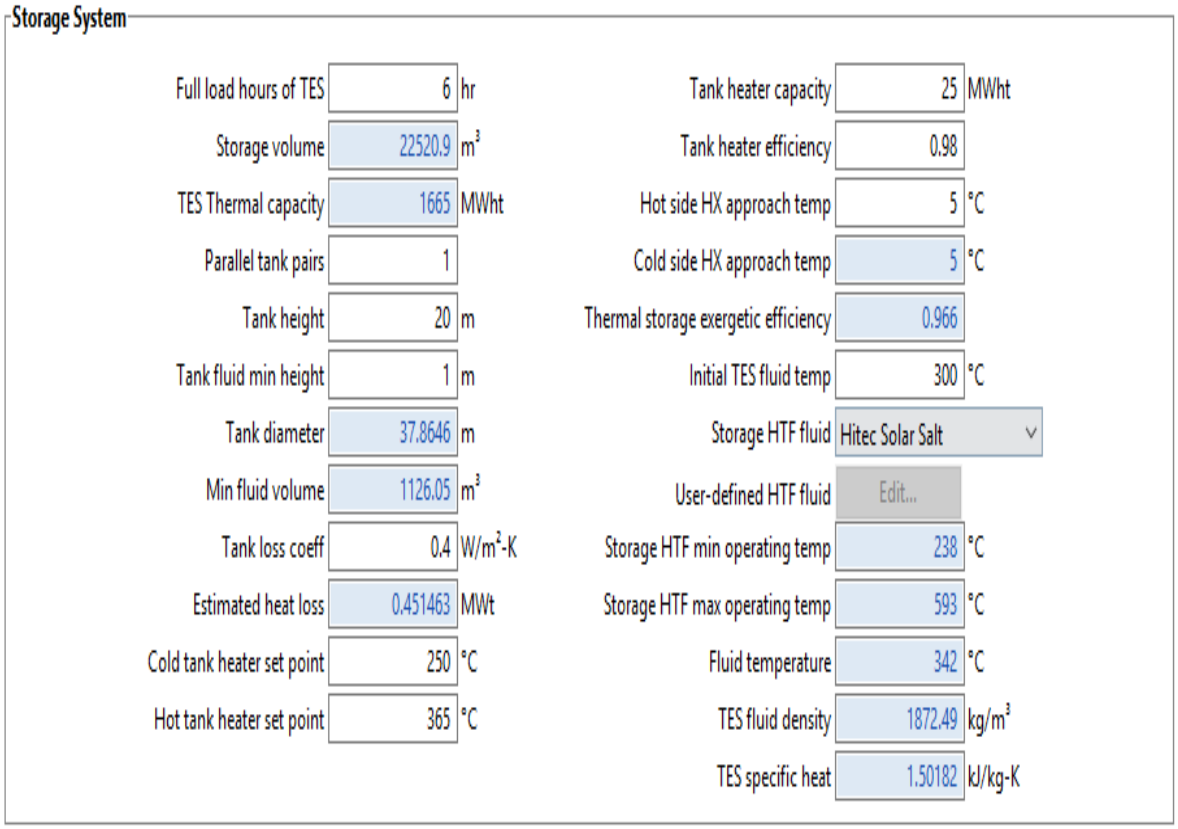

Figure 3.10 Storage system configuration

3.7 Power plant economic analysis

The levelized cost of electricity is the main economical factor used for comparing different energy generation technologies (Solar, wind, biomass nuclear etc.). It is defined as the cost of each unit of energy generated during the analysis period of the selected plant. This factor is calculated using the summation of primary investment and operation and maintenance costs divided by the energy generated from the power plant during its life span. The method used in LCOE calculation is based on net present value approach, where the expenses for investment and the payment flow from earnings and expenses during the system life span are determined based on discounting from a reference date [60].

$$LCOE = \frac{I_0 + \sum_{t=1}^{n} \frac{A_t}{(1+i)^t}}{\sum_{t=1}^{n} \frac{M_{t,el}}{(1+i)^t}} \quad (24)$$

Where:

LCOE: Levelized cost of electricity in Euro/kWh

I_0: Investment expenditures in Euro

A_t: Annual total costs in Euro in year t

$M_{t,el}$: Produced quantity of electricity in the respective year in kWh

i: Real interest rate in %

n: Economic operational lifetime in years

t: Year of lifetime (1, 2, ...n)

Chapter 4. RESULTS AND DISCUSSIONS

Outline:

4.0 Introduction

This chapter gives the different results obtained from the design and simulation of the system. The energy output of two power plants using two different cooling technologies was determined. An analysis of the energy supplied to the city by the power plant using air for cooling and the national grid is exposed. The energy losses from the power plant in form of thermal energy and electricity consumption are determined. Finally, the section ends with an economic analysis of the project.

4.1 Electricity Production

Figure 4.1 shows the monthly energy production by the power plant during the first year of operation, the energy produced is presented separately for each technology of cooling systems. In addition to that, the secondary axis presents the solar irradiation respective to the different considered months.

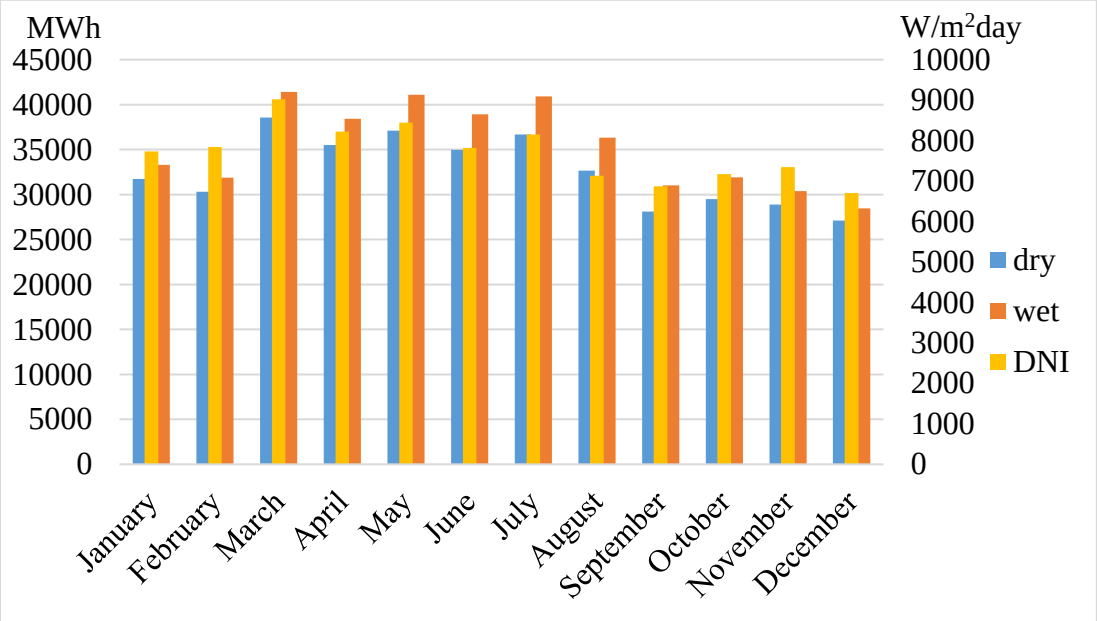

Figure 4.1: Monthly electricity production for 1 year

The best performances of the power plant were recorded during the month of March with a production of 38,575.3 MWh for the power plant using dry cooling system, and 41,421 MWh of energy produced for the power plant running with an evaporative cooling system. As it was

expected the peak of electricity production was found during the month where the solar irradiation was the highest (March).

During the summer season, it was noticed that the ratio of evaporative cooled system electricity production over the system using air was higher than during the remaining months of the year. For example, during the month of June and February where the solar irradiation was almost equal but the energy production was largely different; February (dry: 30,322 MW, wet: 31,876 MW) June (dry: 34,983 MW, wet: 38,918 MW). The difference in the production is due to the other weather parameters mainly the ambient temperature and also the position of the sun through the year (solar incidence angle). Figure 4.2 below shows how the ratio varies throughout the year where it is clearly shown that the performances of the power plant using air for cooling decreases during summer.

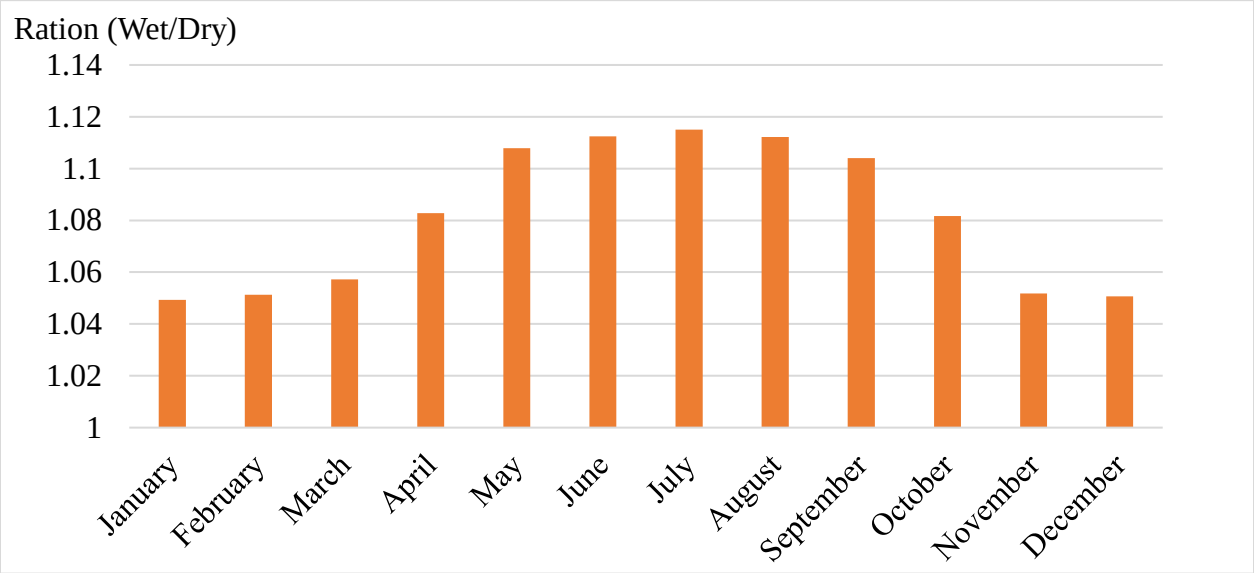

Figure 4.2: Ratio of energy produced by wet and dry cooled power plant

Figure 4.3 shows the difference of the solar incidence angle (θ) between the month of February and June. Since the thermal energy absorbed by the heat collector assembly is proportional to the incidence angle, it was found that the receiver absorbed more thermal energy in the month of June than in February, although the irradiation during the month of February was slightly higher than the one of June.

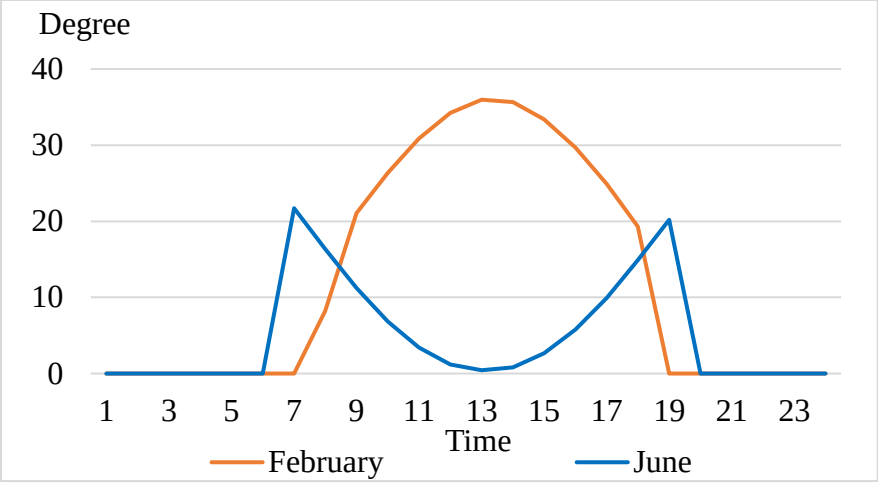

Figure 4.3: Solar incidence angle

Furthermore, the large difference in the ambient temperature between the two months shown in Figure 4.4 also affects the electricity production of the power plant. For the plant using air for cooling the efficiency of the power block was found to be lower compared the one in winter season. The efficiency of the of the cycle for dry cool system was found 35% for the month of February. However, during the month of June the efficiency was 31%. For evaporative cooled system, the efficiency of the cycle was not much affected by the ambient temperature since the efficiency in the month of February was 35% where in June it decreased by 1% to be 34%.

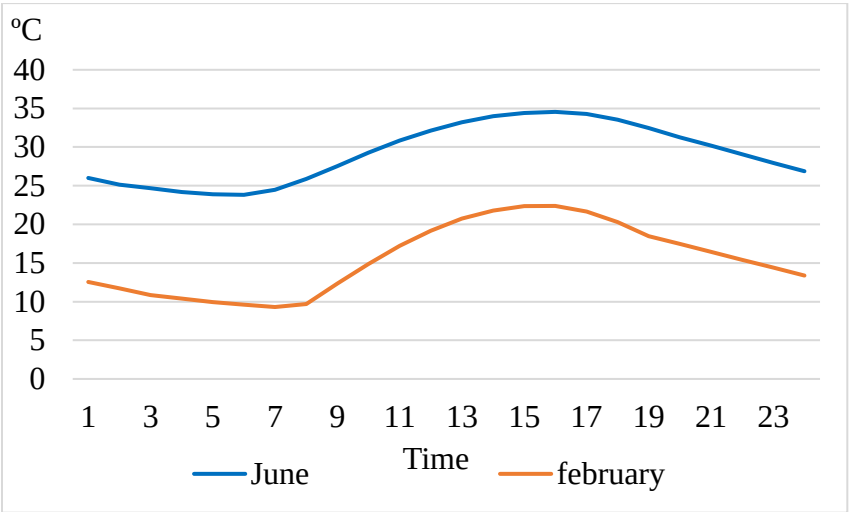

Figure 4.4: Dry bulb temperature

It is clearly shown in the graph that the electricity production from the power plant using evaporative cooling system is higher than the one using dry cooling system. In order to quantify

the difference, the solar efficiencies of the two system, and the capacity factor of each power plant were calculated.

The solar efficiency of the power plant using the two different cooling systems was calculated using:

$$\varepsilon_s = \frac{Actual\ out\ put\ of\ the\ plant}{Total\ incident\ irradiation} * 100$$

Since the capacity factor is the ratio of the actual output during a specific period of time over the amount of energy produced from the power plant when it is working at full nameplate, the equation (20).

Table 4.1: Power plant solar efficiency and capacity factor

	Solar efficiency	**Capacity factor**
Dry cooling	14.5%	44.6%
Evaporative cooling	15.3%	48.3%

According to the results found in Table 4.1 above, the performance of the power plant using water for cooling is slightly higher than the one using air.

4.2 Water Use

Figure 4.5 shows the amount of water flow consumed per hour in the power block and steam generation for the dry and evaporative cooling systems. The water usage in parabolic trough power plant is divided into; parabolic trough washing, steam generation and cooling system. It was found that a huge difference existed between the two systems since the air cooled system use water only for steam generation and the washing of mirrors. However, the evaporative cooling system consumes water 14 times more than the one using air. Furthermore, the highest water consumption was noticed during the months where the solar irradiation was highest specially the month of March where it reaches 277,777.9 kg/h for evaporative system and 8,831.98 kg/h for air cooled system.

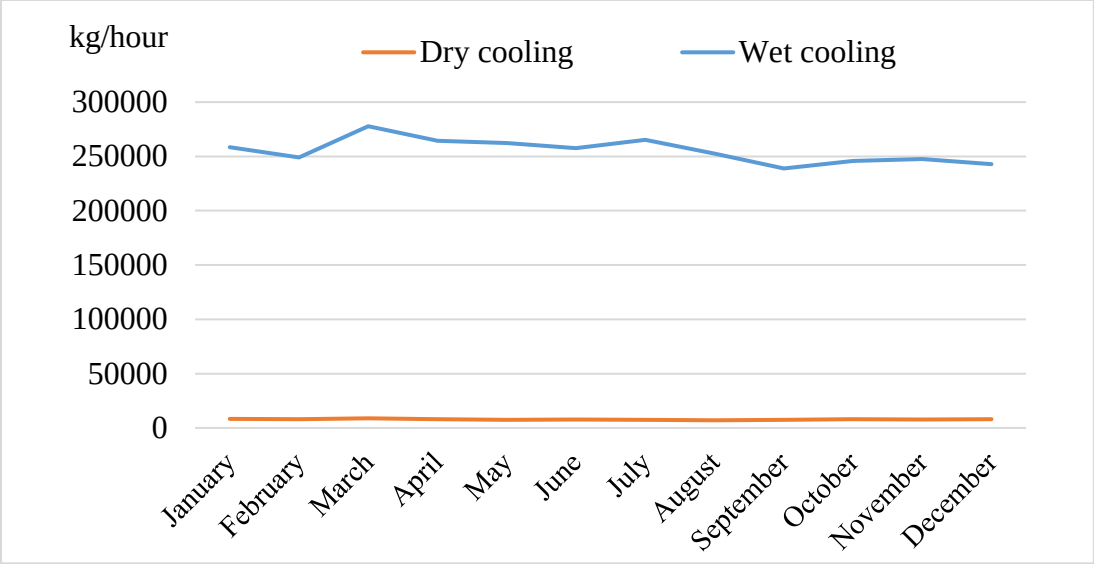

Figure 4.5: Power plant water usage (kg/hour)

In addition to the consumption due to steam generation and power block systems, it was found that the washing of the collectors does not take a big amount of water in wet cooling system comparing to the power block since for a regular washing of two times per week with an amount of 0.7 L for each $1m^2$ of reflective area it consumes around 84,000 m^3 per year, counting for less than 5% from the total water consumption. However, for Air cooled power plant, the water consumed by the washing of mirrors account for almost 60%.

In addition to the enormous quantity of water used in the wet cooling power plant, its scarcity in the region and also the slight difference in electricity production between the two systems. The comparison of the energy produced and the demand, thermal energy storage performances, economic analysis and avoided CO_2 emissions were discussed only for the power plant using air- cooled condensers.

4.3 Load and Electricity Production

Figures 4.6 and 4.8 show the energy demand and supply for the city of Tamanrasset during the two selected moths August and January. The results that was generated shows how the power plant support the grid in order to satisfy the demand of the city.

During the month of January, the system was able to provide up to 1,032,785.5 kWh per day, in the same time the power plant was consuming around 8,670 kWh and it is presented in the graph by negative values. The consumed energy was provided by the grid and it is used by the

power plant to keep the temperature of the heat transfer fluid above the freezing point in the storage tanks and the receivers and also other services related to the operation of the power plant.

During day time and when the solar irradiation was high (from 10 am to 18 pm), the system was generating enough energy to satisfy the needs of the city, supplying the electricity excess to the grid and injecting the excess of thermal energy to the thermal energy storage. On the other hand, the storage tank continued supplying energy till 23 pm when the solar irradiation was not existent. However, from 23 pm to 9 am only the grid was supplying electricity to the city.

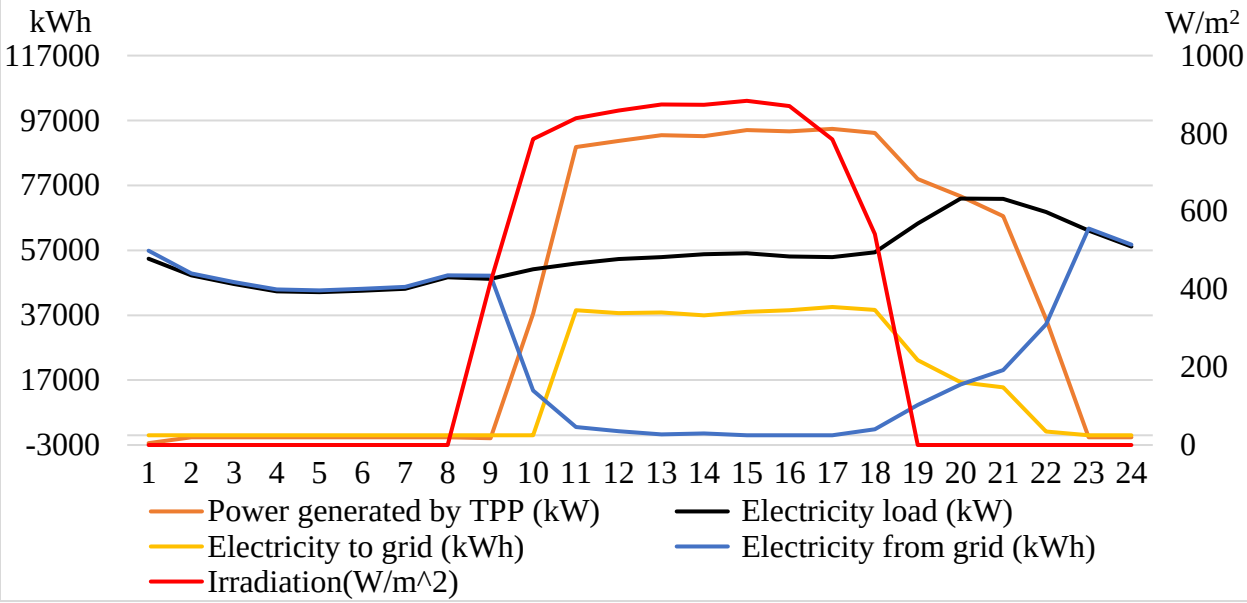

Figure 4.6: January electricity supply

For the whole month of January, the power plant supplied 78% of the energy demand, while the grid supplied the remaining 22%. Table I.1 in the appendix presents the different details of the energy demand and supply system during one day in January.

Figure 4.7 shows the charging and discharging periods of the thermal energy storage. The designed capacity of the storage tank is 1,665 MW_{th}, however, during the month of January it was noticed that the tank was supplied only by 930 MW_{th}. When the sun irradiation was not enough to meet the demand (5 pm), the thermal energy storage started supporting the power block with thermal energy in order to supply enough electricity to the city. However, between 6 to 10 pm only the grid and the thermal energy storage with a share of (91% electricity from the storage and 9% from the national grid) were supplying electricity to the population.

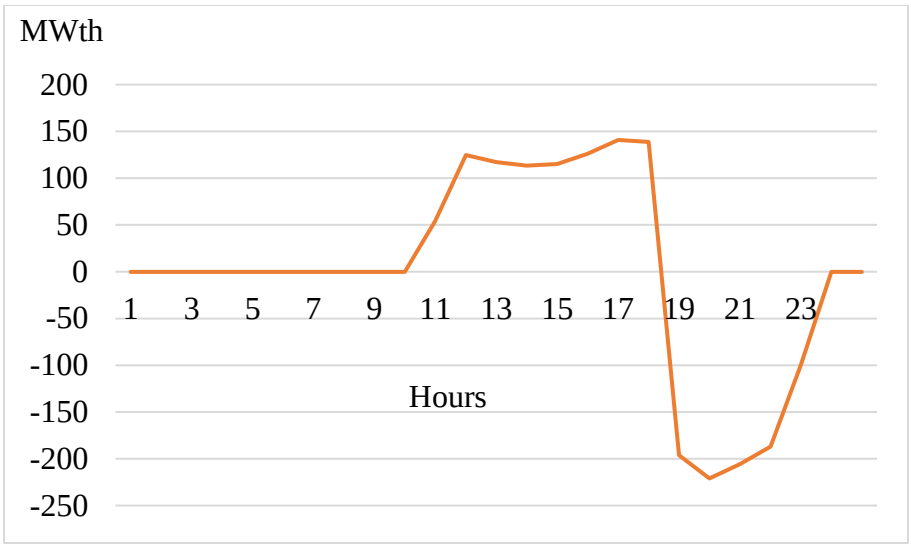

Figure 4.7: Charging and discharging of the TES

Figure 4.8 shows the electricity supply and demand system during the month of August, it is clearly shown by the load curve that the electricity demand is very high in summer than in winter. From the generated results, the power plant was able to cover only 60% from the total demand, and the national grid was feeding the remaining 40% in order to satisfy the needs of the city.

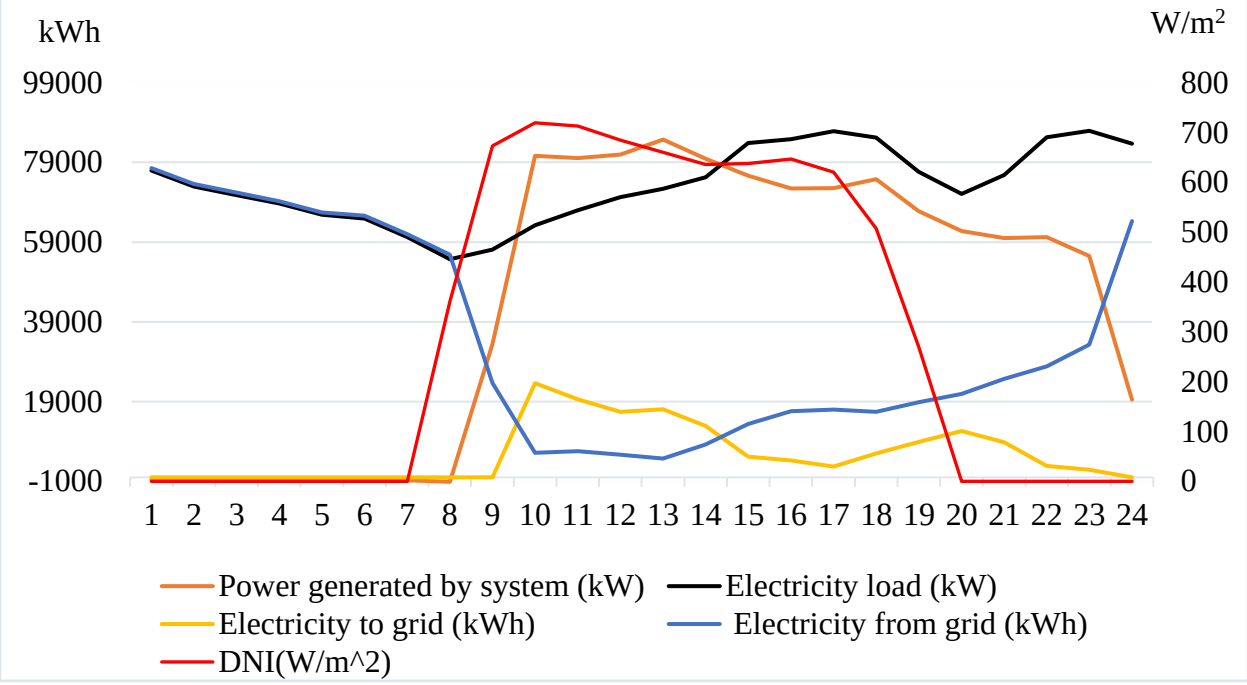

Figure 4.8: August electricity supply

For the month of August, it was noticed that the power plant was able to satisfy the needs of the city only for 5 hours per day from 9 am to 1 pm. However, the production of electricity lasted until midnight. On the other hand, the grid supplied electricity to the system during the whole day, in the same time the power plant was also supplying electricity sometimes to the grid. Table I.2 in the appendix presents the different details of the energy demand and supply system during one day in August.

The electricity produced by the power plant in the month of August was superior to the production in January with a notable surplus of almost 27, 000 kWh. This surplus however has no relationship with the intensity of irradiation, but is a function of the number of daylight hours; 12 hours for August compared to 10 hours for January. Furthermore, it was observed that the losses in the month of August tail those of January owing to the difference in ambient temperatures experienced during the two months. The maximum temperatures for the month of January is recorded at 20 ºC, while the month of August registered a minimum temperature of 25 ºC, with a peak of 35 ºC. This lead to less electricity consumption for the power plant.

Figure 4.9 shows the charging and discharging of the thermal energy storage during the month of August. During the day in presence of sun irradiation the thermal storage was fed by 950 MW_{th}, During the night when the electricity generated directly from sun irradiation was not enough to meet the demand, the storage tank supplied the thermal energy to the steam generation system. Due to the thermal losses from the tanks by convection with the ambient and also the efficiency of discharging process, the thermal energy storage tank supplied 930 MW_{th}. Finally, during the night the electricity that was generated using the thermal energy stored in the tank represented 64% from the demand. However, the grid supplied the 36% that was needed to meet the load demand.

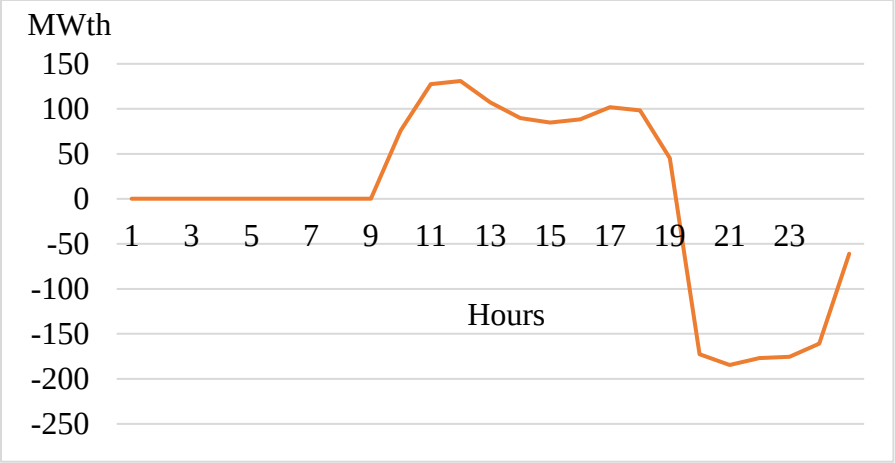

Figure 4.9: Charging and discharging of the TES

4.4 Parasitic losses

Figure 4.10 below shows the different energy losses that occur during the operation of the power plant.

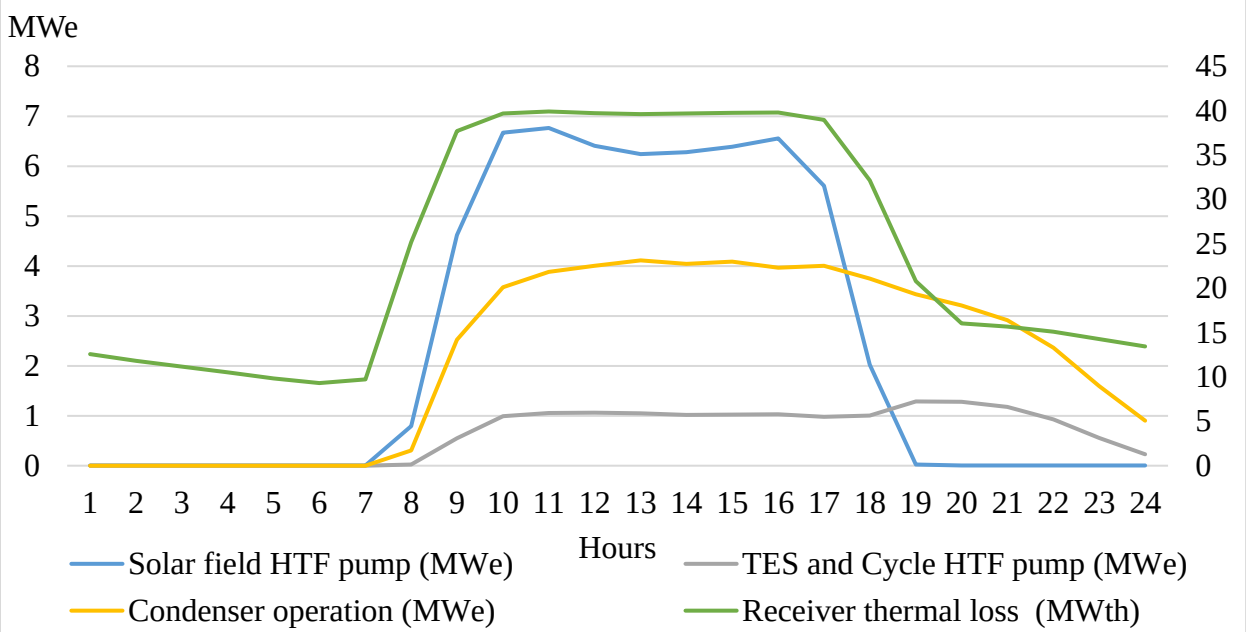

Figure 4.10: Parasitic losses of the system

During the normal operation of the power plant it was noticed that only energy losses due to the solar field heat transfer fluid pump, condenser operation and receiver thermal losses were important. Since the heat transfer fluid pumps in the solar field works only in the morning when the solar irradiation is available, it was noticed that the losses are inexistent during the night time.

However, for the condenser electricity consumption stays almost constant during pick electricity production reaching 4MW, where in the night it decreases with the decrease of electricity production. On the other hand, the pump that circulates the molten salt in the thermal energy storage cycle consumed for charging around 1 MW_e during the day, but in the night time the consumption increased slightly to reach 1.2 MW_e because of the energy storage discharging. These previous losses are called parasitic losses because they refer to the electricity consumed by the power plant itself. However, thermal losses were found to be mainly due to the receiver losses where the latter reached 40 MW_{th} during pick hours and 15MW_{th} when the sun is not present.

4.5 Cost Analysis

In order to calculate the levelized cost of electricity, the different parameters shown in Table 4.2 below were taken into account were taken to estimate the initial cost of investment.

Table 4.2: Cost assumptions for the simulation

SM=2	**Storage= 6 hours Dry-cooled**	
Direct costs		Cost (Labor taken into account)
Land and site improvement	954840 m^2	2008.8 DA/m^2
Solar field	954840 m^2	50220 DA/m^2
Heat transfer fluid system	954840 m^2	5022 DA/m^2
Storage	1665 MW_{th}	7030.8 DA/KW_{th}
Power plant capacity	110 MW_e	88387.2 DA/kW_e
Contingency	Approx. (10%)	6,179,699,563.20 DA
Inflation rate	4.85	
Interest rate	4	
Initial cost	67,976,695,195.20 DA	

In Addition to the initial costs, the operation and maintenance were taken approximately equal to 1% from the initial investment. Furthermore, the cost of insurance and taxes rate were

also taken into consideration. The interest rate of 4% used in this study was obtained from the web site of Trading Economics [61], and the inflation from the web site of the Algerian ministry of finance [62].

Using the equation of the levelized cost of electricity (26), it was found that the LCOE was lower comparing to the international pricing with a value of 8.19 DA/kWh. This low value of LCOE is due to the high potential of solar energy in the site therefore high electricity production. On the other hand, the payback period was calculated and found equal to 8.78 years (the different cost calculations are presented in figures I.3, I.4, I.5 and I.6 in the appendix).

The power plant was designed for a life span of 25 years. On the other hand, the feed in tariff was taken according to the Algerian program for renewable energies with a value of 300% which gives a selling price of 12 DA/kWh for the whole life span factored by the inflation rate [63]. The benefit-cost ratio was therefore found to be 1.73 which mean the project makes profit more than expenses.

Figure 4.11 below shows the cash flow analysis of the designed power plant for the entire lifespan of 25 years.

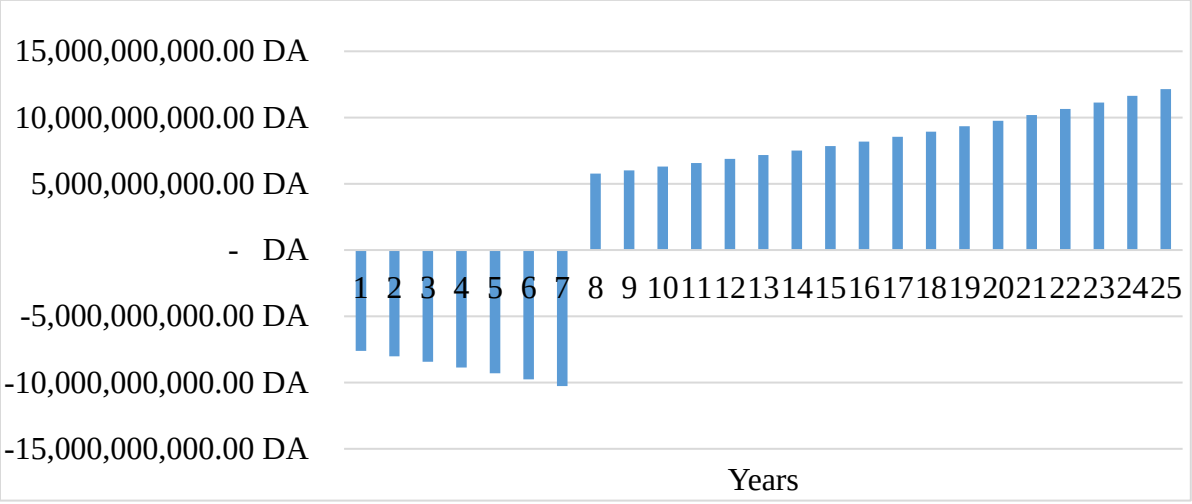

Figure4.11: Cash flow of the investment

The cash flow analysis shows precisely how the amount of money is being transferred into and out of the project. For the first five years, the cash flow was negative which means that the project's liquid assets were negative. However, starting from the second year when the power plant

started running the cash flow was positive, this indicates that the liquid assets are increasing and enabling the project to reinvest in the project, make benefits for the owners and also paying other expenses.

Figure 4.12 below shows a sensitivity analysis of how the levelized cost of electricity can be affected when changing the solar multiple and also storage hours.

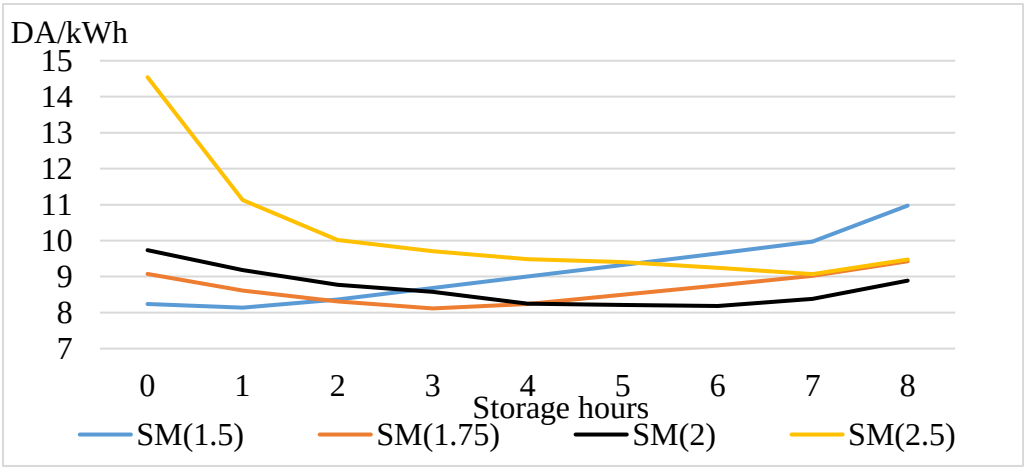

Figure 4.12: LCOE as function of storage hours and solar multiple

It was found that for each solar multiple there is an optimum thermal energy storage hour that gives the lowest LCOE, the lowest LCOE of 8.11 DA/kWh was found in the system that has a solar multiple of 1.75 and 3 hour of energy storage. In the other hand, above the solar multiple of 1.75 it is clearly shown that with the increase in storage hours and solar multiple the cost of energy increases as well. For a given power plant, they are many solar multiples and storage configuration combinations possible. However, the lowest LCOE can be found by varying the storage hours for a fixed solar multiple. For already determined project specification the optimal combination is chosen with taking the LCOE and also the project requirements into consideration.

4.6 CO_2 Gas Emission:

In order to estimate the environmental benefit of the project in terms of CO_2 emissions, a comparison between combined cycle power plant using gas as fuel and the simulated power plant, in average the amount of CO_2 emitted by a combined cycle power plant using gas is 400 kg/MWh [64].

It was found that for the same energy generated for one year the combined cycle power plant can produce almost 2 million tons of CO_2 per year Figure 4.13. Therefore, it is clearly shown that without any harm gas emissions, parabolic trough constitutes a better option than conventional systems for electricity generation.

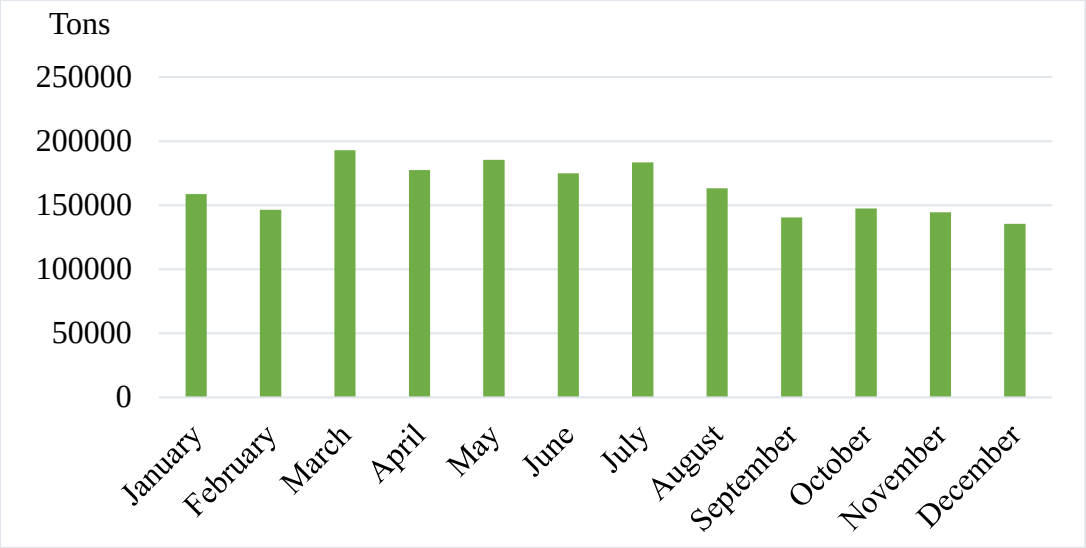

Figure 4.13: CO_2 emissions avoided

Chapter 5. CONCLUSION AND RECOMMENDATIONS

Outline:

5.0 Introduction

This chapter presents conclusion on all the findings of the research in a chronological order of its preset objectives and some recommendations for further researches are outlined herein.

5.1 Conclusion

Algeria has engaged in the promotion of renewable energy resources in order to come up with sustainable and global solutions to mitigate present environmental challenges and also the preservation of conventional energy resources. The renewable energy program that the country has adopted takes into consideration all forms of renewable energy, concentrating solar energy took a share of 10% from the targeted installed capacity. This research dealt with a simulation of 100 MWp parabolic tough power plant using two different cooling systems: dry and evaporative condensers. The power plant was designed with a solar multiple of 2 generating excess energy stored by thermal energy storage working with the globally used technology of indirect two tanks (cold/hot) thermal storage using molten salt. Thereafter, a feasibility study was performed to check whether such project can be implemented in Algeria under the climatic condition of Tamanrasset and also law governing renewable energies in Algeria.

First, different concentrating solar energy technologies were reviewed. Among the four CSP technologies that exist, only central receiver tower and parabolic trough technologies are implemented for large scale electricity production projects. However, in this study parabolic trough technology was adopted because until today it has shown more maturity and cost effectiveness compared to the technology using central receiver tower.

The electricity production of the power plant was found to be different for the two cooling technologies namely, air-cooling and water cooling. The peak of electricity production was found to be in the month of March for both technologies. However, the amount of electricity produced in the power plant using water cooling was higher for all remaining months than the air cooled-system. The ratio of electricity produced from wet over dry cooling systems was found to vary approximatively from 1.04 to 1.12 throughout the year. Therefore, water cooled system performed better than air cooled system over the whole year with marginal difference during winter season and more important difference during summer. During the month of February and June the solar

irradiation was almost equal while the electricity production for both systems was different. For wet cooled system the difference in electricity production was mainly caused by the difference in incidence angle (θ). However, for dry cooled system in addition to the losses caused by the incidence angle, the ambient temperature seemed to affect the efficiency of the power block lowering it from 35% in February to 31% in June.

The capacity factor of both systems was found higher when compared to other renewable energies. However, the capacity factor of evaporative system was found higher than dry cooled system by 4%. Since the capacity factor was higher in evaporative system, the solar efficiency of the system was also higher with 15.3% against 14.5% for air cooled system. On the other hand, water scarcity at the selected location is a major challenge for the implementation of huge water consuming systems. Thus, with a water consumption of 14 times less than water cooled system, air cooled system was found to be more attractive.

The load of the city was compared to the electricity produced by air cooled power plant during two extreme seasons winter and summer. With a peak of 87 MW during summer and 73 MW in winter, it was found that the system was able to cover the major part of the load. During periods where solar energy was not available. Thermal energy storage provided important amounts of energy to support the grid during night peak demand. The losses of the power plant were found to take two forms; parasitic and thermal losses, both losses were important reaching 10 MW_e for parasitic losses during pick hours where for thermal losses due to receiver tubes during pick hours reached 40 MWth

Cost analysis of the system has shown a lower levelized cost of electricity with the value of 8.19 DA/kWh. Furthermore, the thermal energy storage was found to increase the cost of electricity and also reaching an optimum system for each solar multiple. In addition to the benefit-cost ratio that was found to be 1.73, the payback period of 8.78 years has shown that the project is feasible under the economic conditions imposed by the Algerian government. Environmental impact of the power plant was also evaluated and found to be able to avoid a huge amount of carbon dioxide gas emissions reaching 2 million tons of CO_2 per year. Therefore, parabolic trough technology can be considered as clean source of energy for Algeria.

5.2 Recommendations

Energy production varies depending on the potential and also technologies, in this paper the parabolic trough technology performed very well. However, from the international trends, tower power technology also competitively entered the market. Therefore, further study on utilization of tower power technology should be undertaken.

In this study, the ambient temperature was found to have an effect on the performance of the air cooled condenser of the system. Thus, further investigation should be done on the design of the condensers used in the CSP plants in order to overcome the effect of temperature on its performance.

Furthermore, the dust intensity at the site harm the power plant's equipment in the long term. Research should be undertaken to evaluate the negative effects of dust on the power plant specially mirrors and receivers.

BIBLIOGRAPHY

[1] Factbook CIA world. (01 January 2014). "CIA world factbook," [Online]. Available: http://www.indexmundi.com/g/r.aspx?v=81000. [Accessed 7 April 2016].

[2] Reuters T. (10 February 2016). [Online]. Available: http://www.eia.gov/dnav/pet/pet_pri_spt_s1_d.htm. [Accessed 8 March April].

[3] RECREEE., "Latest electricity price schemes price in RECREEE member states," RECREEE, Cairo, 2013.

[4] Boudghene S, Khiat Z, Flazi S. & Kitamura A. (2012). "A review on the renewable energy development in Algeria: Current perspective, energy scenario and sustainability issues," *elsevier*, pp. 4449-4450.

[5] Ministery of Energy. (2015). "Electricité et Gaz," Minister of energy, Algiers.

[6] CDER. (2013). "National Renewable Energy program," [Online]. Available: https://www.cder.dz/spip.php?article1748. [Accessed 5 May 2016].

[7] Gharbi N. (2011). "CDER," [Online]. Available: http://www.cder.dz/vlib/bulletin/pdf/bulletin_021_11.pdf. [Accessed 2 March 2016].

[8] Messai A, Benkedda Y, Bouaichaoui S. & Mohammed B., "Feasibility study of parabolic trough solar power plant under Algerian climate," *elsevier*, p. 3 – 82, 2013.

[9] Boukelia T. & Mecibah M. (2012). "Parabolic trough solar thermal power plant: Potential, and projects development in Algeria," *elsevier*, p. 297.

[10] Boudghene S. (2011). "Algerian renewable energy assessment: The challenge of sustainability," *elsevier*, p. 4507–4519.

[11] Sonia. (7 August 2012). "Tension dans plusieurs villes touchées par des coupures d'électricité," [Online]. Available: http://algeriepatriotique.com/article/tension-dans-plusieurs-villes-touchees-par-des-coupures-d-electricite.

[12] Schnatbaum L. (2009). "Solar thermal power plants," *The european physical journal*, p. 129.

[13] Mohamed A, Bousaad B, Said N. & Ahmed C. (2011). "Dish Stirling technology: A 100 MW solar power plant using hydrogen for Algeria," *elsevier*.

[14] Boudries R. & Dizene R. (2007). "Potentialities of hydrogen production in Algeria," *elsevier,* p. 4481.

[15] ANDI., "Wilaya fe Tamanerasset," Agence national d investisment, Tamanerasset, 2013.

[16] Abbas M. (2016). "Parametric Study of the installation of a Solar Power Tower plant under Saharan Climate of Algeria: case study of Tamanrasset," *ResearchGate,* pp. 357-362.

[17] Honghang S, Gong B. & Qiang Y. (2014). "A review of wind loads on heliostats and trough collectors," *elsevier,* p. 210.

[18] Sarver, T., Qaraghuli, A & Kazmerski L. (2013). "A comprehensive review of the impact of dust on the use of solar energy: History, investigations, results, literature, and mitigation approaches," *elsevier*, p. 698.

[19] Engelstaedter S, Tegen I. & Washington R. (2006). "North African dust emissions and transport," *elsevier,* p. 73.

[20] Arash S, Horenstein M. & Mazumder M. (2013). "Mitigation of Soiling Losses in Concentrating Solar Collectors," *IEEE,* p. 480.

[21] Agnese P, Perignon F, Ferer A, Maïer P. & Pastor M. (1 January 2015). "Les miroirs ardents d'Archimède ont-ils été une arme plausible lors du siège de Syracuse en -215 avant J.C," [Online]. Available: http://cortecs.org/wp-content/uploads/2016/01/CorteX_s21_49_Miroirs_ardents_Archimede_Agnese_Perignon_Fere_Ma%C3%AFer_Pastor.pdf. [Accessed 2 April 2016].

[22] Lovegrove K. & Stein S. (2013). Concentrating Solar Power Technology, Woodhead, 2012.

[23] Behar O, Khellaf A. & Mohammedi K. (2014). "A review of studies on central receiver solar thermal power plants," *elsevier,* p. 14.

[24] Ummadisingu A. & Soni M. (2011). "Concentrating solar power technology potentialand policy in india," *elsevier,* p. 5171.

[25] Kaltschmitt M, Streicher W. & Wiese A. (2007). Solar Thermal Power Plants, Springer Berlin Heidelberg.

[26] Pavlovic T, Radonjic I, Milosavljevic D. & Pantic L. (2012). "A review of concentrating solar power plants in the world and their potential use in Serbia," *elsevier,* p. 3893.

[27] Goswami D. (2015). Principles of solar engineering third edition, New york: Taylor & Francis Group.

[28] Guangdong Z, Wendelin T, Wagner M. & Kutscher C. (2013). "History, current state, and future of linear Fresnel concentrating solar collectors," *elsevier,* pp. 2-11.

[29] Romero M. & Gonzalez-Aguilar J. (2014). "Solar thermal CSP technology," *John Wiley & Sons,* pp. 42-45.

[30] Giostri A, Binotti M, Astolfi M, Silva P, Macchi E. & Manzolini G. (2012). "Comparison of different solar plants based on parabolic trough technology," *elsevier*, pp. 1209-1214.

[31] Price H, Eckhard L, Kearney D, Zarza E, Cohen, G. & Mahoney R.(2002). "Advances in Parabolic Trough Solar Power Technology," *American Society of Mechanical Engineers,* pp. 109-125.

[32] Zarza E. & Moya C. (2012). Parabolic-trough concentrating solar power (CSP) systems, Woodhead.

[33] Baharoon D. & AbdulRahman H. (2015). "Historical development of concentrating solar power technologies to generate clean electricity efficiently – A review," *Elsevier,* p. 996–1027.

[34] Baharoon D. (2014). "Concentrating solar power technologies to generate clean– A review," *Elsevier,* p. 4–14.

[35] Duffie J.& Beckman W. (2013). Solar Engineering of Thermal Processes, New Jersey: USA.

[36] Patnode A. (2006). "Simulation and Performance Evaluation of Parabolic Trough Solar Power Plants," WISCONSIN-MADISON.

[37] Goswami D. & Kreith F. (2016). Energy Efficiency and renewable energy handbook, New york: Taylor and Francis Group.

[38] Forristall R. (2003). "Heat Transfer Analysis and Modeling of a Parabolic Trough Solar Receiver Implemented in Engineering Equation Solver," National Renewable Energy Laboratory, colorado.

[39] Bergman P, Lavine A, Incorpera F. & Dewit D. (2011). "Fundamentals of heat and masss transfer," JOHN WILEY & SONS, United States of America.

[40] Simões-Moreira J. (2012). "Fundamentals of Thermodynamics," in *Thermal Power Plant*, springer, pp. 7-39.

[41] Kehlhofer R. (2009). "Combined-Cycle Gas and steam turbine power plants," PennWell, Oklahoma.

[42] Damerau K, Williges K, Patt A. & Gauche P. (2011). "Costs of reducing water use of concentrating solar power to sustainable levels: Scenarios for North Africa," *elsevier*, p. 4393.

[43] Scott J, Blair N, Pitz-Paa R, Schwarzboezl P. & Cable R. (2001). "TRNSYS modelling of the SEGS VI parabolic trough solar electric generating system," *ASME*.

[44] Swapan B. & Debnath K. (2015). Power Plant Instrumentation and Control Handbook A Guide to Thermal Power Plants, London: Elsevier.

[45] Winter C, Sizmann R. & Vant-Hull L. (1991). Solar Power Plants Fundamentals, Technology, Systems, Economics, Berlin: Springer-Verlag.

[46] Herrmann U. & Kearney D. (2002). "Survey of Thermal Energy Storage for Parabolic Trough Power Plants," *Journal of Solar Energy Engineering*, pp. 145-152.

[47] Kuravi S, Trahan J, Goswami Y, Rahman M. & Stefanakos E. (2013). "Thermal energy storage technologies and systems for concentrating solar power plants," *elsevier*, pp. 285-319.

[48] Gil A, Medrano M, Martorell I, Lazaro A, Dolado P, Zalba B. & Cabeza L. (2010). "State of the art on high temperature thermal energy storage for power generation. Part 1—Concepts, materials and modellization," *Elsevier*, pp. 31-55.

[49] Vignarooban K, Xinhai X, Arvay A, Hsu K. & Kannan A. (2015). "Heat transfer fluids for concentrating solar power systems – A review," *elsevier*, pp. 383-396.

[50] Ameur T. & Mohand A. (2014). "Determination of the optimum design through different funding scenarios for future parabolic trough solar power plant in Algeria," *elsevier*, p. 267–279.

[51] Zaaraoui A, Yousfi M & Said N. (2012). "Technical and Economical Performance of Parabolic Trough Collector Power Plant under Algerian Climate," *elsevier,* p. 78 – 91.

[52] Chukwubuikem C. & Komla, F. (2015). "An Economic Assessment of the Concentrated Solar Power with National Energy Regulator of South African Feed-in Tariff Scheme," *Journal of Energy and Power Sources,* pp. 137-143.

[53] Kariuki K. (2012). "Technical and Economic Analysis of Parabolic Trough Concentrating Solar Thermal Power Plant," Cape town.

[54] Remun J. & Müller S. (2015). Meteonorm, Bern: Meteotest.

[55] Dimitar I. (2010). "Discrepancies in solar irradiation data for Stokholm and Athens," SERC,

[56] Bilgekul. & Huseyin. (2010). "Open courses," [Online]. Available: opencourses.emu.edu.tr/mod/resource/view.php?id=143&redirect=1. [Accessed 8 June 2016].

[57] Wagner M. & Gilman P. (2011). "Technical Manual for the SAM Physical Trough Model," NREL, Colorado.

[58] Geyer M. & Lüpfert E. (2002). "EUROTROUGH - Parabolic Trough Collector Developed for Cost Efficient Solar Power Generation," in *SolarPACES International*, Zurich.

[59] Schott Solar. (2013). "SCHOTT PTR 70 Receivers," Solar Schott, Hattenbergstrasse.

[60] Kost C. (2013). "Levelized Cost of Electricity Renewable Energy Technologies," Fraunhofer Institute For Solar Energy Systems ISE, Freiburg.

[61] Trading Economics (01 April 2016)."Trading Economics," [Online]. Available: http://www.tradingeconomics.com/algeria/interest-rate. [Accessed 15 July 2016].

[62] Ministry of finance (23 June 2016). "Taux d'inflation," [Online]. Available: http://www.mf.gov.dz/index.php. [Accessed 6 July 2016].

[63] Meyer-Renschhausen. (2013). "Evaluation of feed-in tariff-schemes in African countries," *Journal of Energy in Southern Africa,* pp. 56-66.

[64] ESTAP. (2010). "Gas-Fired Power," IEA.

[65] Chellali F, Khellaf A, Belouchrani A. & Recioui A. (2010). "A contribution in the actualization of wind map of Algeria," *elsevier.*

[66] Flowserve. (2016). "Concentrated Solar Power," [Online]. Available: https://www.flowserve.com/Industries/Power-Generation/Concentrated-Solar-Power.

[67] Shahin M. (2009). "Review and Assessment of Water Resources in the Arab Region," *Taylor & Francis,* p. 215.

[68] Comsan. (2010). "Solar energy perspective in Egypt," in *4th Environmental Physics Conference*, Hurghada.

[69] Algerie-monde (2010). "Tamanrasset," [Online]. Available: http//www.algerie-monde.com/hotels/tamanrasset/. [Accessed 04 July 2016].

APPENDIX

Table I.1: Electricity supply and demand system (January)

Time of day (January average)	Power generated by the TPP (kW)	Electricity load (kW)	Electricity to grid (kWh)	Electricity from grid (kWh)
0	-2427.56	54412.6	0	56840.2
1	-593.777	49264.7	0	49858.4
2	-590.931	46605	0	47195.9
3	-590.865	44313.1	0	44904
4	-590.826	44102.4	0	44693.2
5	-590.788	44511.2	0	45102
6	-590.75	45129.5	0	45720.3
7	-590.72	48670.5	0	49261.2
8	-921.725	48233.2	0	49154.9
9	37402	51171.6	0	13769.6
10	88838.6	52915.5	38490	2566.8
11	90734	54283.5	37659.1	1208.59
12	92433.1	54939.1	37795.3	301.269
13	92149.4	55792.6	36924.8	568.002
14	94094.2	56093	38001.2	0
15	93618	55078	38539.9	0
16	94418.4	54886.6	39531.9	0
17	93195	56406.3	38637.4	1848.66
18	78980.7	65234.7	23107.4	9361.44
19	73633.1	72944.3	16318	15629.2
20	67506.1	72802.1	14774.7	20070.7
21	35782.9	68839	1143.31	34199.4
22	-591.164	63121.6	0	63712.7
23	-591.103	58111.9	0	58703
(-): negative values mean energy consumed by the system				

Table I.2: Electricity supply and demand system (August)

Time of day (August average)	Power generated by TPP (kW)	Electricity load (kW)	Electricity to grid (kWh)	Electricity from grid (kWh)
0	-591.061	76963.4	0	77554.5
1	-591	72960.4	0	73551.4
2	-590.944	70794.6	0	71385.5
3	-590.893	68662.2	0	69253.1
4	-590.848	65878.5	0	66469.3
5	-716.751	64903.8	0	65620.6
6	-736.631	60256.1	0	60992.7
7	-1115.82	54700	0	55815.8
8	33467.3	57133.1	0	23665.7
9	80652.1	63230.6	23611.3	6189.83
10	80032.6	67021.4	19567.9	6556.68
11	80959.8	70242.1	16400.9	5683.24
12	84713.4	72364.8	17064.4	4715.85
13	79885.1	75242.5	12873.9	8231.29
14	75628.9	83859	5158.14	13388.3
15	72457.6	84793.8	4225.6	16561.9
16	72514.5	86826.9	2701.82	17014.2
17	74809.6	85238	5996.74	16425.1
18	66744.5	76647.8	8918.69	18822
19	61778.5	71102.8	11575.9	20900.3
20	59977.9	75850	8786.35	24658.4
21	60236.8	85253	2849.86	27866.1
22	55540.6	86905.6	1918.93	33283.9
23	19454.1	83719.7	0	64265.7
(-): negative values mean energy consumed by the system				

Figure I.1: Weather file

Figure I.2: Weather file

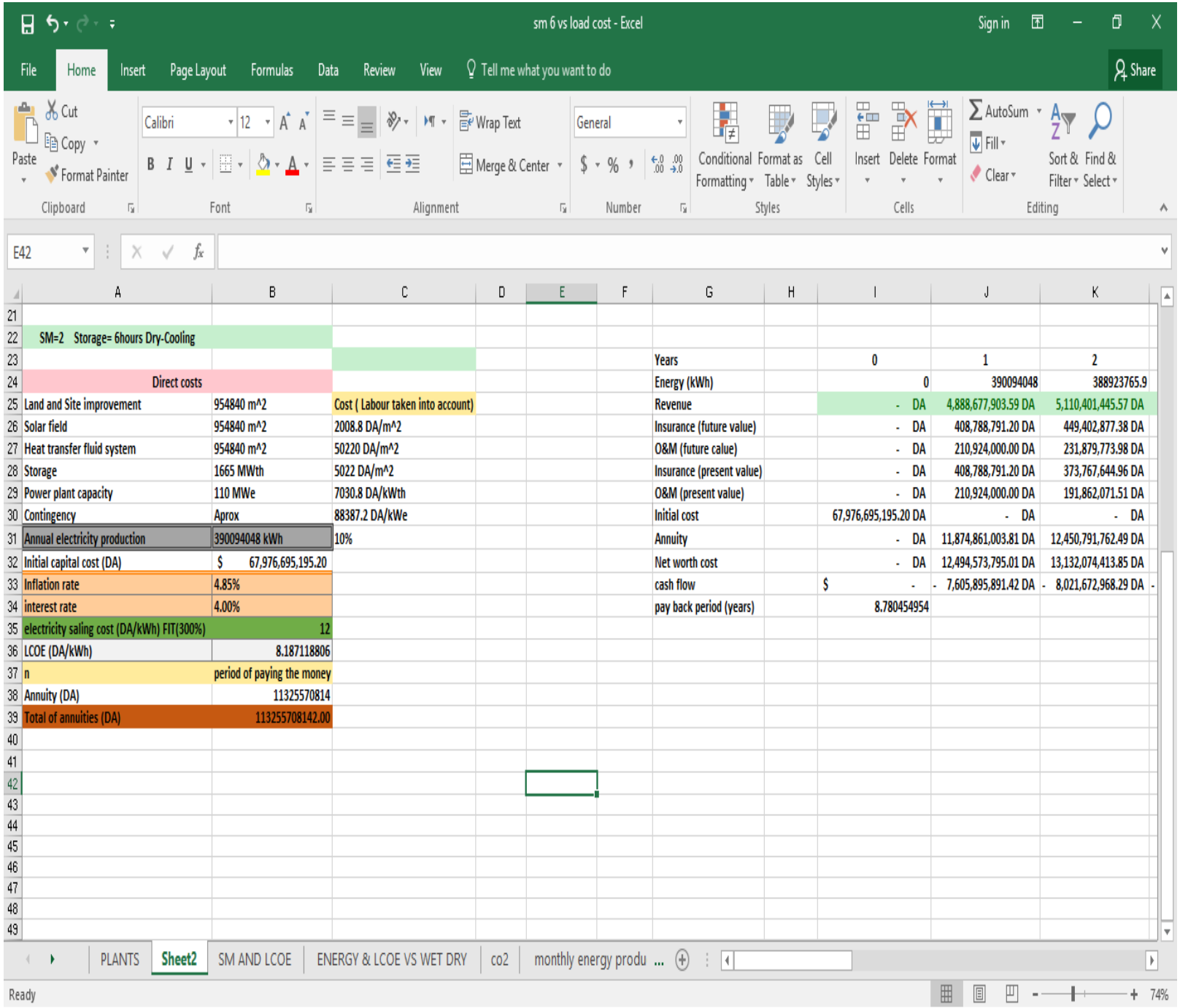

	A	B	C	G	I	J	K
22	SM=2 Storage= 6hours Dry-Cooling						
23				Years	0	1	2
24	Direct costs			Energy (kWh)	0	390094048	388923765.9
25	Land and Site improvement	954840 m^2	Cost (Labour taken into account)	Revenue	- DA	4,888,677,903.59 DA	5,110,401,445.57 DA
26	Solar field	954840 m^2	2008.8 DA/m^2	Insurance (future value)	- DA	408,788,791.20 DA	449,402,877.38 DA
27	Heat transfer fluid system	954840 m^2	50220 DA/m^2	O&M (future calue)	- DA	210,924,000.00 DA	231,879,773.98 DA
28	Storage	1665 MWth	5022 DA/m^2	Insurance (present value)	- DA	408,788,791.20 DA	373,767,644.96 DA
29	Power plant capacity	110 MWe	7030.8 DA/kWth	O&M (present value)	- DA	210,924,000.00 DA	191,862,071.51 DA
30	Contingency	Aprox	88387.2 DA/kWe	Initial cost	67,976,695,195.20 DA	- DA	- DA
31	Annual electricity production	390094048 kWh	10%	Annuity	- DA	11,874,861,003.81 DA	12,450,791,762.49 DA
32	Initial capital cost (DA)	$ 67,976,695,195.20		Net worth cost	- DA	12,494,573,795.01 DA	13,132,074,413.85 DA
33	Inflation rate	4.85%		cash flow	$ -	- 7,605,895,891.42 DA	- 8,021,672,968.29 DA -
34	interest rate	4.00%		pay back period (years)	8.780454954		
35	electricity saling cost (DA/kWh) FIT(300%)	12					
36	LCOE (DA/kWh)	8.187118806					
37	n	period of paying the money					
38	Annuity (DA)	11325570814					
39	Total of annuities (DA)	113255708142.00					

Figure I.3: Economic analysis

Figure I.4: Economic analysis

Figure I.5: Economic Analysis

Figure I.6: Economic analysis

Table I.3: Parasitic losses

Time	Solar field HTF pump	Collector drives	TES and Cycle HTF pump	condenser operation
0	0.00516263	0	0	0
1	0.00510114	0	0	0
2	0.00504495	0	0	0
3	0.00499441	0	0	0
4	0.00494926	0	0	0
5	0.00490919	0	0	0
6	0.00487915	0.0313978	0	0
7	0.790764	0.110168	0.0232353	0.303734
8	4.61644	0.129073	0.551261	2.52399
9	6.66993	0.120835	0.989337	3.57434
10	6.76428	0.121808	1.05865	3.88399
11	6.40473	0.124846	1.06259	4.00687
12	6.23946	0.125848	1.04684	4.11205
13	6.27796	0.125056	1.01924	4.04499
14	6.38795	0.123146	1.02429	4.08668
15	6.55327	0.121692	1.0298	3.96365
16	5.60881	0.126257	0.981173	4.00207
17	2.02094	0.121386	1.00193	3.74578
18	0.0258326	0.0571833	1.28669	3.43294
19	0.00536847	0	1.28261	3.2112
20	0.00536732	0	1.17975	2.91395
21	0.00534261	0	0.926727	2.36417
22	0.0052921	0	0.556037	1.59253
23	0.00522844	0	0.227611	0.901022